Università degli Studi di Cagliari

**PhD Degree**

Industrial Engineering

Cycle XXXII

# Optimal siting and sizing of energy storage devices considering energy generation and consumption uncertainties

Scientific Disciplinary Sector

ING-IND/33


| | |
|---|---|
| PhD Student: | Nayeem Chowdhury |
| Coordinator of the PhD Programme: | Prof. Francesco Aymerich |
| Supervisor: | Prof. Fabrizio Pilo |
| Co-Supervisor: | Dr. Giuditta Pisano |


Final exam: Academic Year 2018 – 2019

Thesis defence: July 2020 Session

This work has been funded from the European Union's Horizon 2020 research and innovation programme under Grant Agreement No 676042

# Table of Contents

# List of Tables

# List of Figures

## Nomenclature

| | |
|---|---|
| $C_n^{RESc}$ | Cost of renewable energy curtailment at node n |
| $C_n^{PLS}$ | Cost of peak load shaving at node n |
| $C_n^{CHPc}$ | Cost of curtailing CHP power at node n |
| $C_n^{CAPEX\_ESS}$ | Storage investment cost at node n |
| $P_n^{RESc}(t)$ | Amount of renewable energy curtailment at node n during time interval t |
| $c_{EN}$ | Energy price in the wholesale market |
| $F$ | Fuel cost for biomass CHP plant |
| $P_n^{PLS}(t)$ | Amount of load curtailment at node n during time interval t |
| $c_E$, $c_P$ | Specific costs of energy storage in terms of energy and rated power respectively |
| $K_S$ | Capital recovery factor |
| $P_n^{RES}(t), Q_n^{RES}(t)$ | Expected active and reactive power production of renewables at time interval t, respectively |
| $P_n^{CHP}(t), Q_n^{CHP}(t)$ | Expected active and reactive power production of CHP at node n during time interval t, respectively |
| $PD_n(t), QD_n(t)$ | Active and reactive power demand of the loads at node n during time interval t, respectively |
| $I_{mn}(t), P_{mn}(t), Q_{mn}(t)$ | Current, active and reactive power flows from m-th to the n-th bus at time interval t, respectively |
| $R_{mn}, X_{mn}$ | Resistance and reactance of the mn-th branch respectively |
| $P_n^g(t)$, $Q_n^g(t)$ | Amount of active and reactive power provided by the upstream connections at node n during time interval t, respectively |
| $S_l(t)$ | Thermal capacity of the line at time interval t |
| $V_{max}, V_{min}$ | Maximum and minimum voltage limits, respectively |
| $P_n^{min\,RESc/CHPc}$ | Lower bound of active power curtailment of renewables and CHP at node n |
| $P_n^{maxRESc/CHPc}$ | Upper bound of active power curtailment of renewables and CHP |

| | |
|---|---|
| | at node n |
| $Q_n^{min\ RESc/CHPc}$ | Lower bound of reactive power curtailment of renewables and CHP at node n |
| $Q_n^{max\ RESc/CHPc}$ | Upper bound of reactive power curtailment of renewables and CHP at node n |
| $RR_n$ | Ramping rate of conventional generator |
| $PC_n^g(t)$ | Amount of produced power from conventional generators |
| $SOC_n(t)$ | State of the charge of storage unit at node n during time interval t |
| $P_n^c(t), P_n^d(t)$ | Charging and discharging power of storage at node n during time interval t, respectively |
| $\eta_c, \eta_d$ | Charging and discharging efficiency of storage, respectively |
| $\alpha_n^c(t), \alpha_n^d(t)$ | Binary variables for charging and discharging of storage at node n during time interval t, respectively |
| $P_n^{c,max}(t), P_n^{d,max}(t)$ | Maximum and minimum limits of charging and discharging power of storage at node n during time interval t, respectively |
| $\widetilde{P_n^{pv}(t)}, \widetilde{P_n^{wind}}(t), PD_n(t)$ | Bounded variables of PV, wind and load at node n during time interval t respectively |
| $\Delta\widetilde{P_n^{pv}(t)}, \Delta\widetilde{P_n^{wind}}(t), \Delta P\widetilde{D_n(t)}$ | Deviation from expected value of PV, wind and load at node n during time interval t respectively |
| $\xi_D^{ub}(t), \xi_D^{lb}(t), \xi_{pv}^{ub}(t), \xi_{pv}^{lb}(t), \xi_w^u$ | Scaled deviations from the random electric loads, PV and wind power generation at time interval t |
| $\Pi_D^+(t)\Pi_D^-(t), \Pi_{pv}^+(t), \Pi_{pv}^-(t), \Pi$ | Dual variables of load, PV and wind at time interval t |
| $\Gamma_i$ | The budget of uncertainty of the uncertain parameter i |

# Acknowledgement

It is an excellent opportunity for me to express my thanks to those who helped me during this journey. First and foremost, I would like to express my gratitude to Prof. Fabrizio Pilo, for his kind supervision throughout these 3 years. It has been an honor and pleasure to work under his able supervision. I would also like to sincerely thank my co-tutor Dr. Giuditta Pisano, for her patience and support during the research and writing of the thesis. I learned a lot from them.

I want to thank my industry tutor Giacomo Petretto, for his time to have countless discussions on complex power system topics and make the workplace comfortable. I would also like to thank Pasquale Salza and Irene Fastelli for being very supportive managers and engaging me on different topics. My colleagues Veronica Malvaldi, Maria Giovanna Vertuccio, Jibran Ali, and Fabio De Simone, who were a constant source of support and kindness.

My gratitude extends to my family, who has been beside me during the time of struggle. I want to thank all the people from Enel, University of Cagliari and MEAN4SG who were involved in this Ph.D. program and made it eventually successful.

# Chapter 1

## Introduction

### 1.1 Summary

The threat of climate change has an impact on our quality of life and the habitability of Earth for many species, including humans. The intergovernmental Panel on Climate Change (IPCC) estimates that, in order to reduce the risk that global temperature increases more than 2°C above preindustrial levels, greenhouse gas (GHG) emissions in developed countries must be descent by approximately 80% below 1990 levels by 2050 [1]. Electricity has an immense role to play to achieve this ambitious goal to reduce the global temperature. Electricity is a critical component in the societal aspect of our daily life to improve the economy, safety, security, and health around the globe. The generation of electricity is growing with the increase of the world population. The electricity generation will continue to increase and is predicted to rise by 70%, from 22126 TWh in 2011 to 37000 TWh in 2030 [2]. At present, the primary source of the majority of electricity consumed is fossil-based fuel. This primary source has recently been dispute due to sustainability and threat to the climate. However, it is obvious to secure a future with an easy-access to high-quality electricity that is sustainable and has less impact on the environment. To achieve that, an energy transition from fossil fuel to sustainable sources is indispensable. The critical transformation of the current energy transition is the emphasis on decentralization as opposed to a more centralized model.

This alteration from centralized to decentralized production will require a unique adaptation of the electric network, especially the distribution network. This adaptation indicates the shift of a passive distribution network to an active network. The active distribution network (ADN) can also be denoted as a smart grid [3].

The current electric power system is comprised of a transmission system and a distribution system. These two systems collectively create an interconnected network with different levels of voltage and currents. This sophisticated network is expensive and time-consuming to build. However, this infrastructure requires to have a cost-effective model to ensure electricity access to a considerable number of customers.

The planning for investment decisions follow-on in the evolution of the distribution grid are multi-layered, long-lasting, and have a substantial influence on the end-user experience. However, these investments are challenging due to inherent uncertainties in the future evolution of load, generation, and technology. The necessity for the distribution grid to become active from a passive network mainly compelled by the integration of weather-dependent distributed energy resources (DER).

DER brings new challenges in the way the power system is planned. DER can introduce bi-directional flow, voltage deviation, and grid congestion problems in the distribution network. These new challenges can affect existing grid reliability and security. Additionally, DER may be connected by various stakeholders that are not accountable for ensuring power quality in the distribution grid. This could indirectly increase the costs of the distribution system operator (DSO). Therefore, DSO is facing a challenging new environment concerning operations and planning of future distribution grids.

In order for the system operator to plan for a cost-effective and intelligent network, it is essential to include optimization and innovative solution into consideration. New innovative solutions such as energy storage could play a vital role in avoiding expensive investment decisions.

Optimization plays a vital role in the operation and planning of electric power systems. From real-time to long-term planning, the most critical power system decisions are supported by a variety of different optimization problems. In dealing with the uncertainty that affects these decisions, today's power system operators usually exploit deterministic optimization models that aim to maintain the reliability of the system and minimize costs. While this approach is valid, it can be expected that the development of new techniques in the area of optimization under uncertainty could yield substantial benefits to this practice. This is the challenge that motivates this Thesis. More precisely, this Thesis proposes models and algorithms to address critical optimization problems in electric power system operations by considering uncertainty through an emerging technique such as Robust Optimization.

OPF is a type of optimization problems where active and reactive power of devices connected to the electric grid can be optimized to minimize a cost function considering the physical constraint of the network. It is a suitable tool to model the operation and planning of distribution systems that contain active elements such as storage and demand response. Due to the high dimension of the distribution network characteristics, alternating current (AC) OPF is the most suitable method. In this thesis, convex relaxations have been chosen to guarantee a low calculation burden and globally optimal solutions. This thesis will emphasis on the development of operations and planning methods to incorporate new challenges in planning and operations for smart grids.

## 1.2 Energy Transition Context

An energy transition can be described as a process that leads to fundamental changes in the way energy is generated and consumed. Such a process is provoked by the policy and technology rather than the availability of resources. In the last couple of decades, the environmental strategy has been dominant to have a sustainable energy system. Especially in the outcome of the Kyoto Protocol, decarbonization has been the main focus of strategy evolution.

An effective energy transition implies a complicated balance between sustainability, competitiveness, affordability, and security of supply. Such a balance is addressed, for instance, by the “trilemma” goals heralded by the World Energy Council [4].

Access to energy services is vital for progressing human advance, fostering social inclusion of the poorest and most susceptible in society, and meeting many of the social development goals (SDGs). In September 2015, 193 countries – developing and developed countries – adopted the Sustainable Development Goals, known formally as the 2030 Agenda for Sustainable Development. The 17 new SDGs goal at ending poverty, improving health and gender equality, protecting the planet, and guaranteeing peace and prosperity for all. For the first time, the SDGs contain a target explicitly focused on warranting access to affordable, dependable and modern energy for all by 2030 (*SDG Indicator 7.1*), signaling an acknowledgment of the necessity of access to advanced energy services in its own right, and of the significance of energy in attaining many of the other development goals. The SDGs identify the integrated nature of development. A deficiency of access to modern energy can make it challenging or impossible for a country to oppose the myriad challenges that it faces, such as poverty (SDG 1), air pollution, low levels of life expectancy and lack of access to essential healthcare services (SDG 3), delivering quality education (SDG 4), adaptation and alleviation of climate change

(SDG 11), food production and security (SDG 2), economic growth and employment (SDG 8), sustainable industrialisation (SDG 9) and gender inequality (SDG 5).

Electricity is at the center of energy transition due to its role for economic and social improvement and its potential to support the decarbonisation plan [5]. Electricity is a primary connection to the exploitation of carbon-free energy resources such as renewables, and nuclear, and its penetration in areas such as transport and heating/cooling can enable their decarbonisation.

Energy and, more specifically, electricity is a vital part of daily activity. Due to the dramatic growth of electrification that mainly drives to achieve deep decarbonization, electricity is now accessible by 86% of the global population [6]. Around 84% of those 14% without electricity access live in rural areas, and over 95% of those residing without electricity are in countries in sub-Saharan Africa and developing Asia, as presented by International Energy Agency (IEA). Since the usage of electricity was started, the development of a country has been closely related to the accessibility and quality of the electricity supply. This has motivated states to invest in the infrastructure development of the power transmission and distribution systems. Due to these investments, power systems have been evolved from small micro-networks to trans-continental networks.

Due to the high dependency on electricity, it is essential to ensure the primary source of electricity. The past decades have seen an expansion of sources for electricity production. As depicted in Figure 1, a frequent upsurge in fossil fuels, specifically coal and gas as well as electricity from nuclear energy is seen between 1990 and 2016. Increasing worries about the sustainability of fossil fuels and the security of nuclear power are the prime movers of the current energy transition.

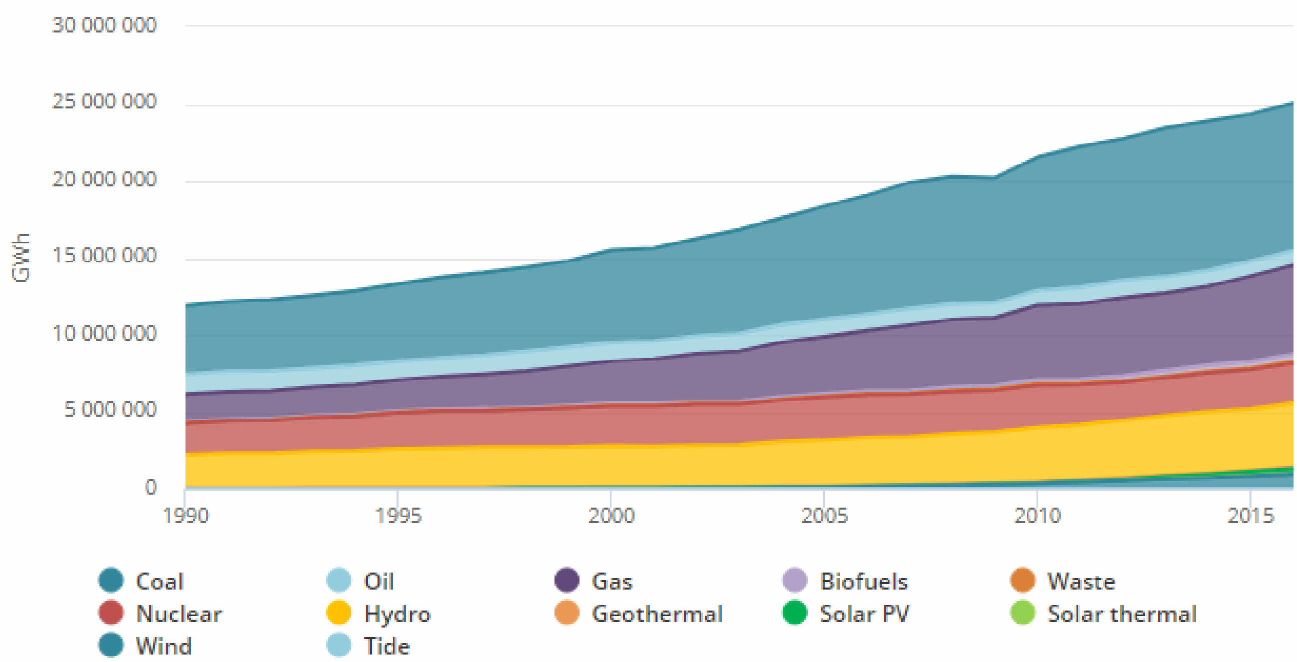


**Figure 1** *World electricity generation by fuel from 1990 to 2016 (Source: IEA)*

The energy transition from "conventional" resources to renewable ones is not the first energy transition in the history of the industrialized world. The first significant energy transition was originated by the discovery of fossil fuels in the early 1700s. The transformation that makes fossil fuels as the primary global energy source took two centuries. In 1995, oil accounted for 50 % of the total primary energy used to produce electricity in Italy. However, because of various oil embargoes and the growing worry of dependence on Middle Eastern countries' oil production, Italy adopted gas as the primary source of energy, besides, to invest more in renewables. Italy is one of the forerunners in the use of renewables. The massive development of renewable energy between 2000 and 2015 was primarily driven by the urge to have energy security and an impact on climate.

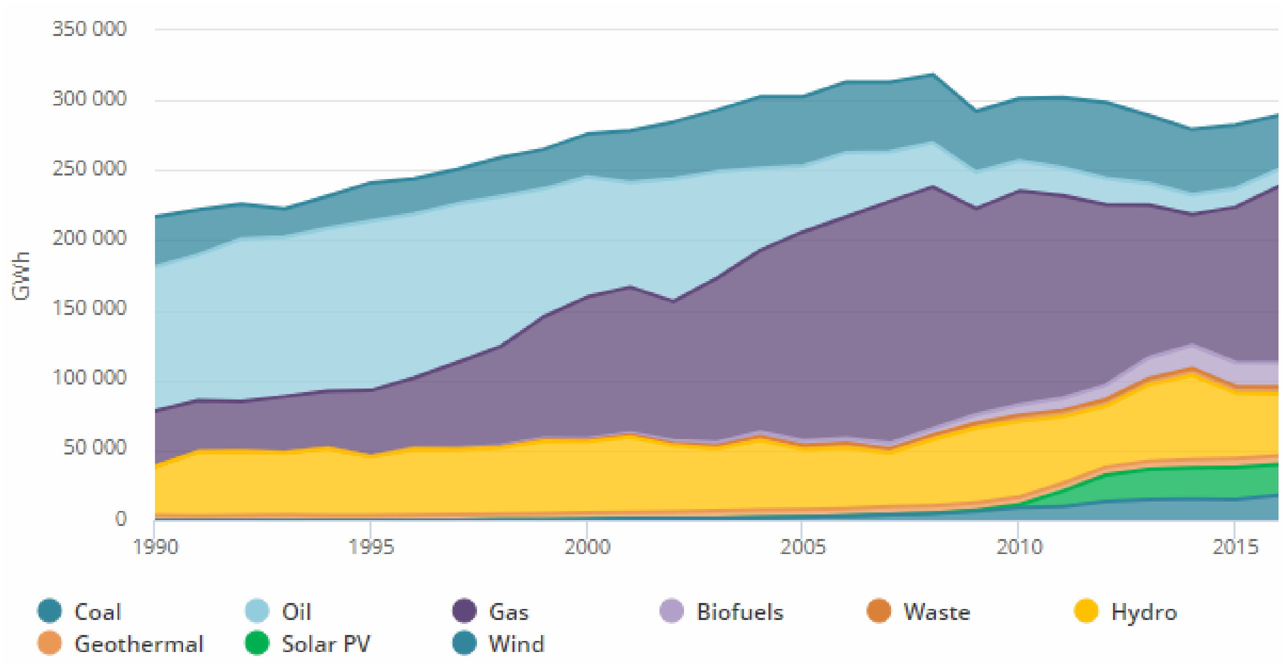


**Figure 2** *Electricity generation in Italy by fuel from 1990 to 2016 (Source: IEA)*

The major energy transition in Italy to renewables was reinforced by firm government policy, massive subsidies, and a strong desire to revitalize. These policies include subsidies, as well as research funded by the European Union, to inspire the growth of decentralized generator technologies and their integration into the grid. The electricity generation in Italy by fuel has been depicted in Figure 2.

The re-invention of the current distribution grid necessitates a passive system to be evolved into an active network with more automation and control strategies. This new active distribution system is often denoted as a smart grid. The smart grid concept aims to ensure sustainability in the power system that includes high quality and security of supply and maintaining at the same time the economic productivity. The subsequent large-scale energy transition is currently emerging and associated in the literature with the term smart grid.

## 1.3 Planning Strategies for Distribution System

### 1.3.1 Increasing demand – new customers

For new customer connections or the growth of the maximum power subscribed by a client, studies addressing existing line capacity are necessary. These studies are often power flow calculations for worst-case circumstances in order to lessen the level of risks. The current development of electric meters allows for a more comprehensive data collection of client consumption. The new, more sophisticated metering devices allow for augmented controllability of appliances and the possibility to connect small decentralized, mostly renewable generators with related tariff systems. This significant push to renovate electric meters has significantly increased the observability and the possibility of controllability in the low voltage (LV) distribution grid.

Nevertheless, the exploitation of the controllability is not yet widely applied. These new smart meters allow for the additional detailed analysis and optimization of existing architecture to avoid unnecessary costly infrastructure investments [7]. The progress of the distribution grid is also reliant on the trends of electric demand countrywide.

### 1.3.2 Integration of distributed generations

The current procedure is to connect decentralized generators includes verification of short circuit security, harmonics produced by the generator, perturbations of the communication system with safety components, flicker in voltage profile, maximum line capacity study, and representing a set maximum possible current injected by the generator. These regulations force the DSO to reinforce existing lines often when installing new generators or creating new separate lines specifically for the generator [7].

### 1.3.3 Tools for distribution network planning with distributed resources

There are two main sets of mathematical tools that exist for distribution grid planning. These tools include the tools that are adopted by current DSO and the more innovative tools that are proposed in the literature. The existing tools used by the DSO comprise different techno-economic indicators to evaluate investment choices.

Power flow analysis is also considered to provide intuitions into the behavior of a distribution grid. The presence of new decentralized generators can extensively affect the current and voltage profiles of a distribution grid. Therefore, comprehensive and accurate power flow models are required to quantify these effects for the smart planning of the decentralized generators.

Current power flow algorithms include the forward/backward sweep, Newton Raphson method [8], [9], fast-decoupled load-flow method [10], z-bus matrix construction method [11], and loop impedance method [12]. A power flow analysis is able to calculate the currents, voltages, and losses in all the branches and nodes (lines, cables, and transformers). This approach provides comprehensive detail of the electric system for a given scenario.

The uses of OPF algorithms for different power system applications have been described in [13]. These algorithms are gathered into three main groups: DC or linear approximations, non-linear convex approximations, and non-convex problems. In the circumstance of distribution grids, DC or linear approximations are often not sufficient for planning and operations algorithms in terms of accuracy. Often DC approximations are used to reduce the calculation time and remove convergence problems by introducing linear constraints.

The full AC power flow models are non-linear and non-convex in nature. The decomposition and heuristic approach is often used to solve nonconvex problems, but that can be expensive from a computational point of view. In the context of the non-linear convex class, there are two main convex relaxations: the SDP relaxation and the SOCP relaxation. Both of these relaxations have been proposed and applied in various cases for distribution power system study. These studies often consider operations of distribution grids [14] - [16]. Few are presented as planning algorithms [17] - [19].

An OPF is able to calculate the optimal setpoints of controllable devices during dynamic analysis. It considers a centralized control that optimizes the whole network.

This suggests that a single actor is controlling all the manageable devices with one primary objective. The OPF becomes unrealistic with the absence of controllability and observability in current distribution grids. However, the integration of decentralized generators could make this control and optimization more complicated.

## 1.4 Issues of renewable energy integration

The integration of distributed renewable energy brings new challenges in the power system operation and planning. The decentralized generators that are often connected to the distribution grid include PV, wind turbines, and micro-hydroelectric generators. These decentralized generators introduce new challenges for the DSOs. These challenges contain bi-directional or increased power flow within the network, voltage profile deviation, and compromised the safety of the equipment. To worsen these challenges, uncertainties in the distribution grid are high due to reduced aggregation effects in contrast to medium and high voltage grids. Random variation in load and generation can create high fluctuations in network power flow, therefore, causing unpredictable changes in the voltage profile.

### 1.4.1 Bi-directional current flow increased

DER connections into the distribution grid can cause a bidirectional current flow problem. If the load is low in an area with high DG installed capacity, the current can flow in the opposite direction. That means current can flow towards the substation end from the decentralized node. This opposite current flow can have effects on safety devices, voltage regulation devices and maximum current limits of distribution lines. Thus, it requires to resize the electrical lines considering the peak load and generation. Safety devices in distribution grids can be extensively affected by an increase or reverse power flow created by DGs. The security devices could get malfunction if the DSs are not disconnected earlier in a faulty situation. And this might damage the insulators, conductors, or the DG plants. DG can increase the existing currents flow through the existing devices; therefore, it could exceed the maximum rated current limits.

### 1.4.2 Voltage regulation devices

DG increases the voltage profile locally where it is installed due to the injections of power into the distribution grid. Active power injection of DG, when associated with local loading of the feeder, can reduce losses in the distribution system. However, if the injection of active power far away from the load, then grid losses can be increased. Reactive power control to support volt/var regulators has been shown to be promising [20].

If DG does not attempt to regulate local voltages, usually switch capacitor banks are unaffected. However, if DG controls local voltages or changes the downstream current of the regulating device, line drop compensation calculations may no longer be precise. The assumptions of downstream voltage are no longer correct if DG changes the local voltage or injects a substantial amount of power into the network. Thus, downstream voltage regulation calculations are no longer precise.

## 1.5 Innovative solution for smart grid

### 1.5.1 Energy Storage Technologies

The influence of renewable energy unpredictability on power systems depends on the penetration level, which is the ratio between installed renewable capacity and peak demand. In most cases, at minor penetration levels, typically less than 15% to 20%, the integration of renewable is not a big issue provided that there is no grid capacity or stability problems. If the penetration level increases, i.e., more than 20%, renewables need to be curtailed during the low consumption periods to ensure grid stability (frequency, voltage, reactive power) [21]. Figure 3 depicts a summary of issues in the integration of distributed generators and their probable solutions. ESSs are one of the highest potentials to solve such renewable integration problems. ESSs can be integrated into power systems to provide all or some portions of the additional regulation control and reserves. Besides, due to its variable nature, renewable can be negatively correlated with load and electricity prices.

ESSs can be installed to store a portion of renewable energy to accommodate wind/PV generation and improve overall system economics and stability. For instance, ESSs can be used to store the wind at night when the load is low and discharge it at peak load periods. Similarly, when wind power surpasses the minimum load at night and has to be curtailed to avoid grid stability problems, ESSs can help to store this curtailed amount of wind power and discharge it during the day to supply loads.

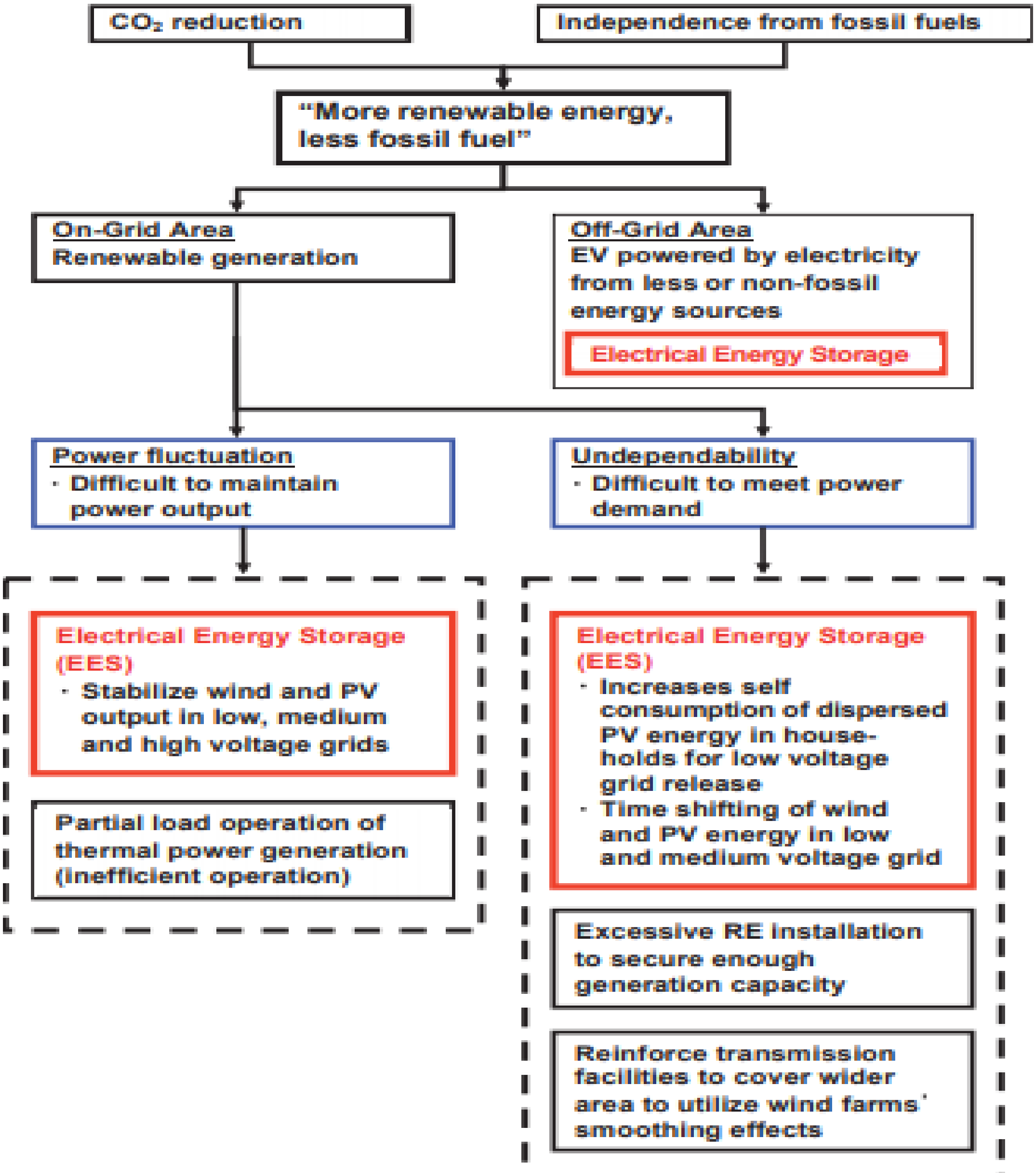


**Figure 3** *Issues with renewable integration and probable solutions [22]*

In general, ESSs can be an option to solve renewable integration issues by providing more flexibility and balancing to wind/solar generation, improving overall system economics and security. They will play an essential part in empowering a low-carbon electricity system with the growing penetration of renewables. The subsequent development of the electricity industry with their corresponding and extensive transmission and distribution networks has drawn interest in using this energy storage technology in recent years. Up to 2005, above 200 PHS systems were in use all over the world, providing a total of more than 100 GW of generation capacity. Though, pressure from deregulation and environmental concerns have led to a decrease in significant investment in PHS facilities, and interest in the grid applications of other forms of ESSs is growing, due to some primary factors including changes in utility regulatory environment, an increasing reliance on electricity in industry, commerce, and the home, power quality, the development of renewable as a significant new source of electricity supply, and environmental requirements. These factors gathered with fast technological growth and reduced ESS unit cost, making their practical use cases attractive. In chapter 2, a review has been performed on different energy storage technologies and their potential applications.

### 1.5.2 Demand Side Management

Demand-side management can be applied passively by giving price signals to end-users and encouraging behavioral changes. Active control of devices is another technique to control the devices or tools that are time non-sensitive. For instance, the washing machine that needs to be completed by a specific period in the evening, but it's not necessary when the washing machine starts to operate. Another example could be domestic water heaters or heat pumps. An approach could be to turn off these devices for specified periods without affecting the comfort of the end-user.

### 1.5.3 Generation and Load Curtailments

A curtailment is an approach of an active reduction of the power of a distributed generator under the ideal power output operational setpoint due to the grid being not capable of using the produced power. This can be caused when the generation is high, and electric consumption is low. The injection to an unloaded feeder from large DG plants could create opposite power flow, over-voltage issues, and line congestion problems. This strategy is suitable when there is no other solution to absorb the renewable power, and it helps to keep the network stable. Often, the curtailments could be cost-effective, but it will harm the payback period of DG.

## 1.6 Research Objectives

As the use of ESSs has been increased in the grid services, and also the cost of storage is decreasing, thanks to the technology development, the planning decision of storage in terms of optimal operation and placement becomes essential for both economic and system security perspectives. The goal is to find a place for ESSs where their applications will be most exploited. The addition of ESSs introduces time correlation characteristics into the planning problem, which is a significant dissimilarity between ESS planning and conventional system planning.

Moreover, the integration of renewable resources into power systems brings challenges for system planning, concerning the high uncertainty in renewable production. Deterministic approaches can not explicitly consider the stochastic nature of weather-dependent sources and hence can not make the right decision. Therefore, it is vital to develop probabilistic techniques for solving the uncertainty issue associated with renewable generations and load. This research aims at dealing with several questions related to the planning of ESSs in power systems with renewable penetration in the electric network:

- Assumed scarcity of data of renewable energy and load, how to decide optimal locations for the ESSs to be installed?
- What is the optimal operational schedule of the ESSs to support the network?
- How to incorporate PV, wind, and load uncertainties into the planning of ESSs in its combined operation with renewables?
- Is it economically convenient for system operators to equip their networks with ESS, instead of paying the DG owner or the customers for their services?

# Chapter 2

## Energy Storage System (ESS): Application & Technologies

### 2.1 Introduction

Energy storage systems (ESSs) have been considered as the vital source of flexibility to support the integration of renewable energy. Earlier studies have revealed the substantial system cost savings by the deployment of ESS, containing investment and operation of generation, transmission, and distribution infrastructures. The challenges associated with meeting demand variations while providing reliable services have historically motivated the use of energy storage devices while at least five factors have driven recent attention in energy storage: technological development of energy storage systems, anomaly in the fossil fuel price, high-value of ancillary services in a deregulated framework of energy market, avoiding high cost of distribution and transmission network reinforcement, and growing penetration of variable weather-dependent renewable generation [23]. The current attention mainly based on potential applications coupling with renewable energy sources, but the usage for the network application is growing recently. In Figure 4, potential applications of ESS technologies have been listed.

This chapter provides an overview of potential applications of storage devices. The leading ESS technologies currently available and underdevelopment are also explicitly described. The technical and economic characteristics of each storage technology are also presented.

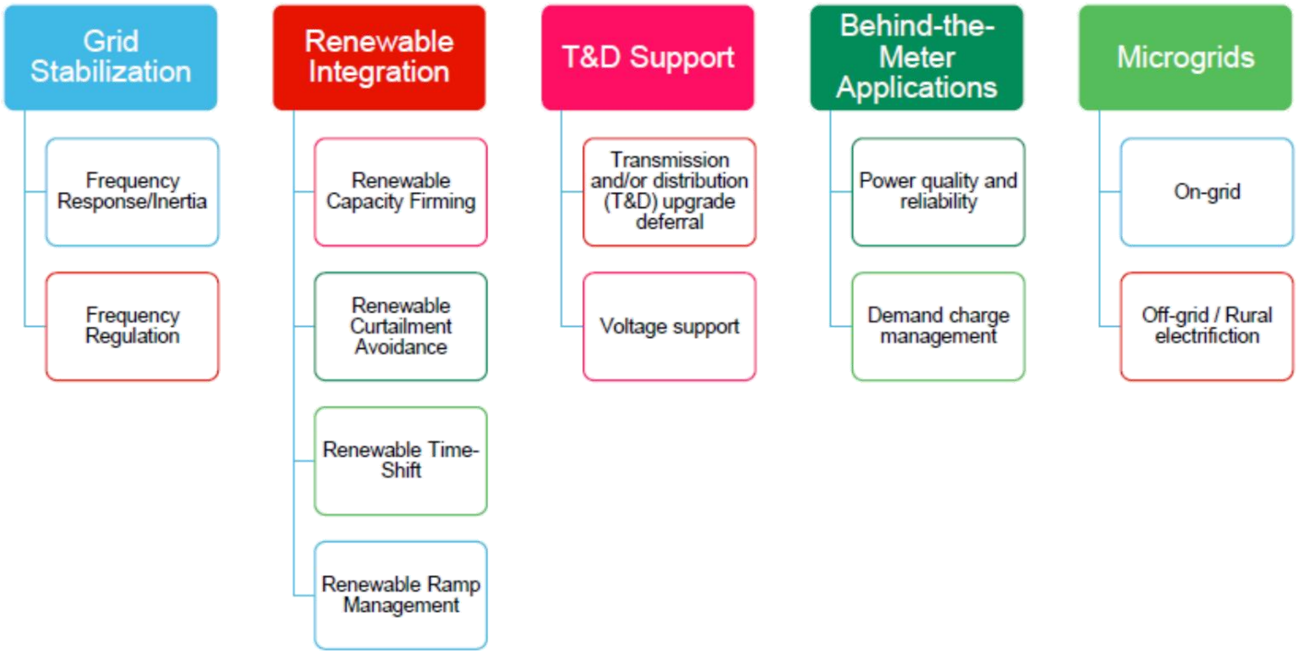


**Figure 4** *Applications of ESS Technologies*

## 2.2 ESS Application

The role of ESSs is to provide flexibility to PV and wind generations due to the variability and uncertainty behavior of PV and wind. Accordingly, renewable energy becomes controllable and dispatchable to meet system loads and meet energy bid in an electricity market. In addition, it can be controlled to utilize available transmission capacity efficiently. The roles of ESSs can be described by the number of uses (cycles) and the duration of operation, as shown in Figure 5. For power quality application, ESSs with high cycle stability and a short period of the operation is required; for time-shifting application, on the contrary, longer storage duration and fewer cycles are necessary [22].

In this section, different ESS applications are described in detail.

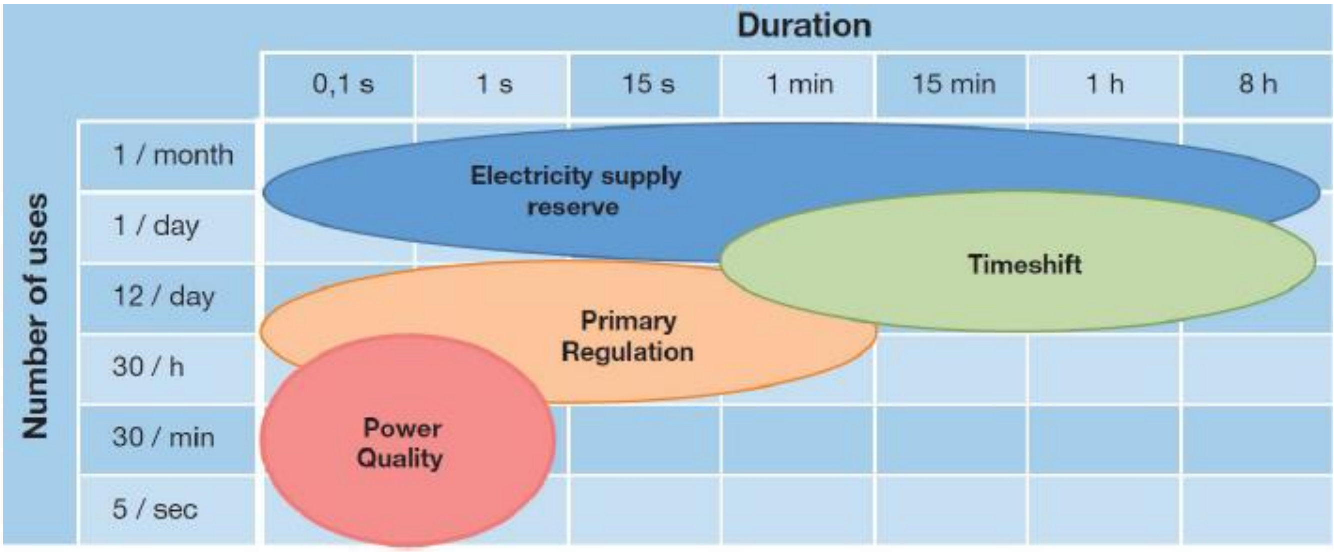


**Figure 5** *Different uses of ESSs depending on frequency and duration of use [22]*

### 2.2.1 Time Shifting

Due to its variable and weather-dependent nature, wind and solar energy might be high at periods of low demand and low electricity prices, and it could be low when demand is high, which might result in wind curtailment. In this case, ESSs can be installed to store the wind or solar energy generated during low demand periods and sell it later at a higher price during periods of high demand. Since this operation of the ESSs effectively shifts wind or solar energy in time, this application is called time-shifting, as shown in Figure 6.

The benefit of using ESSs is expected to be higher with a more significant gap between peak and off-peak of demand. For this application, ESSs are required to have a large energy capacity with an extended charging/discharging duration (from hours to days). Besides, their efficiency is another crucial factor to consider when choosing ESSs for this application, since an outstanding amount of power will be wasted in an inefficient storage device [23].

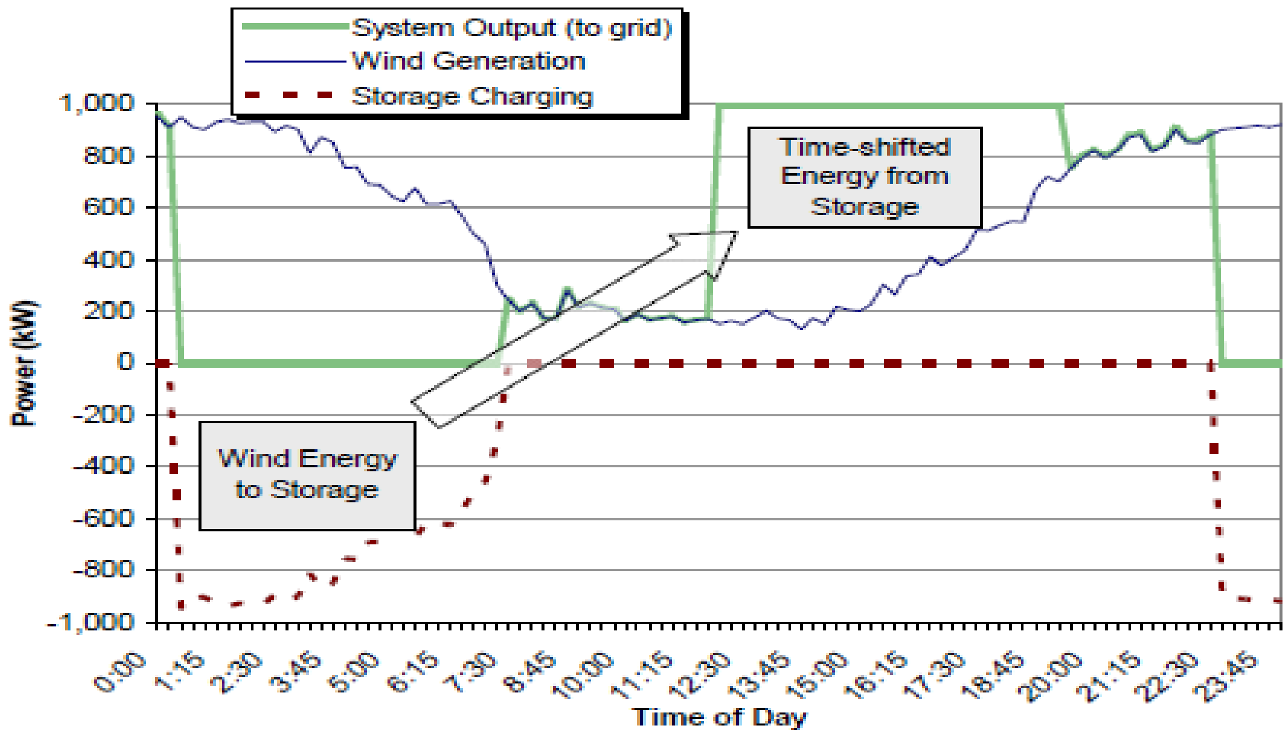


**Figure 6** *Time shifting application*

### 2.2.2 Peak Shaving

Peak Shaving is the process of decreasing the amount of electricity purchased from the utility during peak hours. In peak shaving, the main goal is to handle the peak demand without considering economic aspects, which are the main difference from energy arbitrage application. Since the energy storage system has a fast response and also it is low carbon emitted energy source, it is an optimal solution for this application. According to ABB, the benefits for this application include a reduction in energy cost by reducing peak demand, reduction in energy generation cost by maintaining peak power demand and avoiding investment cost to install more electricity generating units. Usually, the peak shaving application is owned by the electricity consumer, whereas the energy arbitrage application is installed on the supply side [24]. The recent techno-economic analysis shows the cost-benefit study on energy storage systems such as NAS, lithium-ion, lead-acid, and flows batteries for peak shaving applications [25] – [26].

### 2.2.3 Frequency Support

Frequency control allows for reliable power systems, and it happens during the change in the loads. Energy storage helps the power system to correct the frequency mismatch while changing the loads, depicted in Figure 7. Ref. [27] discusses three types of frequency regulation, such as primary, secondary, and tertiary. The primary reserve control balances the frequency in the system within 5-30s. The secondary reserve control acts as a backup of the primary reserve and makes sure to set the nominal frequency, and it usually reacts for 5-15 min [28]. The tertiary control ensures the synchronization between load and generation and also with other generating units. Two case studies in [29] have demonstrated the impact of energy storage devices on frequency regulation for different power system networks such as single and three area power systems.

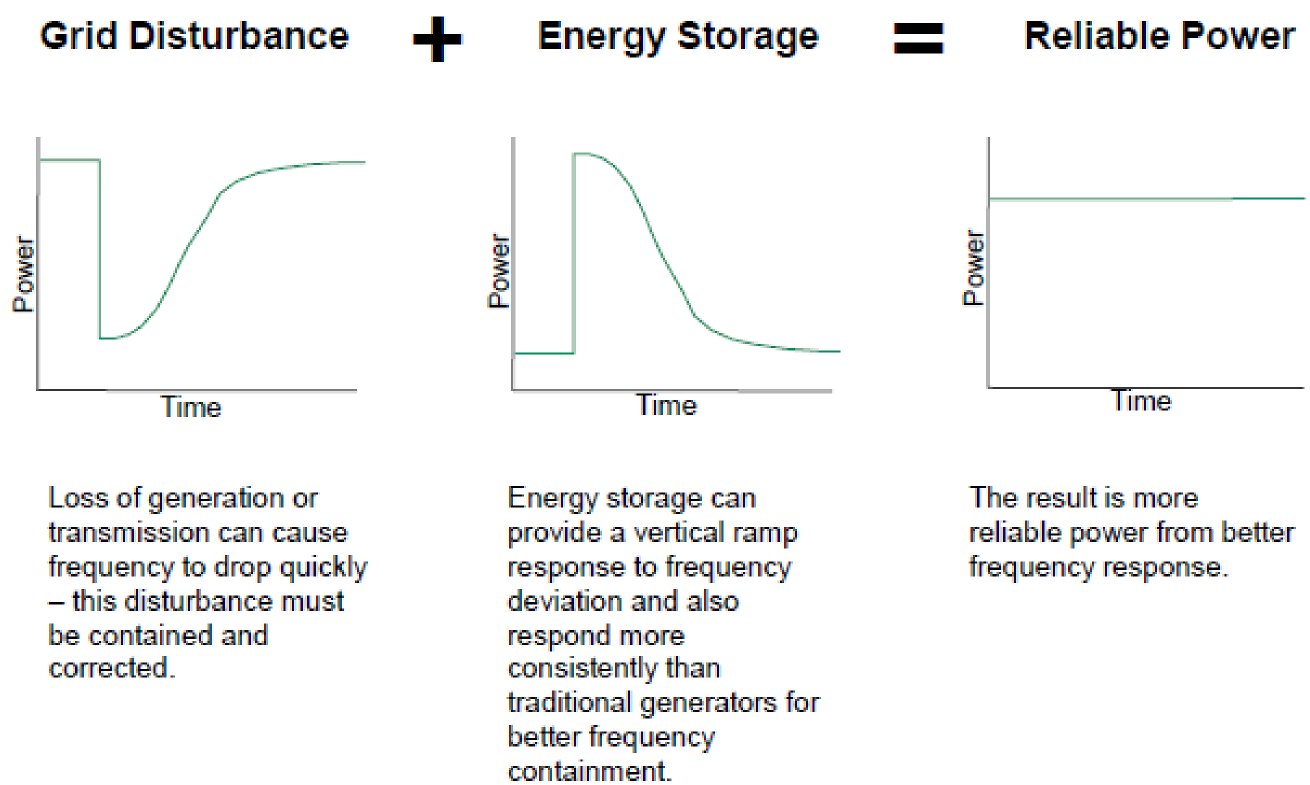


**Figure 7** *Frequency regulation by storage devices*

### 2.2.4 Energy Arbitrage

The penetration of renewable energy creates energy price volatility; during the excess of renewable energy generation, electricity price drops, and the price starts to rise when the renewable generation decreases. The storage system can play an essential role during the volatile situation. The energy storage system can increase the efficiency of the whole power system and optimize it economically. The goal of this application is to store generated electricity from conventional energy sources when the price of renewable generation is high and sell the stored energy during peak power demand hours when the price is high or less renewable energy is being generated. Especially for the microgrid operation, the ESS will store electricity when the generation is higher than the demand and inject the electricity back into the grid system when the demand is higher [30]. The correlation between energy arbitrage with peak demand shaving and load balancing has been discussed in recent research [31]. Another recent case study for the European market shows the impact of PHS and CAES on energy arbitrage applications and also demonstrated new opportunities for energy storage systems on the energy market [32].

Energy markets meet the demand for electricity both in real-time and in the near term. The electric energy market operates two markets of energy: the day ahead and real-time energy markets. The day-ahead market is a forward market; it creates financial schedules for the consumption and production of energy one day before the operating day. Based on demand bids, generation offers, and scheduled bilateral transactions, the locational marginal prices are determined for the next operating day. On the other hand, the realtime market is a spot market; it balances variances between day-ahead scheduled quantities of energy and actual real-time necessities. Based on actual grid operating conditions, locational marginal prices of this market are determined. The daily energy price fluctuations provide an excellent potential profit for arbitrage, by purchasing energy when prices are low during off-peak hours and selling it at higher energy prices during peak hours. Energy storage systems allow an offset in time between energy production and consumption. The capability of storing energy has a significant impact on both the physical characteristics of the electric grid and on the potential revenues of energy market participants.

### 2.2.5 Voltage control

Voltage support is critical in order to have a stable power system and to prevent possible damages to the power system, such as overheating of generation and motors. One way possible to support the voltage is to increase reactive power in the power system. However, increasing reactive power to support the voltage is not always feasible and desirable, especially for the long transmission line, as it is a nonlinear consumer of reactive power. Therefore, the ESS can support the voltage locally by discharging the electricity with the desired voltage level to the power system [24]. The study in [33] has shown case studies where vanadium redox battery has been used to support low voltage (LV) network to solve the voltage rise/drop issues. Other relatively new research in [34] has discussed the optimal allocation of storage devices to support the voltage in the LV network. A supercapacitor bank has shown a potential solution for voltage support of wind plants [35].

### 2.2.6 Spinning Reserve

Spinning Reserve is the reserve system, which can respond quickly when the mismatch between generation and demand happens. The spinning reserve does not get used during the normal operation, but it is always online to support the power system. The spinning reserve storage system can supply power to the power system for more extended periods before the backup system ready to support the system [36]. Recently, a case study [37] has been performed where a virtual energy storage system has been modeled with a flywheel storage system to improve the spinning reserve, which is coordinated the demand response from domestic refrigerators in London.

## 2.3 ESS Technologies

Energy storage technologies can be classified in terms of forms of storage. The categorization of energy storage technologies according to the form of stored energy has been represented in Figure 8. Below a succinct description of energy storage devices that are commonly used.

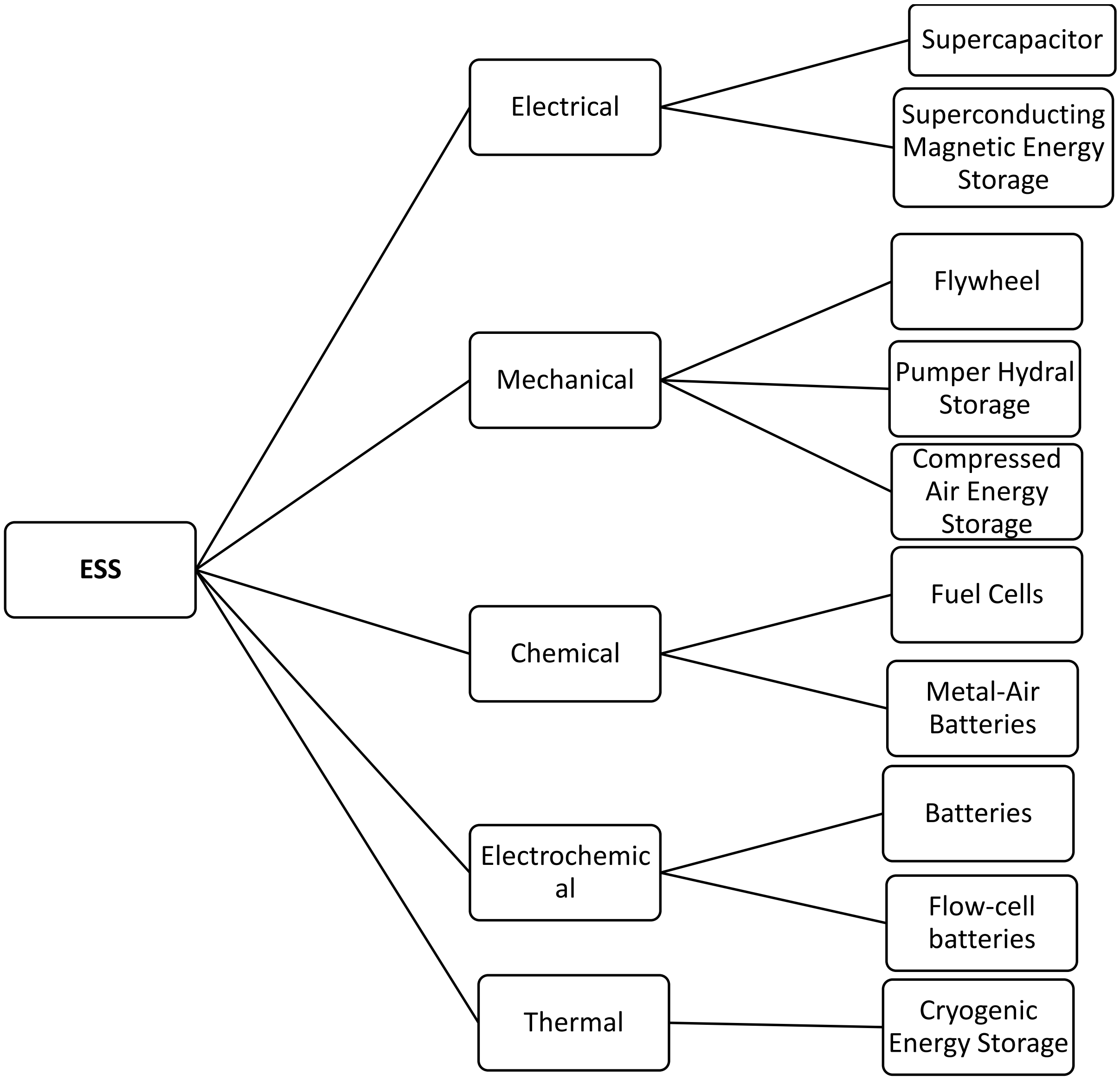


**Figure 8** *Classification of ESS technologies*

### 2.3.1 Electrochemical Batteries

The different electrochemical batteries that are commonly used in the industrial applications are presented in the following sections. That includes Li-ion batteries, NaS, Flow batteries, flywheel, and other storage systems from various technologies.

### *2.3.1.1 Li-ion Batteries*

Li-ion battery chemistries have the highest energy density and are considered safe. No memory or scheduled cycling is needed to enhance battery life. Electronic devices such as cameras, calculators, laptop computers, and mobile phones usually use li-ion batteries, and the uses are high for electric mobility sectors.

Lithium-based batteries are extensively used in small applications, such as mobile phones and portable electronic devices; thus, the annual gross production is around 2 billion cells [38]. Some battery manufactures (SAFT, Shin-Kobe, Japan Storage, Avestor) are developing lithium-based batteries in both high energy and high power configurations for electric vehicles and hybrid electric vehicles [39]. A Lithium technology battery consists of two main types: lithium-ion and lithium-polymer cells [40]. The high energy and power density of lithium-ion cells make them attractive for a wide range of applications, from portable electronics to satellite applications [41]. The ever-growing demand for energy storage requires further researches to improve the performance of this type of power resource. Numerous investigations have been carried out on electrode materials and electrolytes, showing the importance of the choice of these components of the battery. For lithium-ion batteries, the self-discharge rate is shallow at a maximum of 5% per month, and the battery lifetime can reach more than 1500 cycles [38]. However, the lifetime of lithium-ion battery is temperature-dependent, with aging taking its toll much faster at high temperatures, and can severely shorten due to deep discharges. The deep discharge issue makes lithium-ion batteries inappropriate for use in back-up applications where they may become completely discharged. Although Li-ion batteries take over 50% of the small portable devices market, there are some challenges for making large-scale Li-ion batteries. The main hurdle is the high cost due to the special packaging and internal overcharge protection circuits [42].

Regarding its self-discharge, this much relies on temperature, but it has been reported to be around 5% per month [38]. Compared to the Li-ion battery, the lithium–polymer battery operational specifications dictate a much narrower temperature range, avoiding lower temperatures. However, lithium–polymer batteries are lighter, and safer with minimum self-inflammability. Basic chemistry suggests that lithium-based cell technologies are likely to represent the pinnacle of cell development in terms of specific energy density [43]. Lithium-based cell technologies may benefit in the future from better electrodes, plates, current collectors, and seals, complemented by developments in materials processing, fabrication, and manufacturing techniques.

*2.3.1.2 NaS*

In order to achieve much higher power and energy density, some novel energy storage technologies are under research [44]. NaS battery is one of these types, and it has already been employed in power systems for more than 20 projects in Japan and many other worldwide constructions since the 1980s [45].

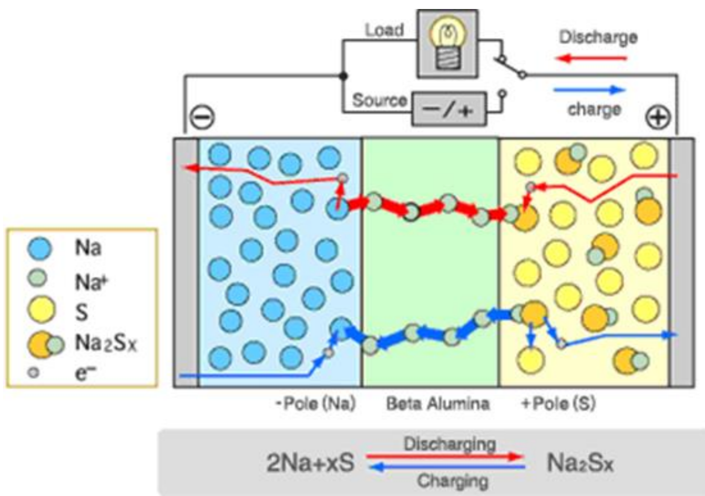


**Figure 9** *NaS technology [46]*

A NaS, as shown in Figure 9, consists of liquid (molten) sulfur at the positive electrode and liquid (molten) sodium at the negative electrode as active materials separated by a solid beta alumina ceramic electrolyte [46]. Compared with the other leading battery technologies, NaS shows much more attractive energy density (four times that of lead-acid battery) and has an extended cycle capability (2500 cycles upon 90% depth of discharge) and a millisecond response for full charging and discharging operations, which presents good potentials to be applied in microgrid applications for power regulations. The energy density and the energy efficiency of this type of batteries are very high 151 kWh/m$^3$ and 85%, respectively [47]. Additional notable features of NaS batteries are no self-discharge, low maintenance, and their 99% recyclability. NaS battery can be widely used in aggregated energy storage. This battery needs particularly useful thermal insulation to reduce heat loss. The structure of the cell is generally used in the form of glass, and the materials used are precious because of the corrosive capacity of liquid sulfur. It is also equipped with an internal heating system that is activated when the temperature drops below a certain limit. With the battery at rest, the thermal autonomy may be a few days. This forces the heating system to be active and connect the battery to the power supply to power it.

This type of battery, characterized by a high typical discharge regimen and high specific energy, is typically used for "energy" applications.

*2.3.1.3 Flow Batteries*

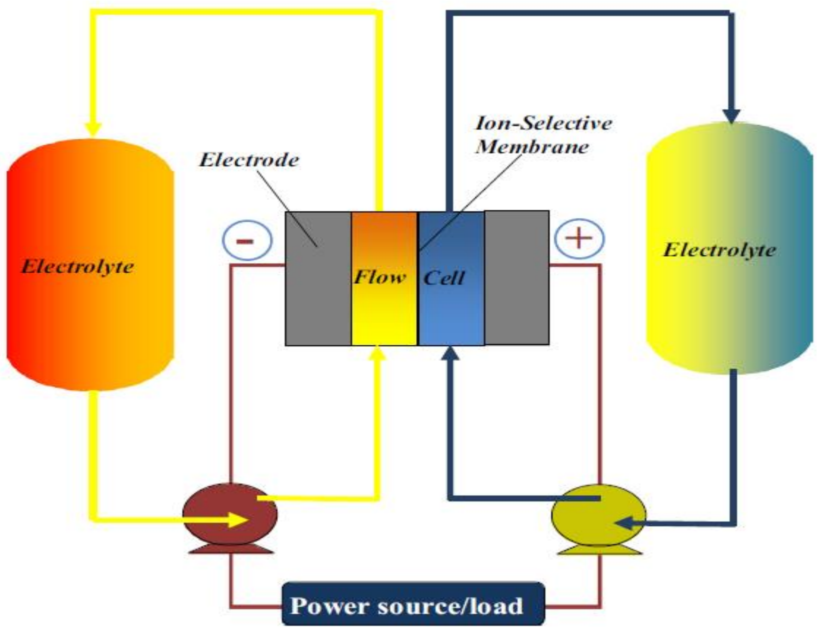


**Figure 10** *Flow Batteries*

Flow batteries (often called redox flow batteries) are a relatively new system. Unlike, conventional batteries, the flow battery store energy in the electrolyte solution. The concept of a flow battery is, the electrolyte consists of electroactive materials are run through a reactor to perform the chemical reaction. The chemical reaction is reversible, which allows charging, discharging and recharging capability. The storage capacity of flow batteries can be increased by merely utilizing larger storage tanks for the electrolyte. Several chemistries are possible for the battery: Vanadium (VRB), Zinc-Bromine (Zn-Br), Polysulphide-Bromide (PSB), Iron-Chromium (Fe-Cr) and Zinc-Cerium (Zn-Ce) [48].

Since 1970 Redox-Flow batteries have been developed. In the US the NASA started development in the early 70s. Different chemistries have been developed (iron chrome, all vanadium, etc.). In the 1980s, mostly the University of New South Wales (UNSW) developed several prototypes. In the 90s, several prototype systems have been tested in the multi kWel range. Especially Asian companies like Mitsubishi Chemicals, Kahima Kita Power Corporation, and Sumitomo, installed and tested these systems. Plants up to 200 kWel and 800 kWh storage capacity have been constructed and operated. In Asia, there are some commercial suppliers of these systems like Golden Energy Fuel Cell (GEFC), Prudent, and Ronke Power. In Europe, AF Gildemeister produces systems within a power range of 10 kWel – 200 kWel. The development work is focused on the cost reduction of these flow systems further. One of the significant cost drivers is the cation exchange membrane. R&D work is performed to develop cheap and cost-effective new membranes on the one hand and to study new Red-Ox couples. Additionally, thinner and more active reaction felts will help to increase the power density of the cell. This will reduce stack size and costs.

#### *2.3.1.4 Lead-acid*

The most mature and cheapest energy storage devices of all battery technologies are the lead-acid battery. These kinds of batteries are based on chemical reactions relating lead dioxide (that forms the cathode electrode), lead (which creates the anode electrode), and sulfuric acid, which acts as the electrolyte. Two major types of lead-acid batteries are flooded batteries, which are the most common topology and valve-regulated batteries, which are subject to extensive research and development [49]. The lead-acid battery has a low cost ($300–$600/kWh), and high reliability and efficiency (70–90%). Apart from the relatively poor performance of the battery at low and high ambient temperatures, and its relatively short lifetime, the main disadvantages of the lead-acid battery are the necessity for periodic water maintenance and its low specific energy and power. Lead-acid batteries also pose difficulties in providing frequent power cycling, often in a partial state of charge that leads to early failure due to sulphation [50].

### 2.3.2 Compressed air energy storage

The compressed air energy storage is a commercially viable technology, which provides ample storage capacity, such as above 100 MW. The idea of compressed air energy storage (CAES) is to compress air using high pressure (approximately 4-8 MPa) through electrical energy. Moreover, when electricity needed, the compressed air is mixed with natural gas; this air-fuel mix will be burned and expanded in a gas turbine and produce electricity through a generator. The first CAES project has been implemented in Germany at Huntorf with a capacity of 290 MW in the year 1978.

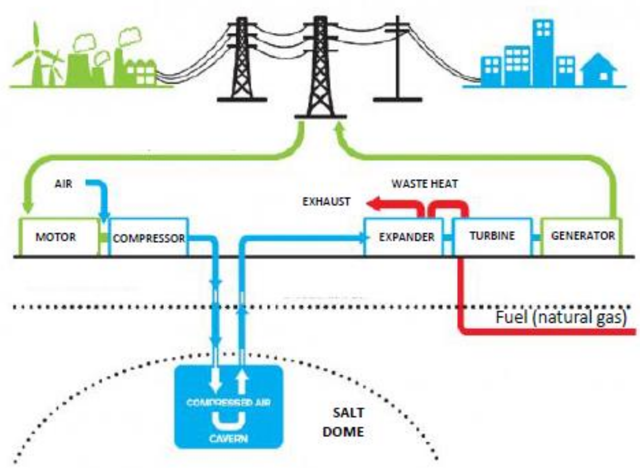


**Figure 11** *CAES System (source: BRUSH group)*

### 2.3.3 Flywheel

The use of flywheel is very primitive [56-58]. The flywheel is defined as a rotating wheel that is used to store mechanical energy. Flywheels are useful for low and medium scale mechanical energy storage systems. The energy stored by a flywheel depends on the mass and radius of the flywheel and the angular velocity. The stored energy of flywheel relies on the speed of the rotating body. With speed, the amount of stored energy increases. In order to move the flywheel, electricity needs to supply from an external circuit. While the flywheel is connected to the grid, it is desirable to have the constant speed that implies keeping the frequency consistent to ensure the grid reliability. The speed of the flywheel can control the frequency of electricity.

Since the low-speed flywheel storage system has long life cycles, low maintenance, and speedy response, it is preferable for the industry. However, it has also disadvantages such as high installation cost, low capacity, and self-discharge problem. The energy storage capacity range of this type of flywheels is 0.2-25 kWh. The efficiency of the flywheel is in the range of 90-95%.

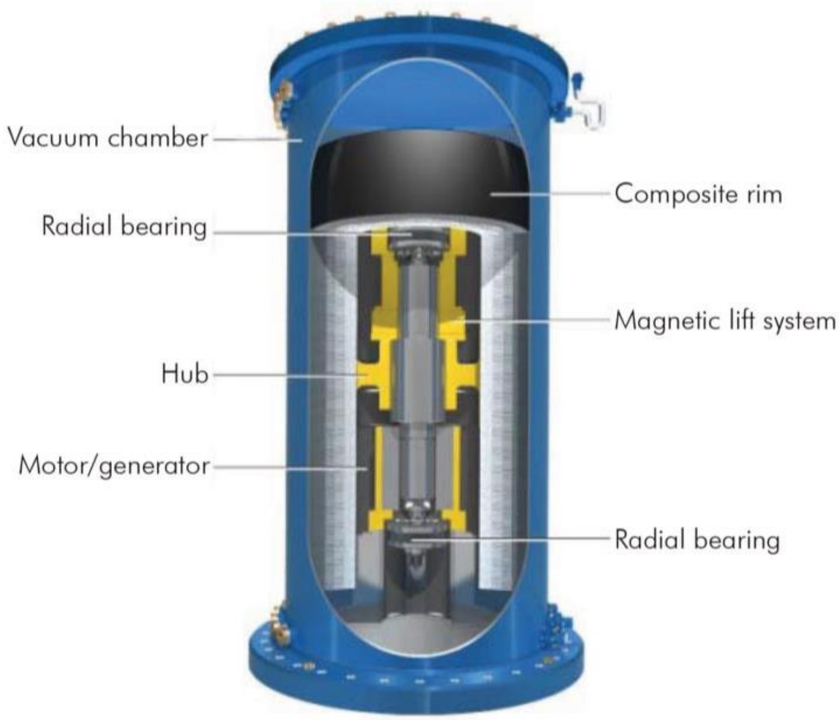


**Figure 12** *Flywheel storage (source: Beacon Power, LLC)*

### 2.3.4 Pumped Hydro Storage

The pumped hydro storage (PHS) technology considered the most mature technology and economically viable. The concept of PHS is to have two water reservoirs at different elevations. There will be a turbine with a generator between the reservoirs to produce electricity. When the electricity is excessive the water will be pumped to an upper reservoir, which implies the charging state and during the electricity demand is higher than supply the water will be discharged from the top to the lower reservoir through the turbine which will produce electricity. Due to PHS's low capital cost, high efficiency, long storage period, the technology is matured in the energy storage market. The typical storage capacity is around 1000 MW, with an efficiency of 71-85% considering the evaporation losses. The drawback of this type of storage system is extensive land use and which implies environmental issues.

### 2.3.5 Thermal Storage

The principle of the thermal storage system is to store thermal energy by heating or to cool the insulated thermal storage medium and use the stored energy during the thermal energy supply-demand mismatch. This technology is mainly used in industrial and residential applications. A comprehensive review has been discussed in [51]. The thermal storage method can store the heat energy in water and inject back the energy when the system needs [52]. The thermal energy storage system can be classified into two types: (i) Low Temperature and (ii) High Temperature. Under the low-temperature thermal energy storage, which considered as underdeveloped [53] two storage technologies such as Aquiferous and Cryogenic energy storages lie.

The aquiferous or chilled water thermal storage uses water, which is iced through a refrigeration processes when the energy price is low or excess of renewable energy and later use for cooling purposes during the peak period. Such storage technology has been installed with a capacity of around 135 MW all over the USA. The most significant storage system is in Texas, the USA, which has a capacity of 90MW at 95°F.

Cryogenic liquids, for instance, liquid air or liquid nitrogen, can be stored for a long time in a vacuum flask at atmospheric pressure. During the electricity demand, the cryogenic liquid is then heated to the surrounding temperature and used to produce electricity by driving a turbine. A pilot plant with a capacity of 300 kW has been developed at the University of Leeds, UK [54].

The high-temperature thermal storage systems are entirely developed and in operation all over the world. Among them, molten salt and phase change material storage system are standard.

Molten salt is usually solid at standard temperature and pressure, but it converts to liquid at high temperatures. The molten salt storage technology stores the liquid salt at high temperatures, and during the peak demand for electricity, the dissolved salt can be used to produce steam for the turbine to generate electricity. In the USA, there are four molten salt storage plants in operation with a capacity of more than 500MW. Spain has the most significant number of molten salt storage plant, which is around 23 plants with more than 1000 MW of storage capacity.

Another high-temperature thermal storage system is a phase change material (PCM) storage system. PCM storage system based on the phase-shifting capability of the material to release or store energy. The usual phase shifting is from the solid phase to liquid, and heat is absorbed and released during this process. The different materials have been studied extensively, and applications of the PCM storage system are illustrated in [55].

## 2.4 Summary

In this chapter, different energy storage technologies and applications are briefly described. The commonly used energy storage technologies in terms of reducing renewable energy curtailments and grid services have been presented. It has been understood that some storage systems are suitable for power-intensive applications such as flywheel and electrochemical batteries. On the other hand, pumped hydro and compressed air energy storage systems are appropriate for energy-intensive applications. The various uses of storage also investigated. The potential of storage goes beyond the services related to energy storage integration; instead, it can provide network services to have a stable and reliable grid.

# Chapter 3

## Convex Optimization for power system

The application of optimization in the power system is inevitable. From the optimal power flow to dispatch generation to the energy market operation, optimization has its role to play. The non-convex optimization problems are difficult to solve to find the global solution, and methods related to the solution approach involve many compromises, e.g., very long computational time, or not always finding the solution. However, the exceptions are the least-square problems, linear programming problems, and convex optimization problems. That being said, it is often hard to express power system formulation in such a way that it is efficient in solving and generate a global solution. The non-convex characteristics of power system formulation motivate to explore the techniques to convexify the non-convex power system problem. The two main benefits of the convex problem over non-convex are [56]-[57]: (i) There are fast and efficient algorithms that can solve large scale convex problems, and (ii) The solution is necessarily a global one, that means optima is always a global one. Since the energy storage planning is a non-convex problem, this chapter briefly introduces the background of convex optimization, and the information is mostly inspired by the *convex optimization* book [58].

### 3.1 Introduction

#### 3.1.1 Mathematical optimization

A constrained optimization problem has the following form

$$\text{minimize } f_0(x) \tag{3.1}$$

Subject to,

$$f_i(x) \le b_i, \quad i = 1 \dots \dots n. \tag{3.2}$$

$$g_i(x) = b_i, \quad i = 1 \dots \dots k. \tag{3.3}$$

Here the function $f_0 : R^n \to R$ is called the objective function, $f_i : R^n \to R, i = 1, \ldots\ldots, n$ is the inequality constraint function, and $g_i : R^k \to R, i = 1, \ldots\ldots, k$ is the equality constraint. The constants $b_1, \ldots\ldots, b_m$ and $b_1, \ldots\ldots, b_k$ are the bounds for the inequality and equality constraints, respectively. The $x$ is a vector that contains the optimization variables as, $x = (x_1 \ldots \ldots x_m)$. A vector $x^*$ is considered optimal if it has the smallest objective value among all the vectors that satisfy the constraints.

When the satisfaction of constraint has been mentioned, it is essential to understand the concept of a feasible set. The set of points that defined the objective and all the constraints is termed as the domain of the optimization problem. For instance, if $D$ is the domain of the feasible points of $f_i$ and $g_i$, a point $x \in D$ is viable if it satisfies the constraints (3.2) and (3.3). The feasible set consists of all the feasible points.

A feasible set P can be defined as equation (3.4),

$$P = \{f_0(x) \mid f_i(x) \le b_i,\ \ i = 1 \ldots \ldots n, \qquad g_i(x) = b_i,\ \ i = 1 \ldots \ldots k.\} \tag{3.4}$$

If the problem is infeasible, then $P = \infty$.

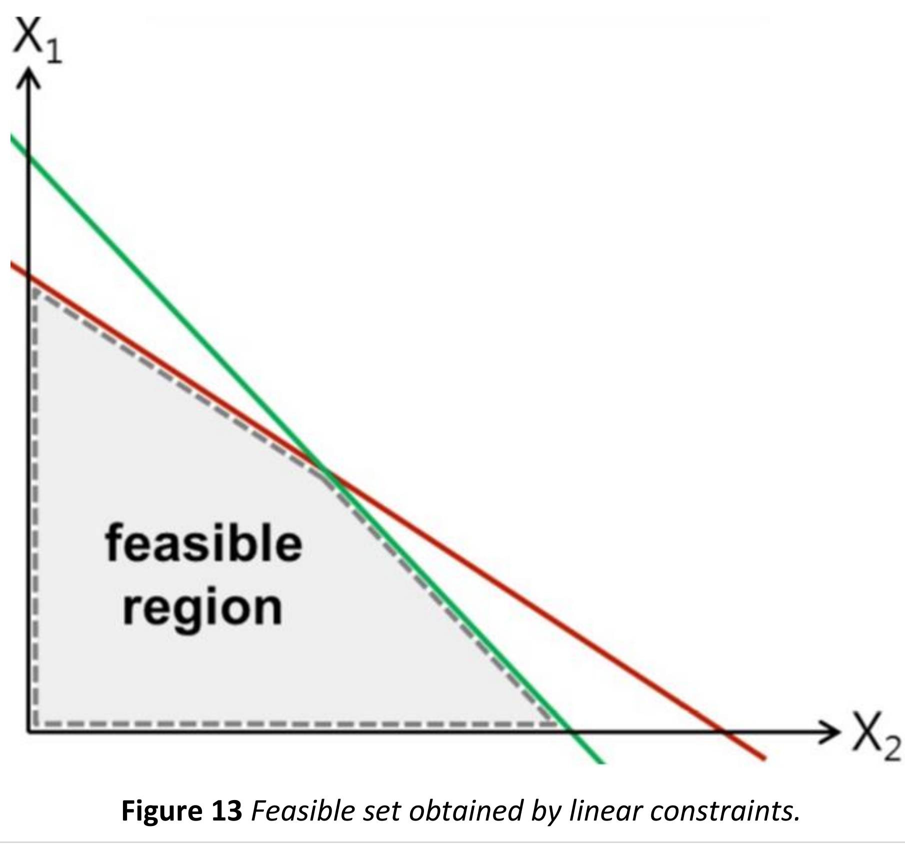


**Figure 13** *Feasible set obtained by linear constraints.*

An example of feasible region has been shown in Figure 13.

### 3.1.2 Local and Global minima

An optimization problem can have several minimal points. A feasible point $x$ can be considered as locally optimal if there is a $R > 0$ such that

$$f_0(x) = \{ f_0(z) | f_i(z) \leq b_i, \ i = 1 \dots \dots n, \qquad g_i(x) = b_i, \ i = 1 \dots \dots k, \qquad \|z - x\|_2 \leq R \} \quad 3.5$$

The above equation (3.5), can be rewritten as,

$$\text{minimize } f_0(z) \quad 3.6$$

Subject to,

$$f_i(z) \leq b_i, \ i = 1 \dots \dots n. \quad 3.7$$

$$g_i(z) = b_i, \ i = 1 \dots \dots k. \quad 3.8$$

$$\|z - x\|_2 \leq R \quad 3.9$$

Here $x$ solves the above optimization problem with variable $z$; this means $x$ minimizes $f_0$ over the points in the feasible set.

On the other hand, the global minimum $x_g$ is a point in the feasible set, $P$ that relates to the smallest value of $f_0(x)$ on its feasible set.

### 3.1.3 Affine set

An affine set can be defined as a set that comprises every pairwise linear combination of points subject to the constraint that the coefficients are real numbers. So to keep it simple, an affine set is a convex set that happens to be infinite.

Let's consider two different points, $x_1$ and $x_2$ and they are in $R^n$. The line passing through $x_1$ and $x_2$:

$$y = \theta x_1 + (1 - \theta) x_2 \quad 3.10$$

A set $S \subseteq R^n$ is affine if the line goes through any two separate points in $S$ lies in $S$. and $x_1, x_2 \in S$. In other words, $S$ contains the linear combination of any two points in $S$, provided the coefficients in the linear combination sum to one.

This concept can be applied to more than two points. If we refer to the point of the form $\theta_1 x_1 + \theta_2 x_2 + \cdots + \theta_l x_l$, where $\theta_1 + \theta_2 + \cdots + \theta_l = 1$, represents an affine combination of the points $x_1 .. \; .....x_l$. Using instruction from the definition of the affine set it can be shown that an affine set holds every affine combination of its points: if $S$ is an affine set, $x_1 .. \; .....x_l \in S$, and $\theta_1 + \theta_2 + \cdots + \theta_l = 1$, then the point $\theta_1 x_1 + \theta_2 x_2 + \cdots + \theta_l x_l$ also belongs to $S$.

If $S$ is an affine set and $a_0 \in S$ , then the set

$$B = S - a_0 = \{x - a_0 | x \in C\} \qquad 3.11$$

Here $B$ is a subspace. Suppose $b_1, b_2 \in B$ and $\gamma, \delta \in \boldsymbol{R}$. Then it can be written $b_1 + a_0 \in B$ and $b_2 + a_0 \in B$, and therefore

$$\gamma b_1 + \delta b_2 + a_0 = \gamma(b_1 + a_0) + \delta(b_2 + a_0) + (1 - \gamma - \delta)a_0 \in B \qquad 3.12$$

The affine hull of $S$ can be defined as the set of all affine combinations of points in some set $S \subseteq R^n$and can be represented as:

$$\text{aff}\, S = \{\theta_1 x_1 + \theta_2 x_2 + \cdots + \theta_l x_l | x_1 .. \; .....x_l \in S, \theta_1 + \theta_2 + \cdots + \theta_l = 1\} \qquad 3.13$$

### 3.1.4 Convex sets

A convex set contains every pairwise linear combination of points subject to the condition that the coefficients are real numbers that sum to 1. A set $S$ is convex if the line segment in any two points in $S$ lies in $S$. For instance, for any two points $x_1, x_2 \in S$ and $\theta$ with $0 \leq \theta \leq 1$, it can be written,

$$\theta x_1 + (1 - \theta)x_2 \in S \qquad 3.14$$

A set is convex if each point in the set can be seen by every other point, along a free straight path between them. All affine set is also convex since it contains the complete line between any two different points in it, and consequently, also the line segment between the points. Figure 14 depicts simple convex and non-convex sets in $R^2$.

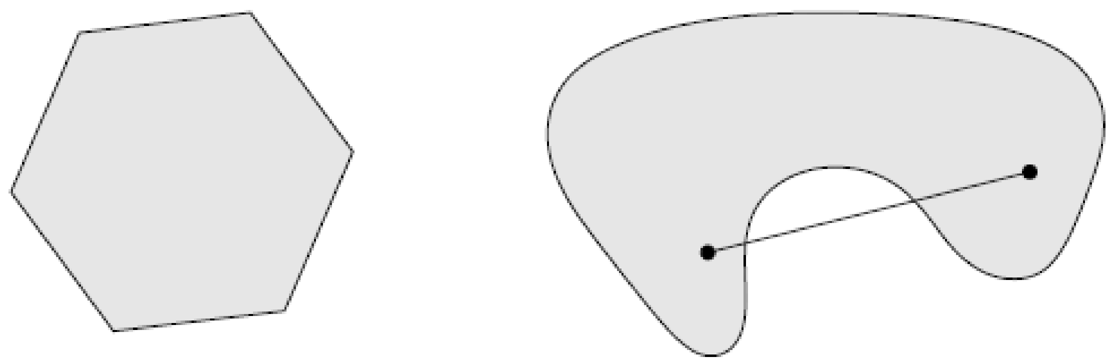

**Figure 14** *Convex set (left) and non-convex set (right)*

As similar to the affine set, if we refer a point of the form $\theta_1 x_1 + \theta_2 x_2 + \cdots + \theta_l x_l$, where $\theta_1 + \theta_2 + \cdots + \theta_l = 1$, and $\theta_i \geq 0, i = 1, \ldots, l$, a convex combination of the points $x_1 \ldots \ldots x_l$. A set is considered to be convex if and only if it comprises all the convex combinations of its points [57].

The convex hull of a set $S$ is the set of all convex combinations of points in $S$:

$$conv\, S = \{\theta_1 x_1 + \theta_2 x_2 + \cdots + \theta_l x_l |\, x_i \in S, \theta_i \geq 0, i = 1, \ldots, l, \theta_1 + \theta_2 + \cdots + \theta_l = 1\} \quad 3.15$$

The convex hull of $S$ is always convex.

## 3.2 Convex Optimization

The standard form of the convex optimization problem can be written as :

$$\text{minimize } f_0(x) \quad 3.16$$

Subject to,

$$g_i(x) \leq 0, \;\; i = 1 \ldots \ldots n. \quad 3.17$$

$$a_i^T x - b_i = 0, \;\; i = 1 \ldots \ldots k. \quad 3.18$$

According to [57], the convex problem should have the following characteristics:

- The objective function has to be convex
- The inequality constraint must be convex and
- The equality constraint has to be affine.

In a convex optimization problem, the aim is to minimize a convex objective function over a convex set.

In this work, two classes of convex problems have been considered: (i) Linear optimization problems and (ii) Second-order cone optimization problems.

The problem is linear if the objective and constraint functions are affine. The general form of a linear optimization problem can be expressed as:

$$\text{minimize } f^T x + d \tag{3.19}$$

Subject to,

$$Hx \leq g \tag{3.20}$$

$$Ax = b \tag{3.21}$$

Where $H \in R^{m\times n}$ and $A \in R^{p\times n}$. It is common to remove the constant from the objective function because it does not affect the optimal or feasible set.

A second-order cone problem can be written in the following way:

$$\text{minimize } f^T x \tag{3.22}$$

Subject to,

$$\|A_i x + b_i\| \leq D_i^T + e_i, \quad i = 1 \ldots \ldots m. \tag{3.23}$$

$$Fx = g \tag{3.24}$$

Where $x \in R^n$ is the optimization variable, $A_i \in R^{n_i\times n}$, and $F \in R^{p\times n}$. The constraint of the following form is called a second-order cone constraint.

$$\|Ax + b\|_2 \leq D^T + e \tag{3.25}$$

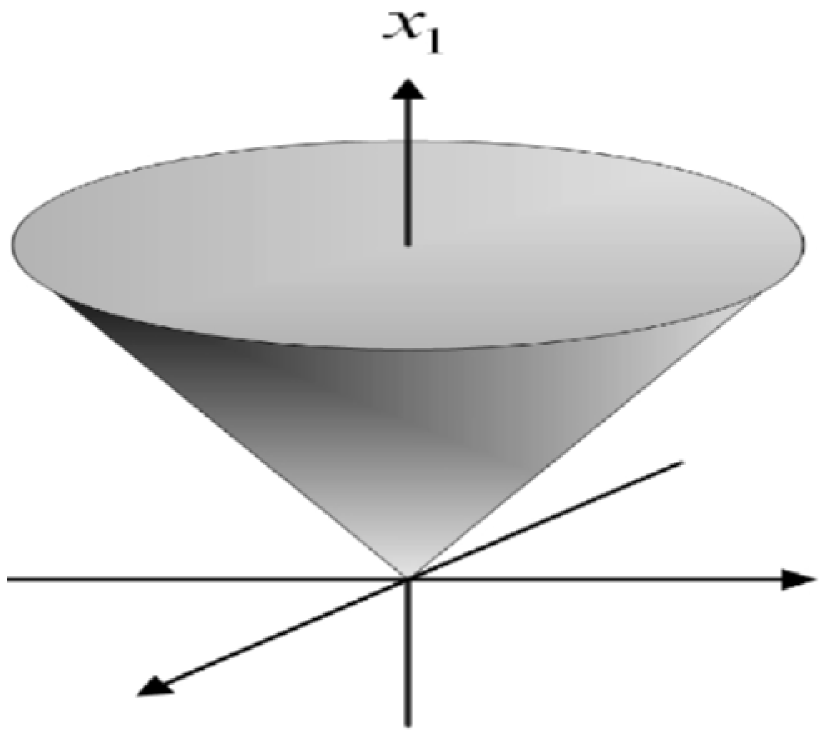


**Figure 15** *Three dimensional second-order cone shape*

## 3.4 Source of non-convexity

Since we are dealing with the power system optimization problem, the sources of non-convexity would be limited to a power system problem. More specifically, from an AC OPF perspective. The primary source of non-convexity is the product of the voltage variables. Also, another source of non-convexity in this work is the investment decision (place of order) that introduces binary variables and integer terms (number of storage).

## 3.5 Techniques for convexification

In the sections below, the convexification techniques to make the non-convex problem tractable have been described.

### 3.5.1 Lift and Project

The lift and project relaxation technique usually used to transform the products of continuous variables. The product of continuous variables in a constraint makes the constraint non-linear. And in order to relax the constraint and make it tractable, lift and project techniques are well exploited.

The key idea in the Lift and Project methods is to try to simulate non-linear programming using linear programming. Since nonlinear constraints are quite powerful: to restrict a variable x to be in {0, 1} it simply adds the quadratic constraint $x(1 - x) \geq 0$. This suggests that nonlinear programming is NP-hard in general. In lift-and-project methods, it introduces the auxiliary variables for the nonlinear terms.

Extra variables $y_{ij} \geq 0$, is introduced with the purpose that $y_{ij}$ signifies the product $x_i x_j$ . This is termed as the lift step, in which it lifts the problem to a higher-dimensional space. The idea is to simply project it to the variables $x_i$ to obtain a solution to the original problem. Provided that, it does not have a way of ensuring $y_{ij} = x_i x_j$ in all solutions of the lifted problem, it still may end up with a relaxed polytope. However, this relaxation can be no worse than the original LP relaxation because of $1 - x_i - x_j + y_{ij} = 0, y_{ij} \geq 0, \Rightarrow x_i + x_j \geq 1$, and any point that is present in new relaxation is in the original one. The lift-and-project relaxation may also be used for any nonlinear terms, such as quadratic terms.

### 3.5.2 Branch and Bound

Branch and bound is an algorithm that commonly used for solving combinatorial optimization problems. These problems are naturally exponential in terms of time complexity and may need exploring all possible arrangements in the worst case. The Branch and Bound algorithm solve these optimization problems reasonably quickly.

In the BB case, the algorithm attempts to avoid searches that are "unusable." Assume that the algorithm can prove that setting $x = 0$ will lead to a value for the optimization quantity of at most $A$ while setting $x = 1$ will lead to a value for this quantity of at least $B$. If $< B$ , then there is no reason even to consider setting $x$ to $0$. The upper bound on $A$ and a lower bound on $B$ permits the algorithm to securely avoid searching a whole amount of the available space: all those cases where $x$ would be set to $0$. This is the power of the method.

### 3.6 Summary

This chapter synthetically recalls the general theory of mathematical optimization. The notion of local and global optima is also described from the capacity of the numerical optimization problems. If the problem is non-convex and non-linear, the resulting outcome often a local optimum. The possible sources of non-convexity have been described. The non-convex problem needs to be convexified to obtain a globally optimum solution. This chapter describes the techniques briefly for convexification, precisely lift and project, and branch and bound.

# Chapter 4

## Optimization under uncertainty

### 4.1 Introduction

Uncertainties are mostly involved in decision-making problems. In general, the energy storage planning in the network is associated with uncertainty from electric loads, solar, and wind power generation. Several factors determine the evolution of each uncertainty. For example, electrical loads are influenced by the level of consumers' activities; the randomness of the solar panel or wind turbine output can be impacted by the radiation of the sun or the speed of the wind and the ambient weather [58].

The traditional paradigm in mathematical programming is to develop a model that accepts that the input data is entirely known and identical to some nominal values. This method, however, does not reflect the influence of data uncertainties on the quality and feasibility of the model output. It is therefore predictable that as the data takes values different from the nominal ones, some constraints may not be maintained, and the optimal solution found using the nominal data may be no longer optimal or even viable. This chapter discusses the approaches that will be adopted during the development of the planning problem of storage, including the robust optimization approach for uncertainty consideration in the model.

#### 4.1.1 Duality theory

The duality theory is very sophisticated and significant in the field of operations research (OR). In the beginning, while this theory has been developed, it was more focused on the linear programming problem. However, it has many applications, especially in areas such as game theory and non-linear optimization problems. The concept of duality theory within linear programming has associated with it a related linear program called its dual. The original problem concerning its dual is termed the primal. In this study, the duality theory has been exploited to reformulate the maximization problem to a minimization one. This situation arises while considering the robust optimization into the deterministic optimal power flow problem.

A general maximization problem can be considered to illustrate the notion of duality theory [59], [60]:

$$\max z = \sum_{j=1}^{l} c_j x_j$$

Subject to,

$$\sum_{j=1}^{l} a_{ij} x_j \le b_i, \;\; i = 1,2, \dots\dots, k \qquad 4.1$$

$$x_j \;\ge 0, \;\; j = 1,2, \dots., l$$

The problem formulated by equation 4.1, considers as a primal problem. The equivalent dual problem of the primal problem can be formulated as:

$$\min v = \sum_{i=1}^{k} b_i y_i$$

Subject to,

$$\sum_{i=1}^{k} a_{ij} y_j \ge c_j, \;\; j = 1,2, \dots\dots, l \qquad 4.2$$

$$y_j \;\ge 0, \;\; i = 1,2, \dots., k$$

As can be seen from the dual problem, equation 4.2, the maximization problem in primal becomes a minimization problem. Furthermore, the constraint with less-than-or-equal-to constraint transformed into a greater-than-or-equal-to constraint. The Table 4-1 illustrates the general transformation rules.

**Table 4-1** *General Transformation rules [59], [60], [61].*

| Primal (min) | Dual (max) | Primal (max) | Dual (min) |
|---|---|---|---|
| $k$ constraints | $k$ variables | $k$ constraints | $k$ variables |
| $l$ variables | $l$ constraints | $l$ variables | $l$ constraints |
| Coefficients of objective function | Right-hand side | Coefficients of objective function | Right-hand side |
| Right-hand side | Coefficients of objective function | Right-hand side | Coefficients of objective function |
| $A$ | $A^T$ | $A$ | $A^T$ |
| Equality constraints | Unrestricted variables | Equality constraints | Unrestricted variables |
| Unrestricted variables | Equality constraints | Unrestricted variables | Equality constraints |
| Inequality constraints $\geq$ $(\leq)$ | Variables $\geq 0$ $(\leq 0)$ | Inequality constraints $\leq$ $(\geq)$ | Variables $\geq 0$ $(\leq 0)$ |
| Variables $\geq 0$ $(\leq 0)$ | Inequality constraints $\leq$ $(\geq)$ | Variables $\leq 0$ $(\geq 0)$ | Inequality constraints $\leq$ $(\geq)$ |

## 4.2 Load, PV and Wind variability

A large number of problems in power system planning require that decisions be made in the presence of uncertainties. Uncertainties, for example, govern equipment failures, electricity demand, and renewable generation, etc. These uncertainty sources can be categorized into two types. The first is configuration uncertainty, which relates to the transmission line, generator, or other equipment failures, in other words, contingencies. The second category is input uncertainty that relates to the limited knowledge of future values of such parameters as electricity demand or generation. Probability distributions and scenario techniques are typical representations of uncertainty. The selection of uncertainty representation depends on the goal of the analysis, the level of underlying uncertainty, and knowledge of the underlying uncertainty [62], [63]. In this work, to have a comprehensive study, uncertainty source, i.e., uncertainty in load, solar, and wind generation, will be studied. Considering uncertainties in power system planning is becoming more critical as renewable energy technologies, especially wind and solar energy, play an increasing role in the portfolio mix of electricity generation. A crucial difficulty in optimization under uncertainty is to deal with an uncertainty space, which is usually huge and might lead to extensive and computationally intractable optimization models. Consequently, proper techniques for modeling random variables have to be applied.

There has been a multiplicity of methodologies developed to deal with the complexity of optimization problems under uncertainty [64]–[72]. Among the references, [70] and [71] are using a robust optimization approach. This chapter discusses the method that will be adopted in the planning problems with ESSs in the next chapter. The theory and methodology of these approaches will be presented.

### 4.2.1 Load Variability

Power systems are planned in such a way that it can manage variable electricity consumption, the load. In Figure 16, the hourly load profile for the year 2010 of four Nordic countries has been presented [91]. In Sweden, Norway, and Finland, the load is noticeably temperature-dependent. Loads during winter are higher than in summer, and due to electrical heating depends on the intensity of cold weather. Unlike wind and solar, load variations are comparative less arbitrary. However, an electric load can change suddenly; for instance, failure of a production line in an industry could impact on the overall grid. Therefore, it is essential to incorporate the load variability in the power system operation and planning models. Short-Term variations of load (order of seconds to hours) are generally small. In the longer-term (order of days to years), changes in load tend to be more predictable. The load follows predictable daily, weekly (weekdays and weekends), and seasonal patterns. For example, there is a clear diurnal pattern of morning hour up variations, late afternoon variations, and evening down differences.

The seasonal change of daylight and changes in the residential use of electricity as the sunlight varies with the season can be observed in the load profiles in different seasons, which results in seasonal variations of the load. The load in each period can be modeled by superimposing a random noise to the mean load, which has been the primary load modeling method in power system analysis. For the whole period considered, the usual practice in modeling the variability of the load is to use a normal distribution.

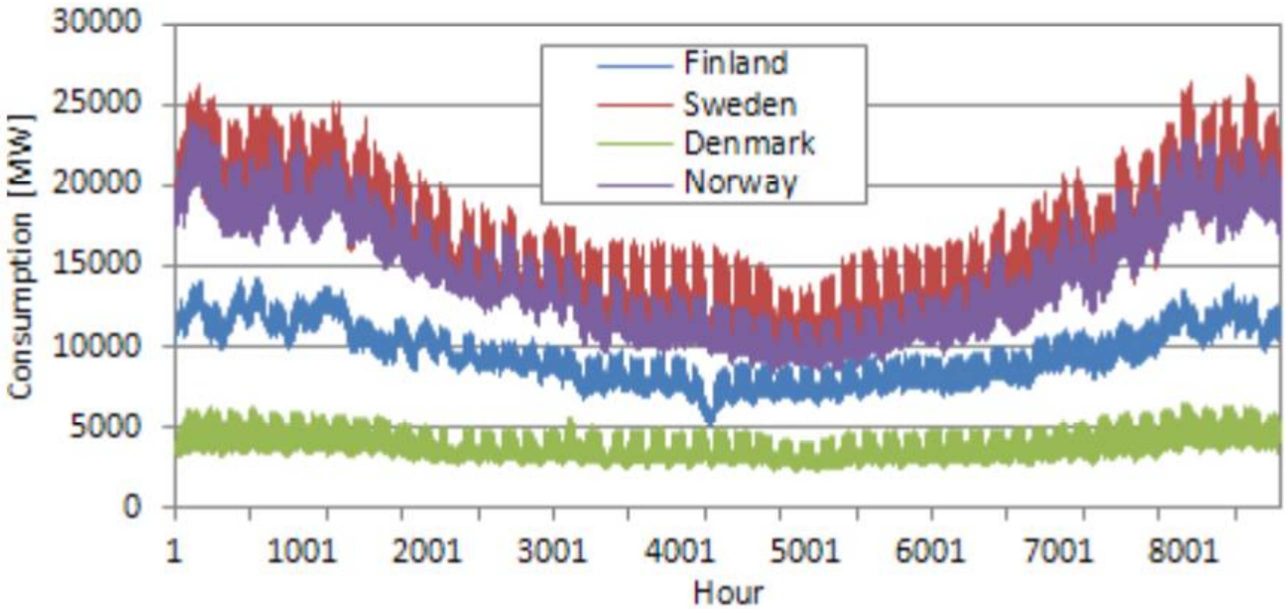


**Figure 16** *Hourly time series of electricity consumption in the Nordic countries in 2010 [73].*

### 4.2.2 Wind variability

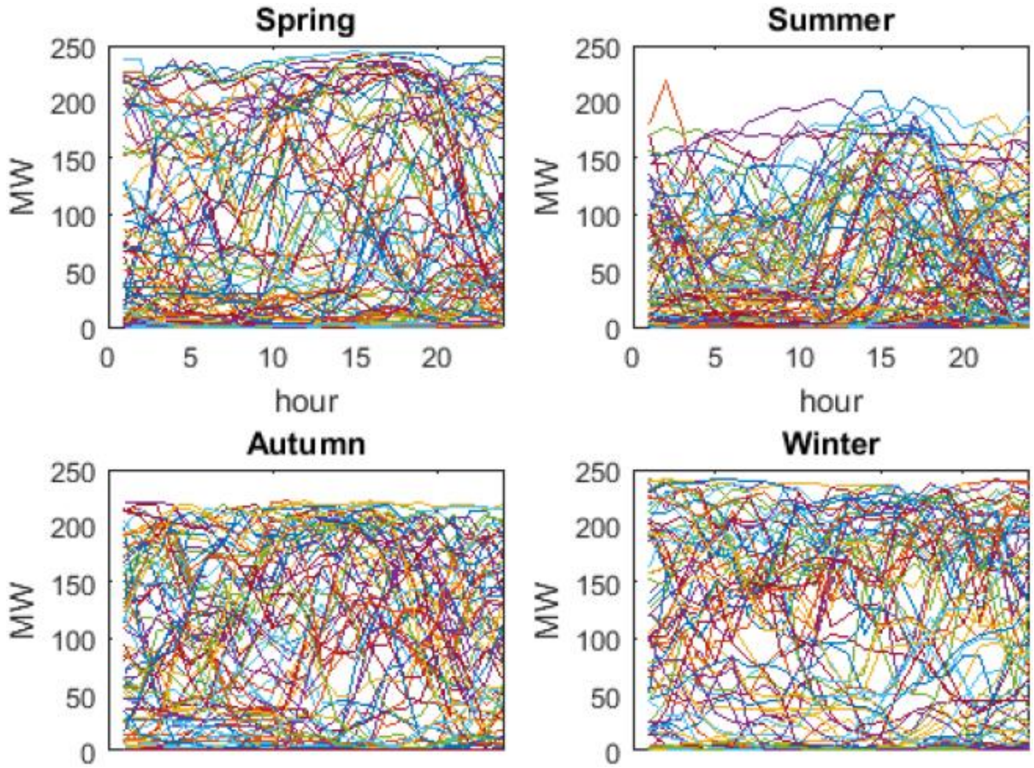


**Figure 17 Daily wind profiles of four seasons [74].**

In Figure 17, the daily wind profiles in four seasons of a year are presented [74]. The key variance is that load variations are better understood than wind or solar variations. As can be observed, wind power output is utterly unpredictable from hour to an hour and from day to day, which may vary between zero and to the rated value for any period. The output of wind power could be very high during the night and low during daytime or vice versa. There is no clear pattern of the daily, monthly, weekly, or seasonal wind power. With this high variability of wind power, information from the daily mean value or normal distribution is insufficient to represent its stochasticity [75],[76].

### 4.2.3 Solar Variability

Another renewable resource, solar energy, is weather dependent. The intermittency of PV power can introduce serious challenges in grid operation/management when large PV plants are integrated with the grid. In Figure 18, the PV output of different patterns such as clear sky, overcast, moderate variability, mild and high variabilities have been depicted. As can be seen, the PV output varies with a different pattern. Usually, Gaussian distribution. The power output of PV models by a generic distribution function such as beta, gamma, or Weibull [77], however, the modeling of PV through probability density function often leads to an inaccurate decision [74]. However, if enough information is available, it is possible to model the uncertain parameters with a known probability density function.

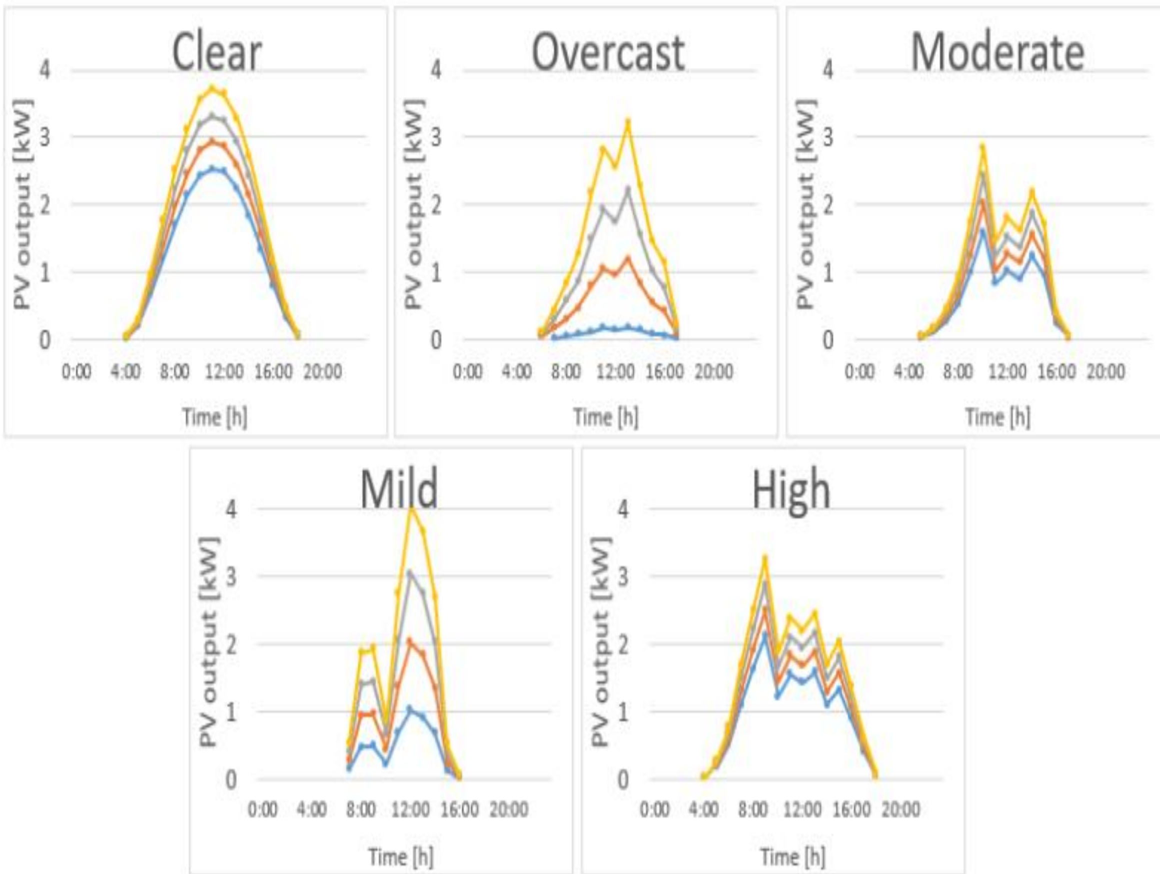


**Figure 18** *PV output for different variability patterns [75]*

Based on the above discussion, it is well understood that the prediction of load profiles and the ou very challenging. Moreover, without considering the intermittent nature of weather-dependent sources could influence power system operation and planning decision. In the following sections, a different approach has been described to deal with uncertain parameters in the optimization problem.

## 4.3 Stochastic Programming

Dealing with uncertainty in an optimization problem necessitates some knowledge about the uncertainty. However, there is often insufficient information about the uncertain parameters; hence, many methods have been developed to model the uncertainty. In stochastic programming, uncertain parameters are represented as random variables with an assumption that their probability distributions can be known or estimated. This programming approach usually leads to specific procedures that take into account the probabilistic aspects.

The field of stochastic programming is concerned with optimization under uncertainty. As the name suggests, its modeling approaches and algorithmic techniques are inherited from mathematical programming, which separates it from the related fields of decision analysis, stochastic control theory, and Markov decision processes. Although mathematical programming is highly recognized and widely used, uncertainty can only be handled by sensitivity or parametric analysis. Stochastic programming overcomes this drawback by including uncertainty explicitly into mathematical programming. Essentially, a stochastic program is a mathematical program in which random variables represent uncertain data, and an appropriate optimization criterion is selected [78].

George Dantzig first introduced Stochastic Programming (SP) in the 1950s. From then, significant development has been observed in developing algorithms for solving them. As a result, SP has become an optimization method in decision making, incorporating uncertainty in large-scale problems. In probabilistic approaches such as cumulant or point estimate method, a deterministic formulation is reserved, and the probability distributions represent uncertain system inputs (e.g., load and generation). Moreover, its optimal solution, i.e., the values of control variables is not influenced by the randomness of uncertain inputs, but they determine only the probability distribution functions of control variables.

In contrast, stochastic programming methods deal with not only uncertain system inputs as random distributions but also form the stochastic formulation for the problem. That is, either the objective function or constraints in the optimization model are described as probability equations or inequalities. The randomness of uncertain system inputs directly influences the optimization result during the solution of stochastic problems [79]. The recourse model for stochastic programing has been first introduced in [80]. The concept of recourse models is taking some decisions after the uncertainty is known. In this case, uncertain parameters are expressed as probability density functions. The decision taken by recourse models without having the complete information of the unknown parameters is called first-stage decisions. After full information is known on the realization of the arbitrary events, recourse actions are taken in later stages.

A simple formulation of the recourse model is the two-stage stochastic optimization model. In the two-stage stochastic optimization model, the set of decisions is separated into two categories. The decision variables of the first stage or for taking here-and-now decision are the variables that have to be decided before the realization of uncertain variables, and when the uncertain parameters are known, further actions can be performed by choosing, at a specific cost, that defines the values of second-stage or wait-and-see variables. These decisions related to the second-stage can be considered as corrective measures against any infeasibility risen because of a particular realization of uncertain parameters. Due to uncertainty, the second-stage cost is a random variable. The goal of a two-stage model is to identify a first-stage decision that is well- put against all probable observations of arbitrary parameters. An optimal solution inclines of having the characteristic that the first-stage decision leaves the second-stage decision in a way to exploit useful outcomes of random events without unnecessary susceptibility to unfavorable outcomes.

### 4.3.1 Two-stage linear stochastic programming

The general form of two-stage linear stochastic programming problem has the following form:

$$\min_{x} f(x) + \mathbb{E}[\Theta(x,\xi)]$$

Subject to, 4.3

$$Ax = b\;, x \geq 0$$

Here, $f(x)$ is the objective function for the first-stage decision, and $\Theta(x,\xi)$ is the optimal value of the second stage problem. The second-stage problem can be written as:

$$\Theta(x,\xi) = \min_y q^T y$$

Subject to, 4.4

$$Bx + Cy = g\ , y \geq 0$$

Here, $x$ is a vector of first-stage decision variables, $y$ is a vector of second-stage decision variables, $\xi = (q, g, B, C)$ are the data of the second-stage problem. The expectation operator $\mathbb{E}$ has been considered at the first-stage problem concerning the probability distributions of the uncertain or random parameters $\xi$. The decision of the first-stage decisions $x$ should be made before the random parameter $\xi$ is known. Therefore, it should be free from the random parameter. On the other hand, the second-stage decision variable $y$ is made after the realization of the random parameter [81]-[82].

### 4.3.2 Gaussian Distribution

One of the most common probability distributions often used in representing the random variables is Gaussian distribution, also known as the Normal distribution. The probability density function of a gaussian distribution for a random variable $\tilde{a}$ is [83]:

$$\mathrm{f}(x) = \frac{1}{\sigma\sqrt{(2\pi)}} e^{\frac{(a-\mu)^2}{2\sigma^2}} \qquad 4.5$$

$$-\infty \leq \mathrm{a} \leq \infty \qquad 4.6$$

$$\sigma \geq 0 \qquad 4.7$$

where, $\mu$ is the mean value of the random variable $\tilde{a}$, $\sigma$ is the standard deviation and $\sigma^2$ is the variance of the random variable.

The typical shape of a Gaussian probability density function is shown in Figure 19. This curve, also known as the bell curve.

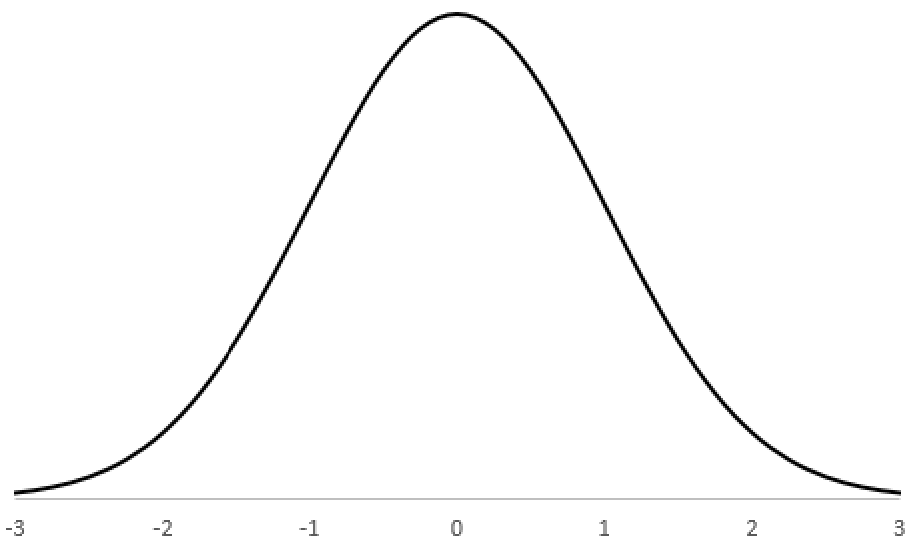


**Figure 19** *Probability density function of a Gaussian distribution*

### 4.3.3 Weibull Distribution

Another commonly used probability distribution often used to represent the approximation of wind speed distribution is the Weibull distribution. Figure 20 shows the graphical representation of the probability density function of the Weibull distribution. The formula for the probability density function of Weibull distribution is [84]:

$$\mathrm{f}(x) = \frac{\gamma}{\alpha}\left(\frac{x-\alpha}{\alpha}\right)^{(\gamma-1)} e^{\frac{(x-\mu)^{\gamma}}{\alpha}} \qquad 4.8$$

where, $\gamma$ represents the shape parameter, $\mu$ is the location parameter, and $\alpha$ is the scale parameter.

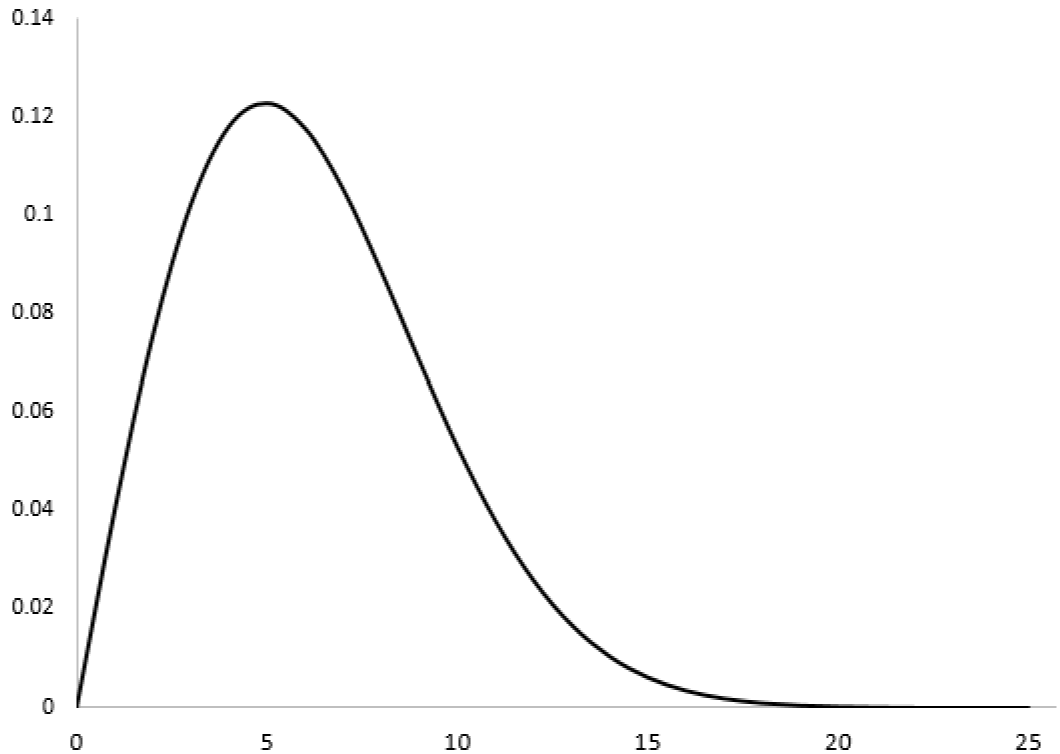


**Figure 20** *Probability density function of a Weibull distribution*

## 4.4 Robust Optimization

Robust optimization can be considered a complementary tool to stochastic optimization in order to incorporate uncertain parameters in the optimization problem. Unlike stochastic optimization, robust optimization does not require the have the probability density function of the uncertain parameters; instead, it needs to define the uncertainty set.

This concept of robust optimization is not new. It was first introduced in 1973 by Soyster [85]. However, this approach to deal with uncertainty caught attention in the late 90s [86]. Since then, several studies have been performed considering robust optimization. One of the relevant studies that applied in this thesis work has been presented in [87]. The authors studied the robust convex optimization problems with polyhedral and ellipsoidal uncertainty sets. However, the application of robust optimization has been extended to semidefinite and least-square problems [88],[89]. The budgeted uncertainty set that has been adopted in this study has been first introduced in [90]. The study demonstrated that using budgeted uncertainty sets can reduce the “price” of robustness. This concept is very relevant, while the problem deals with the planning of the power system where the budget is limited. A comprehensive survey has been performed considering discrete, and interval uncertainty set is [91]. The impact of uncertainty set in the solution and the methodology of reformulation to find the robust counterpart has been studied in [92]. It has been observed that the box uncertainty set often produces very conservative results, and the ellipsoidal uncertainty set can lead to a quadratically constraint program (QCP) of linear programming (LP) problem while reformulating the robust counterpart, that can be often intractable [93]. Keeping this information into consideration, in this study, budgeted or polyhedral uncertainty set has been adopted to solve the robust counterpart efficiently.

### 4.4.1 Application of robust optimization in power system

It has been discussed in the previous chapters that the importance of considering uncertainty in the power system operation and planning is immense. Stochastic optimization has been used to incorporate the uncertainty in the power system model. In order to consider the load variability, multistage stochastic optimization has been used in several studies [94]-[96]. The application also extends to deregulated electricity markets [97]. Due to the fact that having an accurate probability distribution of uncertain parameters is very difficult, and it could lead to a sub-optimal solution, the popularity of using robust optimization has increased.

A two-stage robust optimization technique is used for the unit commitment problem [98]. It considers data uncertainty and attempts to obtain an optimal solution considering the worst-case uncertainty realization. Therefore it uses a box uncertainty set that only considers the extreme points of the feasible space. The solution of the robust optimization problem is guaranteed optimal for a defined uncertainty set [99]. A new mechanism based on robust optimization has been demonstrated in [100],[101]. The study showed the use of robust optimization helped in day-ahead dispatching and determining the reserve with high penetration of renewable energies. A dynamic DC-OPF has been formulated based on robust optimization [102]. The author proposed an affinely adjustable robust OPF that the base-point generation is determined to serve the forecast load that is not met by renewables.

Moreover, it demonstrated that the generation control through participation factors ensures a feasible solution for all realizations of renewables output within a predefined uncertainty set. This OPF formulation has been extended to include the storage on the transmission network, and the problem became mixed-integer linear programming (MILP) problem [103]. The result justified that employing robust optimization helped to minimize the storage investment cost. However, the studies considered a DC-OPF that often produces partial results. Moreover, the adopted box uncertainty sets, which is very conservative and might not be unacceptable for an efficient decision-making process. The conservativeness of the solution can be modified by altering the uncertainty sets [90], based on the level of uncertainty is desired to consider. In [104], a robust unit commitment is formulated considering the security criterion. The problem is then reformulated into a single-level problem using duality theory. In [105], the two-stage robust unit commitment problem under uncertainty from wind power is modeled. To solve the two-stage unit commitment problem, Bender's decomposition technique has been used. A similar model is used in [106], where demand response and wind power considered uncertain parameters. A robust minimax regret model is proposed in [107] to solve the unit commitment problem under uncertainty. The proposed model minimizes the maximum regret of the day-ahead decision from the actual realization of the uncertain real-time wind power generation. A robust DC OPF is introduced in [108] using the conditional value-at-risk concept to alleviate the risk of wind power in the system. As an appropriate investigation of distribution systems necessitates the modeling of an AC OPF, [109] suggests a robust AC OPF where the second-order cone programming (SOCP) used to relax the AC power flow constraints. The DSO trends have been followed in [110], which proposed a methodology for active grid management applying robust optimization is applied to incorporate the spatial-temporal uncertainty. The proposed technique involves the use of a dynamic AC-OPF, guaranteeing a consistent solution for the DSO. Wind and PV uncertainty is developed based on spatial-temporal trajectories, and a convex hull method to create the uncertainty sets for the model is used.

An autonomous microgrid planning technique has been proposed in [111], since this kind of planning is non-convex, this study suggests SOCP relaxation. The uncertain parameters are load and generation. A corrective-preventive approach that is more like a heuristic technique has been used to solve the robust problem. The application of robust optimization also attracts in ensuring the reliability in operation of energy-efficient buildings [112], which considers the electric and thermal loads as the sources of uncertainty.

### 4.4.2 General Formulation

The data entered in the optimization problem usually are not known. This could be due to prediction error, implementation errors, or any measurement errors. The minimax criterion that helps to find the comprehensive robust solution refers: "The robust decision is that for which the lowest (highest) level of benefit (cost) taken across all possible future input data scenarios is as high (low) as possible [113]". However, this approach often suggests a conservative solution, but with proper modeling of uncertainty set can overcome this conservativeness. In the next section, two popular methods have discussed this description, however, it should not be considered as an exhaustive analysis of the robust optimization topic.

#### *4.4.2.1 Soyster Approach*

The first introduction of the robust optimization concept presented by Soyster. The general optimization problem formulation is as follows [114]:

$$\min_x c^T x$$

where, 4.9

$$Ax \leq b$$
$$l \leq x \leq u$$

In the above formulation, $c^T$ is the transpose of vector $c$, $x$ is the solution vector $l$, and $u$ are the upper and lower bounds of the solution vector $x$. The dimension of the vectors is m, and A is a $m * n$ matrix.

The robust formulation of the Soyster approach can be described as follows:

$$\min_x c^T x$$

Subject to, 4.10

$$\sum_j a_{ij}x_j + \sum_{j\in J_i} \widehat{a_{ij}} y_j \le b_i \qquad \forall i$$

$$-y_j \le x_j \le y_j \qquad \forall i$$

$$l \le x \le u$$

$$y \ge 0$$

Here, this approach considers column-wise uncertainty since $y_j$ is one for each column $j$. The second term of the new inequality constraint indicates uncertainty. $y_j$ has to be chosen such a way that for all $i$, the condition $-y_j \le x_j \le y_j$ holds. This approach often considers as a conservative approach because the obtained solution is valid, regardless the value in the given range the coefficients in the matrix A take, but in many applications, it can be considered as a sub-optimum which, however, would not be valid for any possible combination of parameters [114].

### *4.4.2.2 Ben-Tal's approach*

In order to avoid the conservatism, Ben-Tal's proposed following formulation of the robust form [115]:

$$\left\{\min_x [c^T x + d: Ax \ \le b]: (c, d, A, b) \in \mathcal{U}\right\} \tag{4.11}$$

where, $A \in \mathbb{R}^{m*n}$ and $b \in \mathbb{R}^m$ are the coefficient of the constraints, $c \in \mathbb{R}^n$ and $d \in \mathbb{R}$ are the coefficient of the objective function. Here $n$ and $m$ are the numbers of decision variables and the number of constraints, respectively. The data for input $(c, d, A, b)$ are varied in the uncertainty set $\mathcal{U}$.

The input data can be represented as the sum of the nominal values and the associated perturbation. That means, the product of the matrix of basic moves (indicated by $s$) from the nominal values (mentioned by $n$) and the perturbation vector $\xi$. The basic shift and nominal or rated values are defined in [115]:

$$\mathcal{U} = \left\{\begin{bmatrix} c^T & d \\ A & b \end{bmatrix} = \begin{bmatrix} c_n^T & d_n \\ A_n & b_n \end{bmatrix} + \begin{bmatrix} c_s^T & d_s \\ A_s & b_s \end{bmatrix} : \xi \in Z \in R^L\right\} \tag{4.12}$$

As it can be understood from the above formulation that, Ben-Tal's approach is no longer column-wise, but a matrix specifies the uncertainty, that is more comprehensive and flexible.

As it was mentioned earlier, the solution largely depends on how the uncertainty set is being defined. The next section briefly describes the different uncertainty sets.

### 4.4.3 Definition of Uncertainty Set

The application of robust optimization often prefers to have a trade-off between robustness against each physical realization of the uncertain parameter and the size of the uncertainty set.

The worst-case approach mainly deals with the box uncertainty set that contains the full range of realizations for each element of $\xi$ is the most robust choice but the most conservative as well. It guarantees that the constraints are never violated [93].

The box uncertainty set can be defined as:

$$U = \{\xi : \|\xi\|_\infty \leq 1\} \tag{4.13}$$

Where the component in the perturbation vector $\xi \in Z \in R^L$ is considered to be varying in the interval between -1 to +1.

Therefore the box uncertainty set provides a pessimistic solution. A better choice would be using a polyhedral uncertainty set. This set can be expressed as follows:

$$U = \{\xi \in \mathbb{R}^L : \|\xi_\infty\| \leq \Gamma\} \tag{4.14}$$

where the real vector of dimension L $\xi$ is the only knowledge available, namely perturbation vector, that varies inside a given interval. $\|\xi_\infty\|$ defines the continuous uniform norm of $\xi$ and $\Gamma$ is the measure of the uncertainty.

This type of uncertainty set also called a budgeted uncertainty set since the level of robustness can be adjusted with $\Gamma$. It is important to properly select the budget of uncertainty $\Gamma$ in order to have a reasonable solution maintaining sufficient robustness of the model. In this work, the polyhedral uncertainty set has been adopted since it produces a sufficiently robust solution if the budget of uncertainty is chosen based on the uncertainty level one wants to accept. As $\Gamma$ increases, more uncertain the considered scenario, and less risky becomes the solution. In this study, the polyhedral uncertainty set has been adopted since it produces a comprehensive view with different levels of uncertainty.

Another commonly used uncertainty set is the ellipsoidal uncertainty set. And the general formulation is:

$$U = \{\xi \in \mathbb{R}^L: \|\xi_\infty\| \leq \Omega\} \qquad 4.15$$

Though the ellipsoidal uncertainty set leads to better objective value, however, it gives rise to a CQP for an uncertain LP, therefore, more intractable from a computational point of view. The three commonly used uncertainty sets have been graphically represented in Figure 21.

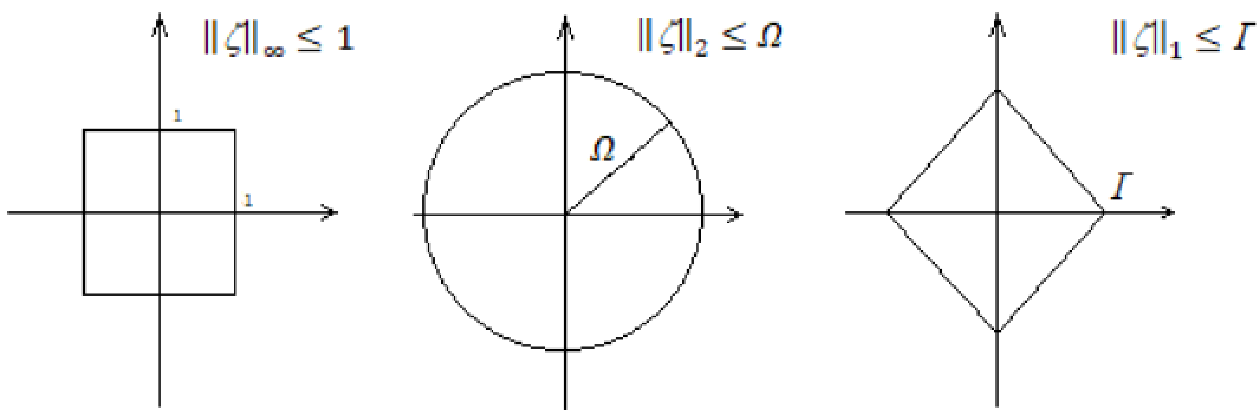


**Figure 21** *Graphical representation of uncertainty sets [59]*

## 4.5 Solution methodology

Robust optimization problem usually contains an infinite number of constraints due to imposing worst-case formulation and hard constraints. Therefore, it is often computationally intractable in its current form. Generally, there are two approaches to deal with this kind of situation [112]: (i) Robust reformulation technique or Analytical approach and (ii) Adversarial approach. In this thesis work, a systematic robust reformulation approach has been adopted.

## 4.6 Analytical approach

After selecting the uncertainty set, the next step is to reformulate the robust optimization model to make it tractable. The robust reformulation approach consists of three systematic steps. Below each step has been discussed for a polyhedral uncertainty set.

### 4.6.1 Worst Case Reformulation

First of all, it is necessary to rewrite all the constraints containing elements affected by uncertainty in such a way that the sum of deviations is maximized in order to account for the worst possible case. This is done by isolating the shift of the variable from its nominal value and determining the budget of uncertainty $\Gamma$ that limits the total deviation.

For a worst-case analysis, when taking into account the uncertainty, we consider the following problem:

$$\max cx$$

Subject to

$$\sum_{j=1}^{n} a_{ij}x_j + max \sum_{j \in J_i} \widetilde{a_{ij}}\, \xi_{ij} x_j \leq b_j \qquad 4.15$$

$$l \leq x \leq u$$

For the *i-th* constraint, the auxiliary problem can be formulated as follows:

$$max \sum_{j \epsilon J_i} \widetilde{a_{ij}}\, \xi_{ij} |x_j|$$

Subject to

$$\sum_{j \epsilon J_i} |\xi_{ij}| \leq \Gamma_i \qquad 4.16$$

$$\left|\xi_{ij}\right| \leq 1 \qquad \forall_i, j\epsilon J_i$$

### 4.6.2 Forming the Dual

To make the problem tractable, the dual of the previous inner maximization problem is formed. This technique can be exploited because the optimal values of the two objective functions correspond due to the strong duality theorem:

$$\min z_i\,\Gamma_i + \sum_{j\epsilon J_i} p_{ij}$$

Subject to

$$z_i + p_{ij} \geq \widetilde{a_{ij}} y_i \qquad \forall_i, j\epsilon J_i \qquad 4.17$$

$$\left|x_j\right| \leq y_j$$

$$z_i, p_{ij}, y_j \geq 0$$

Where $z_i, p_{ij}$ are shifts from the nominal values.

### 4.6.3 Robust reformulation

Finally, the new variables and the new constraints have to be added to the original model. Incorporating model into the original problem, the robust linear counterpart is formulated as:

$$\min cx$$

Subject to

$$\sum_{j=1}^{n} a_{ij} x_j + z_i \Gamma_i + \sum_{j\epsilon J_i} p_{ij} \leq b_i$$

$$l_j \leq x_j \leq u_j \qquad 4.18$$

$$z_i + p_{ij} \geq \widetilde{a_{ij}} y_j, V_i, j \epsilon J_i$$

$$-y_j \leq x_j \leq y_j$$

$$z_i, p_{ij}, y_j \geq 0$$

The above model is immune of uncertainty and tractable.

## 4.7 Adversarial approach

If a tractable robust reformulation technique cannot model the robust counterpart, an adversarial approach can use to solve the problem. This approach first considers a finite set of scenarios for the uncertain parameter. In the beginning, the finite set of scenarios only considers the nominal scenario. And then, the robust optimization problem, which has a limited number of constraints, is solved. If the solution is robust feasible, then the robust optimal solution is obtained. Otherwise, it needs to find the scenario that is making the last found solution infeasible. In other words, searching for the scenario of increasing the infeasibility. When that scenario found, it has to be added in the finite set of scenarios and solve the robust optimization problem. This approach can also be termed as a heuristic approach [116].

## 4.8 Summary

This chapter provides a concise theoretical background of different approaches to deal with uncertainty in the optimization problem. The methods are stochastic optimization and robust optimization. Generally, stochastic optimization requires to have a probability density function of uncertain parameters. On the other hand, the robust optimization technique only needs information on the uncertainty set, which basically the bounds or the limits that represent the deviation from the nominal values. The different types of uncertainty sets have been defined in this chapter. The solution techniques for robust optimization are mainly two: Robust reformulation and adversarial approach. The robust reformulation approach that has been adopted in this thesis has been described. The efficient reformulation of robust optimization problem becomes tractable that can be solved using off-the-shelf solvers.

# Chapter 5

## Deterministic Optimal Power Flow (OPF) formulation of energy storage planning

### 5.1 Introduction

In 1962, Carpentier was first formulated the OPF problem. And that has turned into a major method for security and economic analysis in support of power system operation and control. An OPF problem finds the optimal solution to an objective function subject to the power flow constraints and other operational constraints such as generator minimum and maximum output constraints, transmission stability and voltage constraints, and limits on switching mechanical equipment. There are a number of OPF formulations with different constraints, objective functions, and solution methods. Formulations that use the exact AC power flow equations are known as AC OPF. Simpler versions that assume all voltage magnitudes are fixed and all voltage angles are close to zero are known as DC OPF. DC stands for direct current, but it might confuse: DC OPF is a linearized form of a full AC OPF, not a power flow solution for a direct current network.

OPF algorithms are effective and efficient at investigating the active distribution networks for operation and planning purposes. The two main problem resolution approaches to solve the high-dimensional, and non-convex problems include linear convex relaxation of power flow constraints and heuristic techniques. A heuristic two-step process with a master and a sub-problem is proposed in [117] for storage siting and sizing problems. This approach first adopts a heuristic algorithm to solve the placement and sizing problem of storage. And then, a multi-period AC OPF with multi-objective function takes into account network parameters such as voltage, losses in the network, and energy costs. Another study uses particle swarm optimization for a comprehensive sizing and placement algorithm [118]. An alternative heuristic method, an artificial bee colony, was used to find the optimal place and size of the storage system [119]. A heuristic approach has been adopted for a multi-objective problem considering both distribution and transmission networks [120]. It should be mentioned that the heuristic algorithms are computationally intense and are not guaranteed to return a globally optimal solution [121]. A complete DG portfolio sizing and siting problem have been solved using a mixed-integer linear programming approach [122]. However, the mixed-integer method uses a DC OPF, and the calculation time is high, and scalability to large network sizes has not been addressed.

Convex relaxations of the power flow equations reduce the high computational burden and ensure a global optimum. The relaxation of the power flow constraints into a second-order cone has already been theoretically explained and detailed mathematically [123]. An impedance model was adopted to develop the optimal placement and sizing algorithm [124]. Optimal siting and sizing of storages utilizing a linearized DC power flow for transmission planning with a consideration of maximum investment cost are presented in [125]. However, this DC linearization is not accurate for the high R/X ratio in the LV distribution networks that suggest electrical losses that are non-linear. Though few, the use of an AC OPF for optimal placement [126] or optimal sizing [127] is also found in the literature. In [128] it explores a two-step procedure to size and finding an optimal location for storage using a relaxed power flow constraint.

Nevertheless, this sizing procedure estimates the power and energy imbalances at PV nodes and sizes the battery systems to lessen these mismatches. Therefore, this methodology sizes the battery systems to reduce PV injection when power quality becomes an issue. The method for sizing the storage does not compare the cost with curtailment cost. The algorithm also does not study the possible benefits of storages participating in an electricity market. A SOCP OPF algorithm is then exploited in the second step to place the size battery systems.

## 5.2 Deterministic AC OPF model

For the sake of better understanding, this section will briefly describe the process of convexification that has been adopted in this study. As mentioned earlier, a second-order-cone relaxation has been used in this study to relax the AC OPF. In this study, the convex dist-flow relaxation has been extended to incorporate the binary variables for the storage placement problem. The SOC and CDF relaxations are considered to be equivalent [129].

In this section, the fundamental power flow equations are derived. A power network is comprised of a variety of components such as generators, lines, buses, and loads. The network can be represented as a graph (B, L), where B represents the set of buses, and L represents the set of lines [130].

The AC power flow equations are developed on complex quantities for current I, voltage V, admittance Y, and apparent power S, which are linked by the physical properties of Kirchhoff's Current Law (KCL),

$$I_i^g - I_i^d = \sum_{(i,j)\in L} I_{ij} \tag{5.1}$$

According to Ohm's law

$$I_{ij} = Y_{ij}\left(V_i - V_j\right) \tag{5.2}$$

and the definition of AC power,

$$S_{ij} = V_i I_{ij}^* \tag{5.3}$$

Uniting these three properties yields the AC power flow equations,

$$S_i^g - S_i^d = \sum_{(i,j)\in L} S_{ij} \quad \forall i \in N \tag{5.4}$$

$$S_{ij} = Y_{ij}^* |V_i|^2 - Y_{ij}^* V_i V_j^*, \quad (i,j) \in L \tag{5.5}$$

The above equations are nonlinear and non-convex that define the power flow in the network. And the primary source of nonconvexity is the product of voltage variables, $V_i V_j^*$, and it is also an NP-hard problem.

The general properties of AC power flow can be represented utilizing the equations 5.1 – 5.4.

The absolute square of Ohm's law is,

$$I_{ij} I_{ij}^* = \left(Y_{ij} V_i - Y_{ij} V_j\right)\left(Y_{ij}^* V_i^* - Y_{ij}^* V_j^*\right) \tag{5.6}$$

$$\left|I_{ij}\right|^2 = \left|Y_{ij}\right|^2(|V_i|^2 - V_iV_j^* - V_i^*V_j + \left|V_j\right|^2) \quad 5.7$$

The absolute square of AC power,

$$S_{ij}S_{ij}^* = \left(V_iI_{ij}^*\right) \ \ \left(V_i^*I_{ij}\right) \quad 5.8$$

$$\left|S_{ij}\right|^2 = |V_i|^2\left|I_{ij}\right|^2 \quad 5.9$$

Absolute square of voltage products

$$\left(V_iV_j^*\right)\left(V_iV_j^*\right)^* = \left(V_iV_j^*\right)(V_jV_i^*) \quad 5.10$$

$$\left|V_iV_j^*\right|^2 = |V_i|^2\left|V_j\right|^2 \quad 5.11$$

To calculate the line loss, it can be written the power flow equation as follows,

$$S_{ij} + S_{ji} = Y_{ij}^*(|V_i|^2 - V_iV_j^* - V_jV_i^* + \left|V_j\right|^2) \quad 5.12$$

Since the above formulation is nonconvex, to solve the formulation efficiently, it needs to convexify the non-convex term. Specifically, in this study, second-order cone relaxation has been derived.

SOC relaxation utilizes two fundamental intuitions. First, it uses the lift and project technique. That describes as lifting the product of voltage variables $V_iV_j^*$ into a higher dimensional space or namely W-space. Therefore the term becomes,

$$W_i = |V_i|^2 \quad i \in B \quad 5.13$$

$$W_{ij} = V_iV_j^* \quad \forall(i,j) \in L \quad 5.14$$

The above formulation is convex. However, this relaxation in W-space can strengthen by taking the absolute square of voltage products property,

$$\left|W_{ij}\right|^2 = W_iW_j \quad \forall(i,j) \in L \quad 5.15$$

$$\left|W_{ij}\right|^2 \leq W_iW_j \quad \forall(i,j) \in L \quad 5.16$$

The above equation is a convex second-order cone constraint, that can be solved using off-the-shelf solvers.

### 5.2.1 Power flow formulation

Based on the above devised second-order cone programming relaxation, in this section, the power flow formulation has been presented. Due to the better convergence characteristics, in this study, the branch flow model (BFM) has been used [131].

The active and reactive power flows in the proposed OPF problem is formulated as in equation (5.17) and (5.18).

$$P_n^g(t) + P_n^{RES}(t) - P_n^{RESc}(t) + P_n^{CHP}(t) - P_n^{CHPc}(t) - PD_n(t) + P_n^{PLS}(t) - P_n^c(t) + P_n^d(t) - \sum_{m\epsilon\theta_n} R_{mn} \cdot I_{mn}^2 = \sum_{m\epsilon\theta_n} P_{mn}(t) \quad 5.17$$

$$Q_n^g(t) + Q_n^{RES}(t) - Q_n^{RESc}(t) + Q_n^{CHP}(t) - Q_n^{CHPc}(t) - QD_n(t) - \sum_{m\epsilon\theta_n} X_{mn} \cdot I_{mn}^2 = \sum_{m\epsilon\theta_n} Q_{mn} \quad 5.18$$

Where $(P_n^{RES}(t);\ Q_n^{RES}(t))$ and $(P_n^{CHP}(t);\ Q_n^{CHP}(t))$ define the expected RES and CHP production in terms of active and reactive powers, $PD_n(t)$ and $QD_n(t)$ are the active and reactive power delivered to the load connected to the *n*-th node, $I_{mn}(t)$, $P_{mn}(t)$, and $Q_{mn}(t)$ are respectively the current, the active and the reactive power flowing in the branch from the *m*-th bus to the *n*-th one, $R_{mn}$ and $X_{mn}$ are the resistance and reactance of the *mn*-th branch. $P_n^c(t)$ and $P_n^d(t)$ are the charging and discharging power of the storage at time $t$. $P_n^g(t)$ and $Q_n^g(t)$ are the active and reactive power provided by the upstream connections (slack bus of the network). The values of $P_n^g(t)$ and $Q_n^g(t)$ are zero except for the first node.

The voltage drop and corresponding current flow in the branch $mn$ can be calculated by (5.2) and (5.3) respectively

$$V_m - V_n = I_{mn}(R_{mn} + jX_{mn}) \quad 5.19$$

$$I_{mn} = \left(\frac{P_{mn} + jQ_{mn}}{V_m}\right)^* \quad 5.20$$

The current flow on the branch $mn$ can be placed in (5.2) to obtain the following equation:

$$(V_m - V_n)V_n^* = (P_{mn} - jQ_{mn})(R_{mn} + jX_{mn}) \qquad 5.21$$

Considering the associated voltage angle of each bus (5.21) can be written as

$$V_m V_n(\cos\theta_{mn} + jsin\theta_{mn}) - V_n^2 = (P_{mn} - jQ_{mn})(R_{mn} + jX_{mn}) \qquad 5.22$$

From (5.22), identifying the real and imaginary parts and squaring them, the following equation can be derived, that can be used to obtain the voltage across the branch $mn$

$$V_m{}^2 = V_n{}^2 - \mathbf{2}(R_{mn}P_{mn} + X_{mn}Q_{mn}) + (R_{mn}^2 + X_{mn}^2)I_{mn}^2 \qquad 5.23$$

The magnitude of the current flow $\mathrm{I}_{\mathrm{mn}}^2$ can be obtained as

$$I_{mn}^2 = \frac{P_{mn}^2 + Q_{mn}^2}{V_m^2} \qquad 5.24$$

$$P_{mn}^2(t) + Q_{mn}^2(t) = S_l^2(t) \qquad 5.25$$

In order to effectively formulate a SOCP problem, two new variables are introduced [155],

$$i_{mn}(t)v_m\,(t) = S_l^2(t) \qquad 5.26$$

Here $i_{mn} = |I_{mn}|^2$ and $v_m = |V_m|^2$

### 5.2.2 Energy Storage system model

The storage was modeled as either an apparent power injection or an apparent power load for a given node at a given time period.

$$SOC_n(t) = SOC_n(t-1) + \left(P_n^c(t)\cdot \eta_c - \frac{P_n^d(t)}{\eta_d}\right)\cdot \Delta t \qquad 5.27$$

$$0 \le P_n^c(t) \le \alpha_n^c \cdot P_n^{c,max}(t) \qquad 5.28$$

$$0 \le P_n^d(t) \le \alpha_n^d \cdot P_n^{d,max}(t) \qquad 5.29$$

$$SOC_{n,min} \le SOC_n(t) \le SOC_{n,max} \qquad 5.30$$

$$\alpha_n^c(t) + \alpha_n^d(t) \leq 1 \quad 5.31$$

where $\alpha_n^c(t)$ ϵ [0 or 1] and $\alpha_n^d(t)$ ϵ [0 or 1].

The state of charge (SoC) of energy storage devices is calculated by considering the initial state of charge and charging and discharging efficiencies $\eta_c$ and $\eta_d$ (eq. (5.27)). To restrict the maximum charging and the depth of discharging and for avoiding the simultaneous charging and discharging, the binary variables $\alpha_n^c$ and $\alpha_n^d$, of which only one can be different from zero, have been considered in equation (5.28)-(5.31). Finally, eq. (5.32) is added to force the SoC to be equal at the beginning and the end of the considered time horizon *T*. .

$$SOC_{n,0} = SOC_{n,T} \quad 5.32$$

It is worth mentioning that during the estimation of the charging and discharging power of the storage unit, a quadratic term has arisen due to the multiplication of binary and integer variables. A decomposition technique has been used to linearize the relevant constraints by rewriting constraints in the form of (5.33) as in (5.34) and (5.35) to avoid the bilinear terms.

$$x <= y \cdot z \cdot c \quad 5.33$$

$$x <= y \cdot z_{max} \cdot c_{max} \quad 5.34$$

$$x <= z \cdot c \quad 5.35$$

The continuous and integer variables are respectively variable in $[0, x_{max}]$, $[0, c_{max}]$ and $[0, z_{max}]$.

### 5.2.3 Distributed Generator modeling

The equation (5.36) -(5.37) imposed the active and reactive power curtailment associated with RES and CHP generators. In equation (5.36), $P_n^{min\ RESc/CHPc}$ represents the lower bound of the active power curtailment of RES and CHP generators. In this study, the lower bound value of curtailment has been chosen as 0, which means the generators curtail all of their capacity. The upper bound, $P_n^{maxRESc/CHPc}$, has been considered the capacity of the generators based on the expected values of each time step.

$$P_n^{min\ RESc/CHPc} \leq P_n^{RESc/CHPc}(t) \leq P_n^{maxRESc/CHPc} \quad 5.36$$

$$Q_n^{min\ RESc/CHPc} \leq Q_n^{RESc/CHPc}(t) \leq Q_n^{maxRESc/CHPc} \quad 5.37$$

## 5.3 Multi-temporal OPF with ESS

The objective function (OF) of the deterministic model consists of minimizing the operational extra-cost that should be maintained for complying with the technical constraints. Such cost includes the penalty terms for RES ($C_n^{RESc}$) and for biomass combined heat and power (CHP) curtailment ($C_n^{CHPc}$), and the cost of shaving the peak loads ($C_n^{PLS}$). Furthermore, since the goal of the thesis is to evaluate the contribution of energy storages to the management of the network, even in uncertain conditions, the investment cost $C_n^{CAPEX\_ESS}$ to be sustained for the storage allocated in the network is added to the operational cost, as in (5.38).

$$\min C_{tot} = \min\left\{\sum_{n=1}^{N}\left[C_n^{RESc} + C_n^{CHPc} + C_n^{PLS} + C_n^{CAPEX\_ESS}\right]\right\} \quad 5.38$$

Subject to voltage and current limits, power flow equations, and storage technical constraints. In the following, each cost term and constraints are detailed.

*Penalty for RES curtailment* $\mathbf{C_n^{RESc}}$

To strongly penalize the generation curtailment of RES, the cost of curtailed energy from RES due to network constraint violations has been monetized as twice the price of energy paid in the wholesale market $c_{EN}$ (here, 58 €/MWh, according to the average Italian energy selling price), as in (5.39).

$$C_n^{RESc} = \sum_{t=1}^{T} 2 \cdot c_{EN} \cdot P_n^{RESc}(t) \qquad n = 1 \cdots N \quad 5.39$$

where $P_n^{RESc}(t)$ is the energy curtailed at the time interval t by the RES generator connected to the n-th bus of the network.

Since the increment of the network, hosting capacity may be quantified via the possibly avoided curtailment of RES production, the smaller this term, the better the storage allocation solution.

*Penalty for biomass CHP curtailment* $\mathbf{C_n^{CHPc}}$

This cost for biomass CHP curtailment is assumed as the fuel cost *F* [€/MWh] (here, 80 €/MWh) increased by 20%. This assumption allows penalizing also the CHP curtailments, with high cost as in (5.40).

$$C_n^{CHPc} = \sum_{t=1}^{T} 1.2 \cdot F \cdot P_n^{CHPc}(t) \qquad n = 1 \cdots N \qquad 5.40$$

where $P_n^{CHPc}(t)$ is the energy curtailed at the time interval *t* by the biomass CHP connected to the *n*-th bus of the network.

*Peak load shaving cost* $\mathbf{C_n^{PLS}}$

Regarding the term referred to the Customers, in this thesis, only the cost of shaving the peak loads has been considered, by assuming that it is not possible to fully control the customer demand but only cut a quote of their consumption in some critical conditions. It is assumed, as the RES curtailment, that this curtailed energy is paid at twice the energy price $c_{EN}$ to penalize load curtailment with the higher cost, as renewable generation curtailment, as in (5.41).

$$C_n^{PLS} = \sum_{t=1}^{T} 2 \cdot c_{EN} \cdot P_n^{PLS}(t) \qquad n = 1 \cdots N \qquad 5.41$$

where $P_n^{PLS}(t)$ is the energy curtailed at the time interval *t* to the customer connected to the *n*-th bus of the network.

*Storage investment cost* $\mathbf{C_n^{CAPEX\_ESS}}$

The storage investment cost ($SC_n$) is a function of the size of the storage in terms of rated power and energy as in (5.42).

$$SC_n = c_P \cdot P_n^{rated} + c_E \cdot E_n^{rated} \qquad n = 1 \cdots N \qquad 5.42$$

where $c_P$ and $c_E$ are the specific costs of the ESS adopted technology, reliant respectively on the power rating $P_n^{rated}$ and the nominal capacity $E_n^{rated}$ of the *n*-th ESS located in the network (here $c_P$ =200 €/kW and $c_E$ =400 €/kWh according to the market cost of Lithium-ion technology ).

In order to consider this cost in the objective function (5.38) only a daily quote of $SC_n$ is added to the operational terms of (1), calculated as in (5.43).

$$C_n^{CAPEX\_ESS} = \frac{K_S}{365} \cdot SC_n \qquad n = 1 \cdots N \tag{5.43}$$

where $K_s$ is a capital recovery factor (here $K_s$=0.1, for considering 10 years as ESS lifetime).

In this thesis, it is supposed that the storages are DSO owned and managed for relieving contingencies. Thus, the ESS OPEX (operational expenditures) is not considered in the optimization. According to this point of view, it is supposed that the minimization of the network operational cost, in terms of reduction of the curtailed power from RES and to loads, that would be necessary to relieve contingencies, represents the only incomes that allow DSO to pay back EES CAPEX (capital expenditures) and ESS OPEX. A term that takes into account the depreciation of the ESSs due to their use could be included, but in this study, this cost is assumed negligible.

## 5.4 Summary

In this chapter, the mathematical formulation of a multi-period AC OPF for energy storage planning in the distribution network has been derived. The complete derivation of the second-order cone program of an AC OPF problem is presented in this chapter. The OPF model is formulated to reduce the PV, Wind, and CHP curtailments and also minimize the load shedding. The storages are used to support the distribution network. It is assumed that DSO owns the storages, and it is managed to relieve contingencies. Therefore, in this model, the operational cost of storage has not been considered.

# Chapter 6

## 6. Robust optimal placement for energy storage system

Uncertainties of distributed generation and load are comparatively high in the distribution grid in comparison to transmission grids. Uncertainties in daily operations can have substantial effects on the operational costs of distribution grids. Therefore, the flexibility of load and generation should be considered to optimize operational costs better and postpone network reinforcement. The robust day ahead robust scheduling of the flexibilities of load and DG can strengthen the daily operations. The robust scheduling means considering the uncertain variables such as weather conditions and other associated uncertainties. In this chapter, in order to validate the proposed model and approach, two case studies have been performed.

### 6.1 Robust reformulation

As described in chapter 4, the robust reformulation approach will only convert the constraints that are affected by uncertainty. In other words, the constraints that consist of uncertain parameters need to be formulated in such a way that the constraints become immune of uncertainty.

Though the fundamental of this solution approach has been described in chapter 4, the reformulation technique for this specific application will be discussed here.

The robust reformulation technique for distribution network planning is detailed in the next section.

## 6.2 Robust reformulation (Distribution network)

Assume that all the decision variables should be considered before the revealing of the uncertainty from solar power, wind generation, and electric loads. In the active power balance in chapter 5, equation 5.17, uncertainties $P_n^{RES}(t)$ and $PD_n(t)$ are modeled as symmetric and bounded variables $\widetilde{P_n^{pv}(t)}$, $\widetilde{P_n^{w}(t)}$ $and$ $\widetilde{PD_n(t)}$. It should be mentioned here that $P_n^{RES}(t)$ consist of solar and wind generations. The uncertainty takes values as in the following equation 6.1 - 6.3,

$$\widetilde{P_n^{pv}(t)} = P_n^{pv}(t) + \Delta\widetilde{P_n^{pv}}(t) \quad \widehat{P_{pv}^{lb}} \leq \Delta P_{pv}(t) \leq \widehat{P_{pv}^{ub}} \tag{6.1}$$

$$P_n^{\widetilde{wind}}(t) = P_n^{wind}(t) + \Delta\widetilde{P_n^{wind}}(t) \quad \widehat{P_{wind}^{lb}} \leq \Delta P_{wind}(t) \leq \widehat{P_{wind}^{ub}} \tag{6.2}$$

$$\widetilde{PD_n(t)} = PD_n(t) + \Delta\widetilde{PD_n(t)} \quad \widehat{P_D^{lb}} \leq \Delta P_D(t) \leq \widehat{P_D^{ub}} \tag{6.3}$$

In the robust model, the objective function, in chapter 5 (equation 5.38), is identical to the deterministic model. The only constraint that is affected by uncertainty is the electric power balance equation. The electric power in the network should be met when the worst case of uncertainties occurs. For the power balance equation, the worst case would occur at the maximum increase of the electric loads and the maximum decrease in solar and wind power generation. Therefore, the robust formulation becomes as in equation 6.4 – 6.7.

$$min\, C_{tot} = min\left\{\sum_{n=1}^{N}\left[C_n^{RESc} + C_n^{CHPc} + C_n^{PLS} + C_n^{CAPEX\_ESS}\right]\right\} \tag{6.4}$$

Subject to,

$$\begin{aligned} P_n^g(t) + P_n^{RES}(t) - P_n^{RESc}(t) + P_n^{CHP}(t) - P_n^{CHPc}(t) - PD_n(t) + P_n^{PLS}(t) \\ - P_n^c(t) + P_n^d(t) + max\{P_D^{ub}(t) * \xi_D^{ub}(t) + P_D^{lb}(t) * \xi_D^{lb}(t) \\ - P_{pv}^{ub}(t) * \xi_{pv}^{ub}(t) - P_{pv}^{lb}(t) * \xi_{pv}^{lb}(t) - P_{wind}^{ub}(t) * \xi_{wind}^{ub}(t) \\ - P_{wind}^{lb}(t) * \xi_{wind}^{lb}(t)\} - \sum_{m\epsilon\theta_n} R_{mn} \cdot I_{mn}^2 = \sum_{m\epsilon\theta_n} P_{mn}(t) \end{aligned} \tag{6.5}$$

$$\xi_D^{ub}(t) + \xi_D^{lb}(t) + \xi_{pv}^{ub}(t) + \xi_{pv}^{lb}(t) + \xi_{wind}^{ub}(t) + \xi_{wind}^{lb}(t) \leq \Gamma_1(t) \tag{6.6}$$

$$\xi_D^{ub}(t), \xi_D^{lb}(t), \xi_{pv}^{ub}(t), \xi_{pv}^{lb}(t), \xi_{wind}^{ub}(t), \xi_{wind}^{lb}(t) \leq 1 \quad 6.7$$

Where $\xi_D^{ub}(t), \xi_D^{lb}(t), \xi_{pv}^{ub}(t), \xi_{pv}^{lb}(t), \xi_{wind}^{ub}(t), \xi_{wind}^{lb}(t)$ are the scaled deviations from the random electric loads, solar, and wind power generation. $\Gamma_1(t)$ is the budget of the uncertainty of uncertain parameters at time *t* that lies between 0 to 1, where 0 being the deterministic case and 1 defined the most robust case.

To make tractable the above problem, the following subproblem in equation 6.8 - 6.10 need to be formulated into the corresponding dual problem by introducing dual variables $\lambda_1(t), \Pi_D^+(t)$, $\Pi_D^-(t), \Pi_{pv}^+(t), \Pi_{pv}^-(t), \Pi_{wind}^+(t), \Pi_{wind}^-(t)$ for constraints 6.9 – 6.10.

Subproblem:

$$\begin{aligned} max\{P_D^{ub}(t) * \xi_D^{ub}(t) + P_D^{lb}(t) * \xi_D^{lb}(t) - P_{pv}^{ub}(t) * \xi_{pv}^{ub}(t) - P_{pv}^{lb}(t) * \xi_{pv}^{lb}(t) \\ - P_{wind}^{ub}(t) * \xi_{wind}^{ub}(t) - P_{wind}^{lb}(t) * \xi_{wind}^{lb}(t)\} \end{aligned} \quad 6.8$$

Subject to

$$\xi_D^{ub}(t) + \xi_D^{lb}(t) + \xi_{pv}^{ub}(t) + \xi_{pv}^{lb}(t) + \xi_{wind}^{ub}(t) + \xi_{wind}^{lb}(t) \leq \Gamma_1(t) \quad 6.9$$

$$\xi_D^{ub}(t), \xi_D^{lb}(t), \xi_{pv}^{ub}(t), \xi_{pv}^{lb}(t), \xi_{wind}^{ub}(t), \xi_{wind}^{lb}(t) \leq 1 \quad 6.10$$

The robust counterpart after applying the duality theory is formulated as in 6.11 – 6.15.

$$min\ \lambda_1(t)\Gamma_1(t) + \Pi_D^+(t) + \Pi_D^-(t) + \Pi_{pv}^+(t) + \Pi_{pv}^-(t) + \Pi_{wind}^+(t) + \Pi_{wind}^-(t) \quad 6.11$$

Subject to,

$$\lambda_1(t) + \Pi_D^+(t) \geq \widehat{P_D^{ub}}(t), \lambda_1(t) + \Pi_D^-(t) \geq \widehat{P_D^{lb}}(t) \quad 6.12$$

$$\lambda_1(t) + \Pi_{pv}^+(t) \geq -\widehat{P_{pv}^{ub}}(t), \lambda_1(t) + \Pi_{pv}^-(t) \geq -\widehat{P_{pv}^{lb}}(t) \quad 6.13$$

$$\lambda_1(t) + \Pi_{wind}^+(t) \geq -\widehat{P_{wind}^{ub}}(t), \lambda_1(t) + \Pi_{wind}^-(t) \geq -\widehat{P_{wind}^{lb}}(t) \quad 6.14$$

$$\lambda_1(t), \Pi_D^{\pm}(t), \Pi_{pv}^{\pm}(t), \Pi_{wind}^{\pm}(t) \geq 0 \quad 6.15$$

Finally, the tractable robust model can be formulated as follows,

$$min\, C_{tot} = min\left\{\sum_{n=1}^{N}\left[C_n^{RESc} + C_n^{CHPc} + C_n^{DR} + C_n^{CAPEX_{ESS}}\right]\right\} \quad 6.16$$

Subject to

$$P_n^{g}(t) + P_n^{RES}(t) - P_n^{RESc}(t) + P_n^{CHP}(t) - P_n^{CHPc}(t) - PD_n(t) + P_n^{PLS}(t) - P_n^{c}(t) + P_n^{d}(t) + \lambda_1(t)\Gamma_1(t) + \Pi_D^{+}(t) + \Pi_D^{-}(t) + \Pi_{pv}^{+}(t) + \Pi_{pv}^{-}(t) + \Pi_{wind}^{+}(t) + \Pi_{wind}^{-}(t) - \sum_{m\epsilon\theta_n} R_{mn}\cdot I_{mn}^{2} = \sum_{m\epsilon\theta_n} P_{mn}(t) \quad 6.17$$

Moreover, the constraints 5.18 - 5.32 and 6.12 – 6.15 form the tractable problem.

The new model does not contain any uncertainty and is formulated as a mixed-integer second-order conic programming (MISOCP) problem that can be solved efficiently using CPLEX that uses a branch and cut algorithm to find the integer feasible solution.

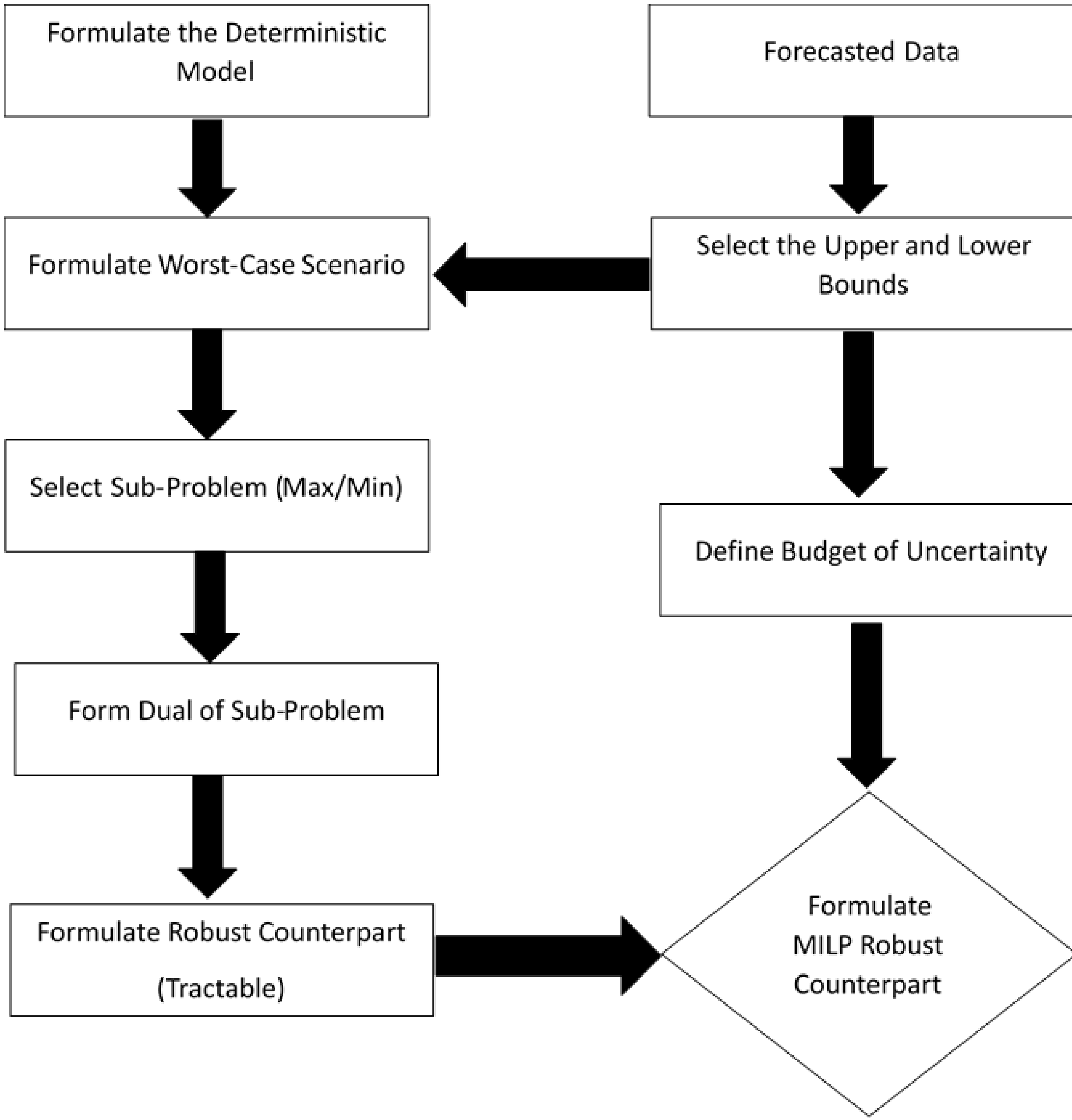


**Figure 22** *Flow chart of the robust reformulation solution approach*

The solution methodology can be explained by the flow chart in Figure 22.

## 6.3 Case Study (Distribution network)

The procedure has been applied to a test distribution network derived from the ATLANTIDE project [133]. The MV network, shown in Figure 23, representative of the industrial ambit, is constituted by

100 nodes, subdivided in 7 feeders supplied by a Primary Substation equipped with a 25 MVA HV/MV transformer. The total demand is about 30 MVA (372 GWh/year), and the total installed DG capacity is 34 MW (27.2 GWh/year), as a mix of wind, PV, and biomass CHP generators.

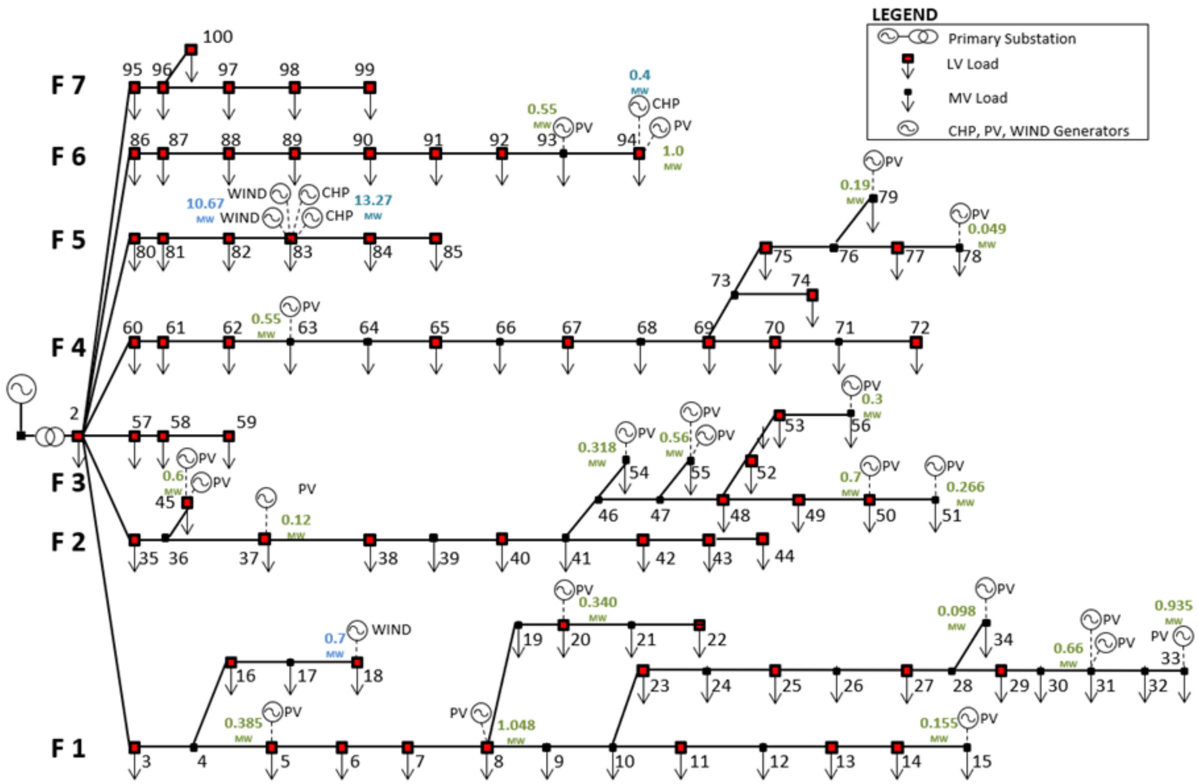


**Figure 23** *Test distribution network*

The mathematical formulation of the RO for an AC OPF based energy storage planning tool has been programmed in GAMS (General Algebraic Modeling System) and solved using CPLEX 25.1.1 on a 2.30 GHz personal computer with 4GB RAM. In this experimental study, the worst case has been considered when the load is high ($\xi_{D,t}$=1) and wind and PV generation is low ($\xi_{pv,t}, \xi_{w,t}$= -1).

For the sake of a comprehensive view, in the following, the results obtained by the application of the described optimization to the network of Figure 23 in twelve typical days, differentiated between working days, Saturdays and holidays (Sundays included), and between seasons, have been reported. The time horizon of 24 h of each typical day has been considered with a time step of 1 h. Three scenarios have been considered: the certain one (solved by the deterministic OPF) and two uncertain scenarios with different values of risk ($\Gamma = 0.5$ and $\Gamma = 1$), both solved with RO. Furthermore, for highlighting the advantages provided by the storage systems the case of deterministic optimization (certain) without storage has been added to the previously described cases.

All the buses of the test network were assumed candidates for storage placement. The available ESS were considered of 1.0 MW/2 h storage capacity. The efficiencies for charging and discharging were considered 90% each, which gives an overall roundtrip efficiency of 0.81. The initial state of charge (SOC) has been considered 25% of its capacity. The cost Lithium-ion technology in this study has been considered as €200 for each kW of rated power, €400 for each kWh of rated energy.

In these typical days, some under-voltage conditions occur in the most distant nodes from the HV/MV transformer and, thus, for solving these issues, it is necessary to resort to the load peak shaving. Furthermore, some lines suffer for overloading depending on the non-coincidence of load demand and DG production. ESSs prove to be useful for reducing the curtailment of the demand and production as detailed in the next subsections.

*Generation and load profiles*

The generation and load profiles were simulated according to the ATLANTIDE load and generation daily curves, that provide for different kinds of customers (i.e., industrial, residential, commercial and agricultural) and for several technologies of DG (i.e., wind turbine, PV and CHP biomass based) the hourly consumption/production for each typical day. An amount of 22 PV systems was assigned to 20 nodes. The size of these systems is between 49 – 1048 kW. Node 8 has the biggest PV system, whereas the lowest one is connected to node 78. Node 83 comprised of two wind generators and CHP plants. Figure 23 depicts the nominal power of the PV, Wind, and CHP of each node.

The load profiles indicated a peak load of 18.69 MW during the spring working day and 18.14 MW during the summer working day with an average load of 13.79 MW and 13.38 MW respectively. As an example, the demand and production profiles and their balance at the HV/MV interface, during the spring working day, are shown in Figure 24.

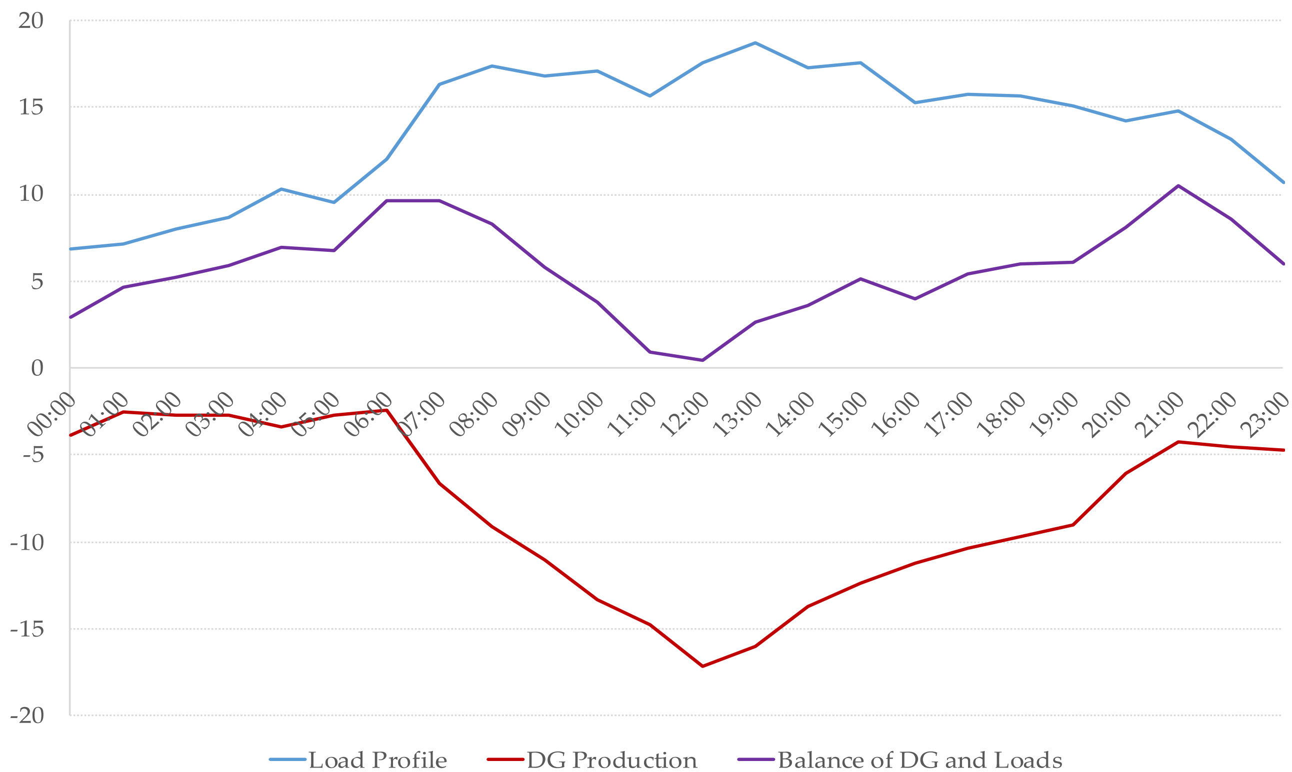


**Figure 24** *Load-production profiles of the whole network for the Spring working typical day*

### 6.3.1 Storage Placement

The optimization results of storage position for each typical day for the three considered cases have been enumerated in Table 6-1. It is worthy of mentioning that the results are substantially incremental: the intermediate case includes the location of the deterministic case, and the robust case (no risk) includes, in turn, the intermediate one.

Table 6-1The ESS optimal positions may change from one typical day to another even for the same case, but the results can be summarized by considering a given solution valid for all the twelve typical days. In the following, it has been assumed that the placement in one bus or in a close one in two different typical days can be considered the same placement. In particular, for instance, the bus 83 and the bus 84 in the deterministic case, that are the solutions for the TD6, and the TD8 respectively, can be considered as a unique optimal position around the bus 83.

On the contrary, if two busses, even close, appear in the solution of the same day they are both considered necessary and two ESS have to be placed on that nodes (e.g., the busses 83 and 85 in the results of all the cases for the TD12 or the busses 83 and 84 in the results of the intermediate and robust cases for the TD5). By applying these rules, the total number of ESS that has to be placed in the three cases are reported in the last row of Table 6-1. It is worthy of mentioning that the results are substantially incremental: the intermediate case includes the location of the deterministic case, and the robust case (no risk) includes, in turn, the intermediate one.

Table 6-1It is worthy of mentioning that the results are substantially incremental: the intermediate case includes the location of the deterministic case, and the robust case (no risk) includes, in turn, the intermediate one.

Table 6-1 *Storage placement for each typical day for the three considered cases*

| **Typical Days** | **Deterministic Case** | **Intermediate Case** | **Robust Case** |
|---|---|---|---|
| TD1 - Winter Working day | 10, 32 | 10, 32, 77 | 10, 32, 48, 77 |
| TD2 - Winter Saturday | - | - | - |
| TD3 - Winter Holiday | - | - | - |
| TD4 - Spring Working day | 10 | 10, 34 | 10, 34 |
| TD5 - Spring Saturday | 84 | 83, 84 | 83, 84 |
| TD6 - Spring Holiday | 84 | 84 | 84 |
| TD7 - Summer Working day | - | - | - |
| TD8 - Summer Saturday | 83 | 12, 83 | 12,32, 83 |
| TD9 - Summer Holiday | - | - | - |
| TD10 - Autumn Working day | 12 | 12, 27 | 12, 27, 69 |
| TD11 - Autumn Saturday | 84 | 84 | 69, 84 |

| | | | |
|---|---|---|---|
| TD12 - Autumn Holiday | 83, 85 | 83, 85 | 83, 85 |
| **Total number of ESS** | **4** | **5** | **6** |

In order to analyze the impact of renewables and load uncertainty on the investment of the energy storage in the distribution network, one of the worst-cases of renewables (PV, wind, or biomass-based) and loads combinations are considered. The worst-case scenario considered in this work is when the loads have upper bound values, and the renewables have lower bound values. Three cases are considered by varying the loads and renewables uncertainty bounds. In the first case, the budget of uncertainty is zero ($\Gamma = 0$), i.e., the profiles of load and renewable generations are assumed following the forecasted values. In the second case, the value of budget of uncertainty for both load and renewables considered 0.5 ($\Gamma = 0.5$) that is between the zero (deterministic) and 1 (robust or worst case). In the third case ($\Gamma = 1$), the considered worst-case scenario has been evaluated. In this case, the uncertainty sets of loads and renewables are considered broader to take into account the possible extreme coordinates of the uncertainty set.

The following figures compare the results of the studied cases (i.e., no control, deterministic OPF no storage, deterministic OPF with storage, intermediate and robust). In particular, these results are related to the most critical typical day, the winter working day (TD1). For the sake of clarity, the figures refer only to the feeder F1 that is the longest feeder of the test network depicted in Figure 23 (i.e., the last bus is about 14.2 km far from the primary substation).

The simulation of no control case also suggests generation curtailment (*no control* case refers to a simple load flow studies that help to understand the network conditions), especially in feeder 6. Furthermore, it was observed over current issues in the line of nodes 80-81, 81-82, and 82-83. It was observed when the biomass plant starts to operate, it creates line congestion, and thus, generation curtailment occurs.

Figure 25 shows the voltage profiles occurring at 9:00 am of the winter working typical day, because, among other time intervals, this one was proved that experiments the greatest load curtailment; The allowable voltage range had been considered 0.95 p.u. as the lower bound and 1.05 p.u. as the upper bound of the voltage.  Figure 26 and Figure 27 show the load curtailed during the winter and autumn working days respectively. The balances of DG production and curtailed demand for winter working day are depicted in Figure 28, and the same information for the autumn working day is illustrated in Figure 29. Moreover, the ESS charging/discharging optimal profiles of one of the ESS optimal positioned in the feeder F1 are shown in Figure 30 (bus 10 of Figure 23). As it is evident by the results, all the optimizations allow to solve the under-voltage conditions occurring in the long feeder F1 (Figure 25); the more conservative the optimization (i.e. by passing from certain to uncertain, intermediate and robust, optimization) the smaller the demand curtailed (Figure 26 and Figure 27); in the feeder F1 no generation curtailment results from the optimizations, thus the balance of production and demand (curtailed) is closer to the original one (no control) in the robust case (Figure 28 and Figure 29). It is worth noting that the difference between the voltage value at the sending end (the MV busbar of the primary substation) is lower in the no control case than the other cases because the implemented model of the HV/MV transformer is very simple and strongly suffers for the high demand, not curtailed in the control case. These results together with the ESS operation, are discussed more in detail in the next subsections for each optimization case.

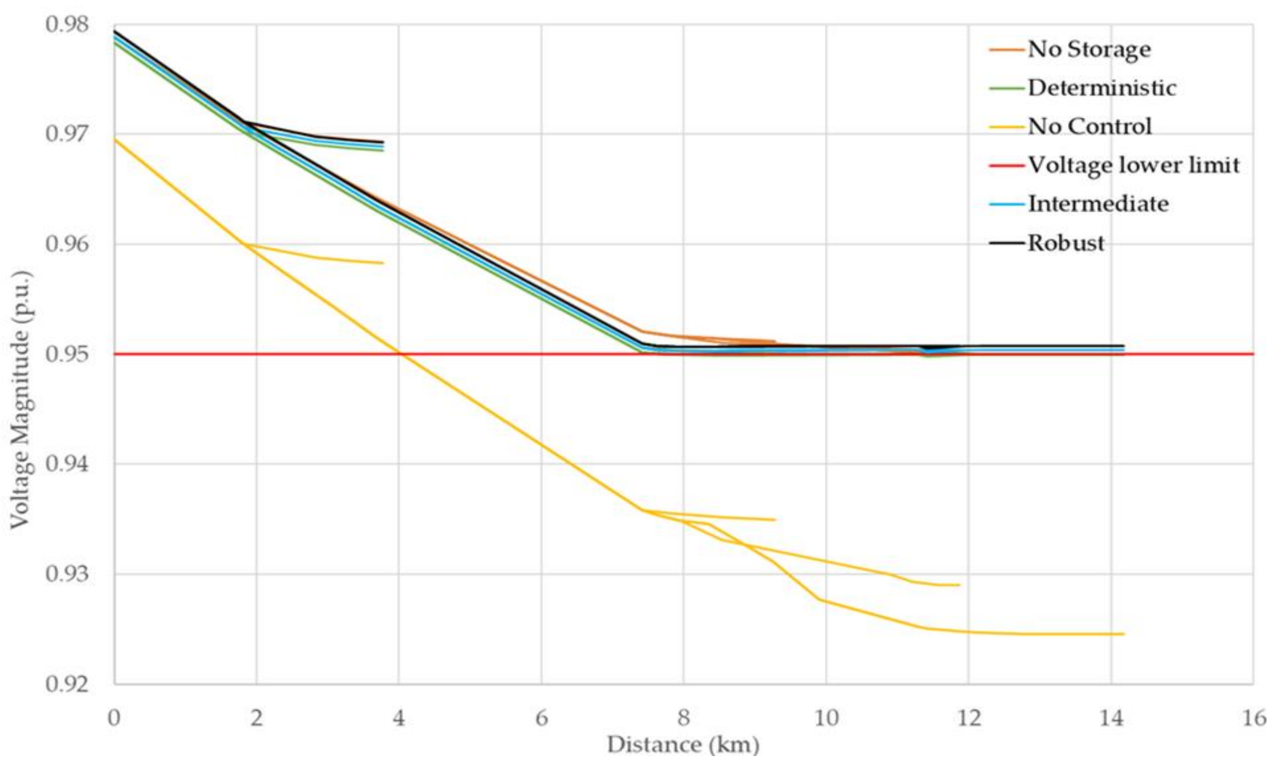


**Figure 25** *Voltage profiles of feeder F1 for no control, no storage (certain deterministic OPF without storage) and deterministic (certain deterministic OPF with storage), intermediate and robust cases at 9:00 am of the winter working day.*

### 6.3.2 Influence of budget of uncertainty

#### 6.3.2.1 Deterministic case (with and without storage)

Due to the absence of uncertainty, in this case, the load and renewables profiles will remain the same as the predicted values. It was witnessed that during the deterministic case with storage, at least four storages need to cover their requirements. The ESS optimal positions can change from one typical day to another, but, by summarizing the results in the twelve typical days, (Table 6-1) they were located two in the two lateral branches that start from the node 10 (feeder F1, positions are 10 or 12 and 32). The third and fourth ESSs have to be located around the node 83 (feeder F5, positions are two among 83, 84 and 85). It is essential to observe that node 83 is the node that has the highest number of renewables and CHP connected; thus, it is noticeable to consider that as a privileged position for storages.

The highest load curtailment was experienced during the typical day of winter working day (TD1) with the amount of 51.77 MWh/day for the case without storage and 30.46 MWh/day for the case with storage. Apart from the winter working day, the autumn working day (TD10) has experienced the most load curtailments that account for 32.47 MWh/day for without storage case and with the integration of storage, it became 14.05 MWh/day. The autumn Saturday or semi-holiday (TD11) had experienced the highest generation curtailment due to the line congestion in feeder 6 (F6 in Figure 23) with the amount 62.7 MWh/day. However, this amount has minimized to 48.2 MWh/day by integrating storage.

By focusing on the feeder F1, as it is evident from Figure 25, the nodes of this feeder have under-voltage issues in the no control case, and any optimization forces to resort load shedding (Figure 26). By comparing these two certain cases, is it worth noticing that if the ESSs are not available for the optimization (deterministic OPF no storage) much more demand has to be curtailed (i.e., 41.62 MWh/day of the no storage case vs. 20.97 MWh/day in the case with storage for winter working day). In the case of autumn working day (TD10), these values become 27.33 MWh/day (for no storage case) and 12.18 MWh/day (for deterministic with storage case), as shown in Figure 27.

The daily operation of the ESS has been optimized as well as the optimal position. For instance, during the winter working day, the daily operation profile of the ESS located around the bus 10 is shown in Figure 30, and the balances of demand and production, with and without ESS. At the beginning of the day, the ESS started to charge, keeping the final balance of demand, DG production (minimal in the first hours of the day), and charging power for ESS so low to do not negatively impact the network operation. At around 7:00 am, when the morning peak starts, the storage discharges for reducing the power demand and keeping the voltage profile within the limit (Figure 25). In Figure 31, the optimized daily operational profiles for the autumn working day have been described. In this typical day, the ESS is placed around the bus 12. Similar to the operations of winter working day, the ESS started to charge at the beginning of the day and discharges during the demand is higher. Specifically, the ESS discharges from 08:00 -10:00, 12:00-21:00, as shown in Figure 31. Around 11 am the storage charges to avoid any violation of technical constraints due to DG production.

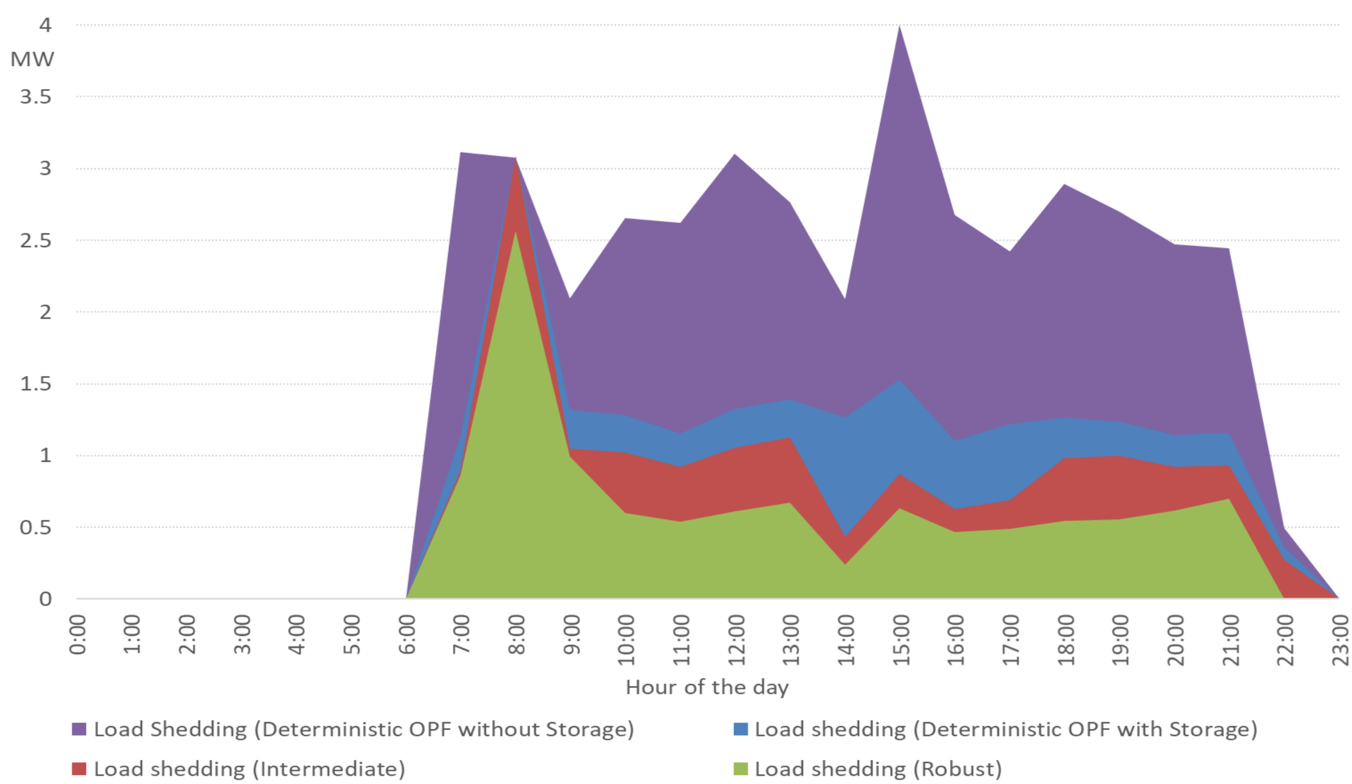


**Figure 26** *Load curtailments experimented by the feeder F1 for the no storage (certain deterministic OPF without storage), deterministic (certain deterministic OPF with storage), intermediate and robust cases on the winter working day.*

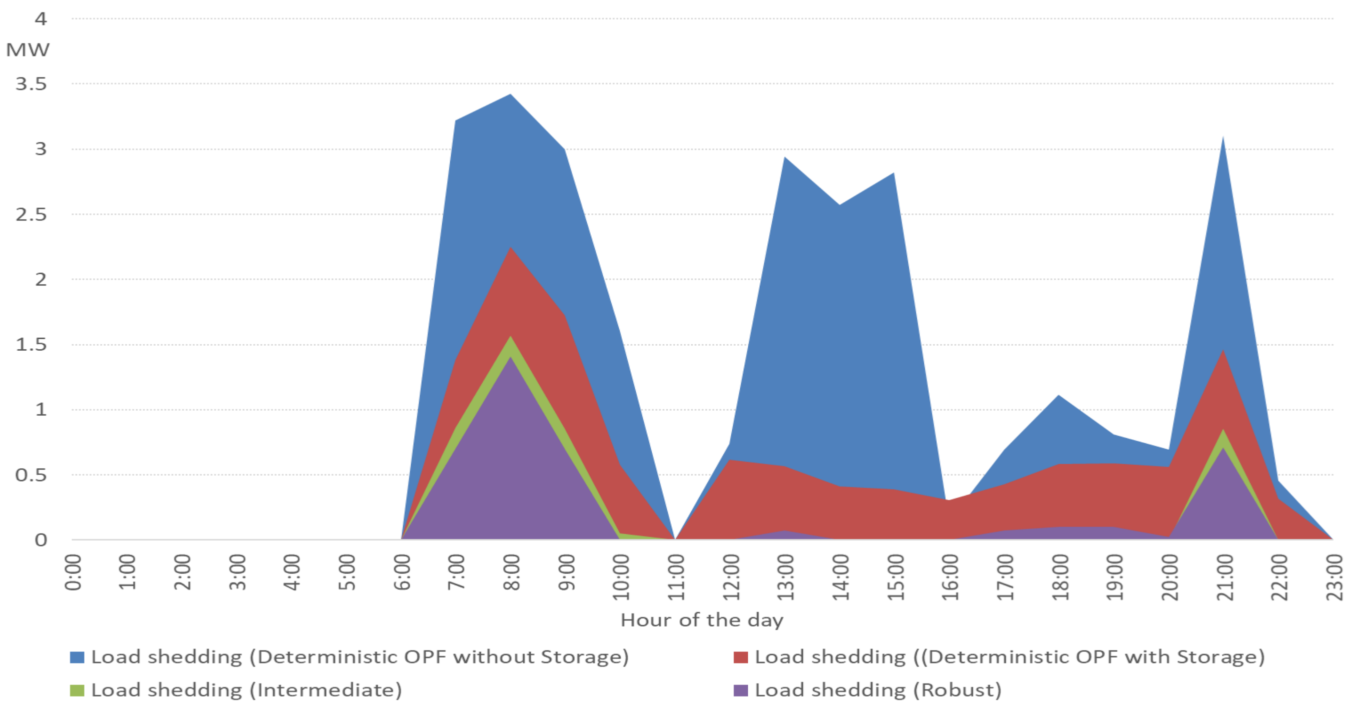


**Figure 27** *Load curtailments experimented by the feeder F1 for the no storage (certain deterministic OPF without storage), deterministic (certain deterministic OPF with storage), intermediate and robust cases on the autumn working day*

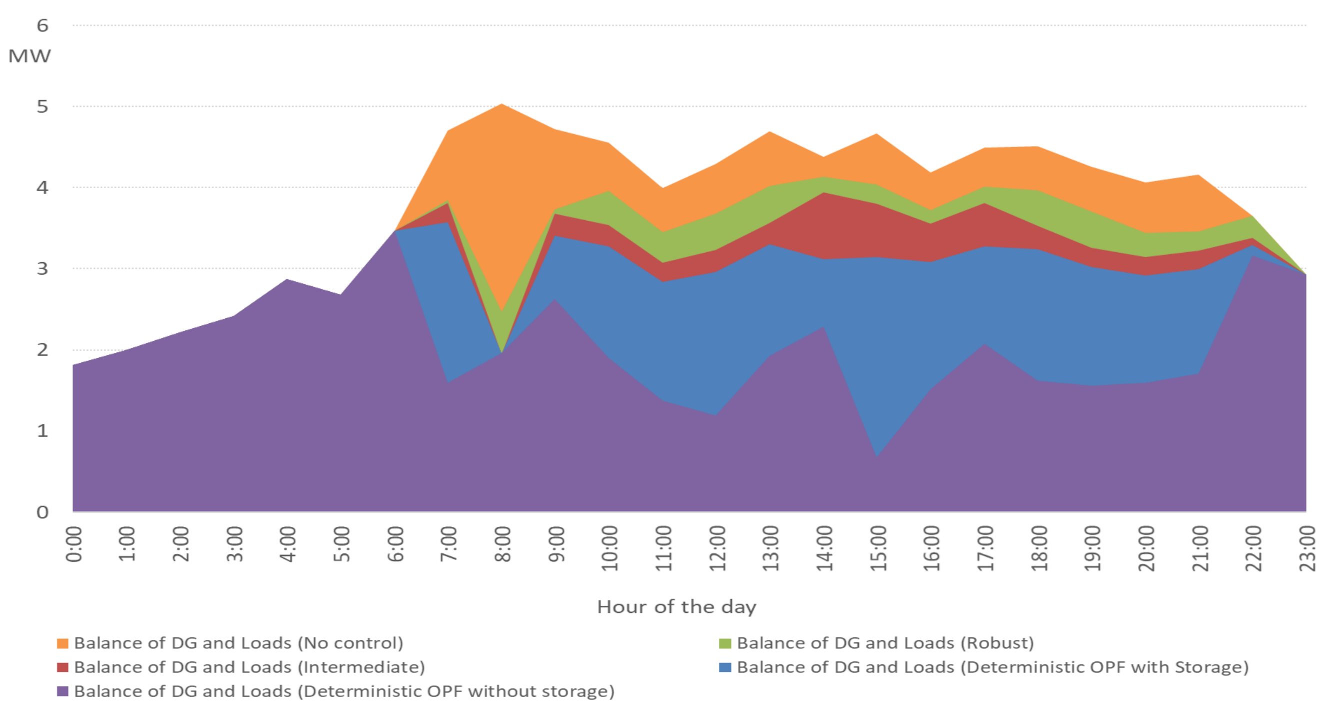


**Figure 28** *Balance of DG production and curtailed demand of the feeder F1 for the no control, no storage (certain deterministic OPF without storage), deterministic (certain deterministic OPF with storage), intermediate and robust cases on the winter working day.*

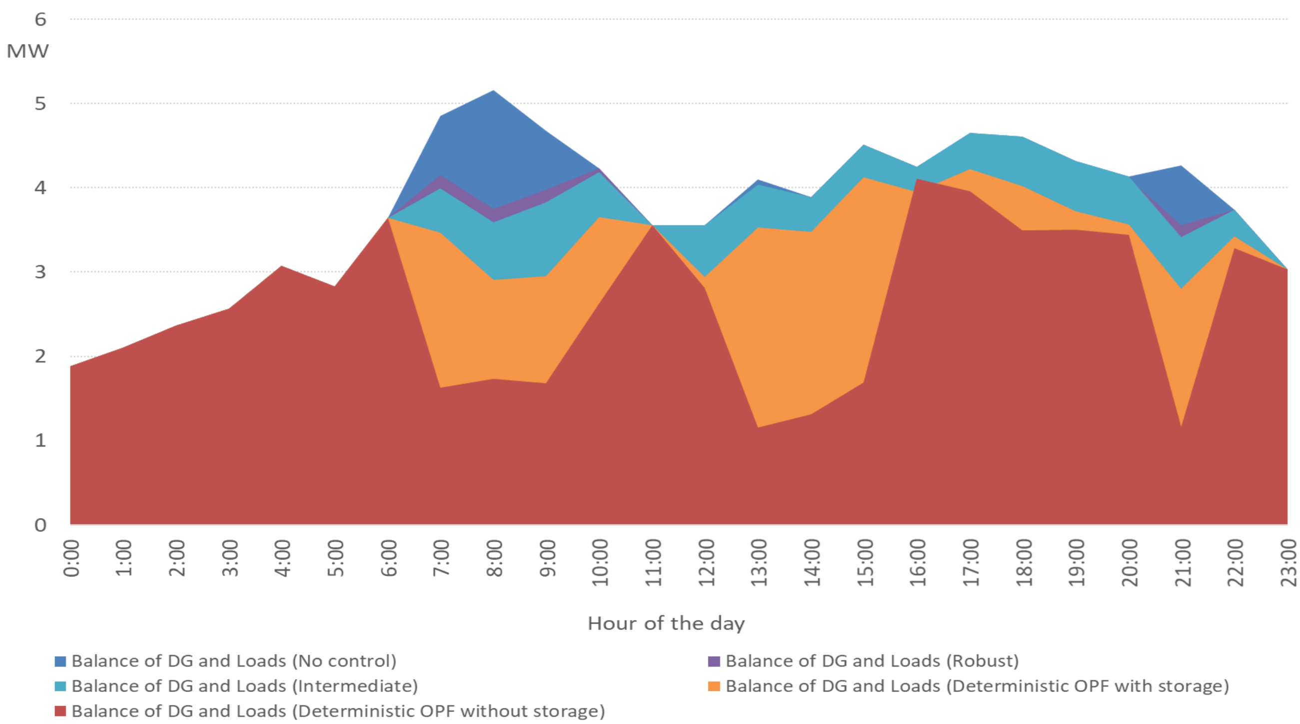


**Figure 29** *Balance of DG production and curtailed demand of the feeder F1 for the no control, no storage (certain deterministic OPF without storage), deterministic (certain deterministic OPF with storage), intermediate and robust cases on the autumn working day.*

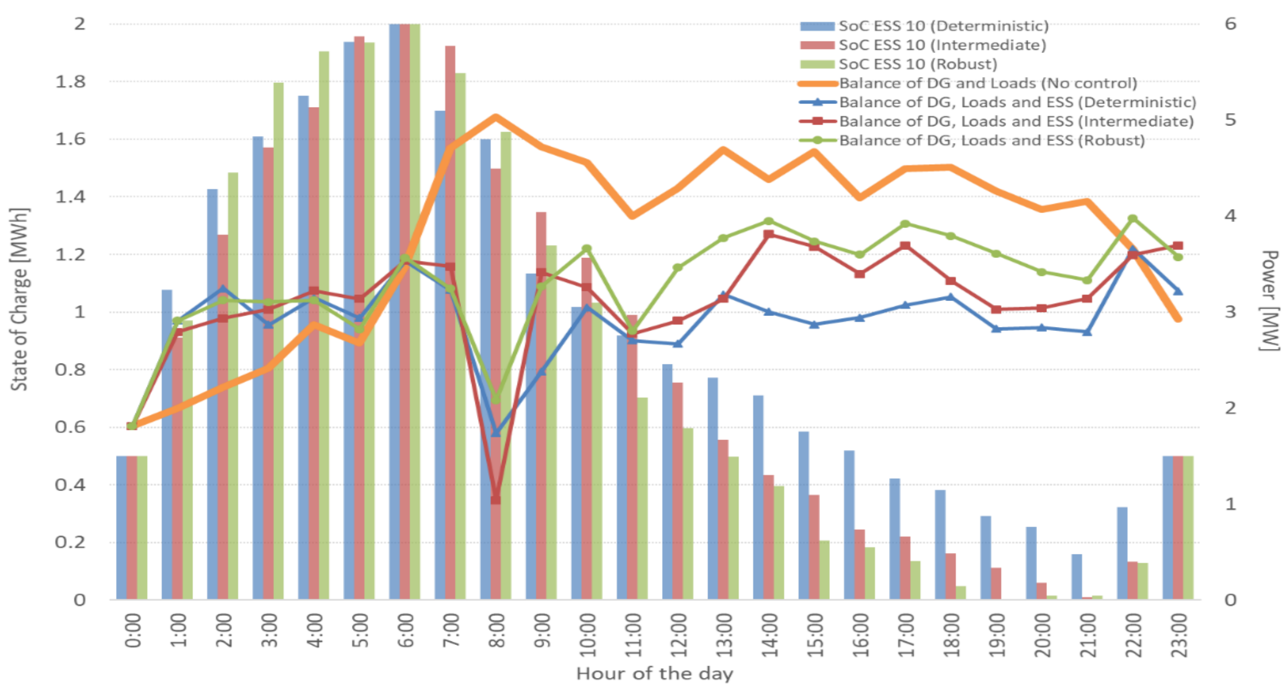


**Figure 30** *Charging/discharging profiles of ESS optimal positioned in the bus 10 of the feeder F1 for the deterministic (certain deterministic OPF with storage), intermediate and robust cases on the winter working day and balances of powers (DG, Loads and ESS) in the same cases. The no control case has been added for comparison.*

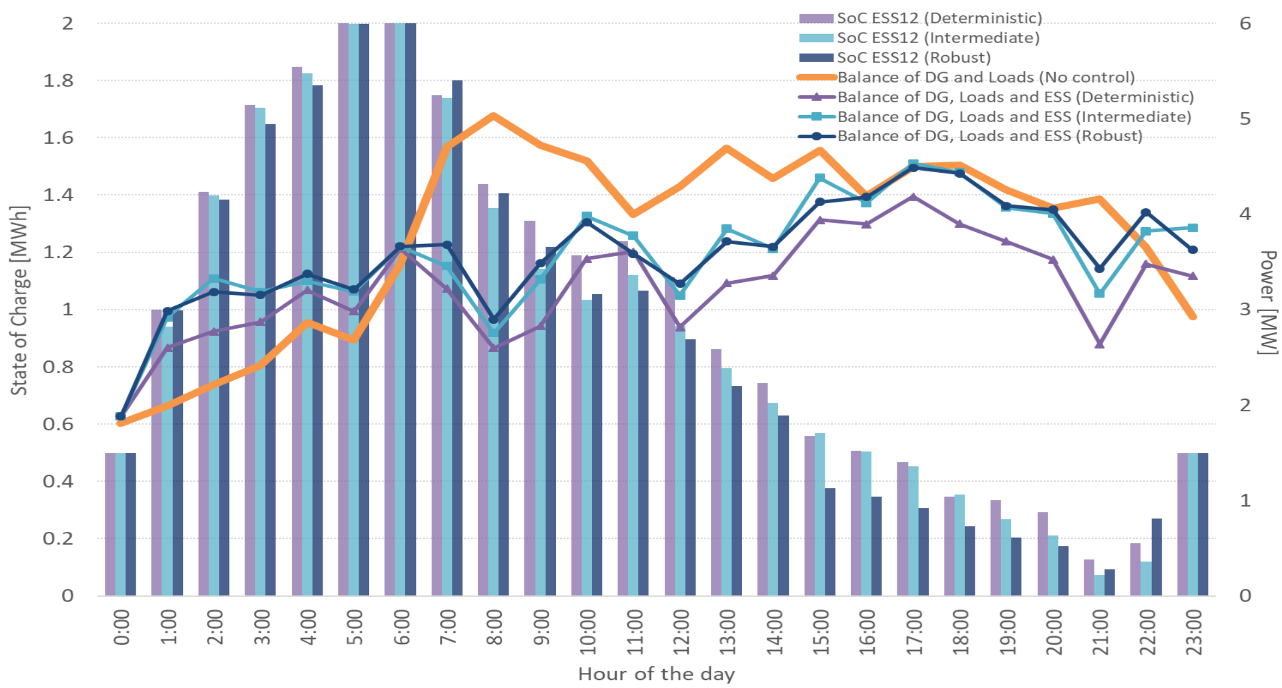


**Figure 31** *Charging/discharging profiles of ESS optimal positioned in the bus 12 of the feeder F1 for the deterministic (certain deterministic OPF with storage), intermediate and robust cases on the autumn working day and balances of powers (DG, Loads and ESS) in the same cases. The no control case has been added for comparison.*

### 6.3.2.2 Intermediate case

In this case, a narrow uncertainty bound is considered. The budget of uncertainty for the uncertain parameters has been considered as $\Gamma = 0.5$. The optimization algorithm will look for a solution inside the specified uncertainty bound. From Table 6-1, by considering the simulation results of the twelve typical days, and assuming the most conservative hypotheses (i.e., the final result is the union of the results obtained for each typical day), the intermediate case suggests at least five storage systems to be installed: two in the feeder F1 and two in the feeder F5, as in the deterministic case, plus one ESS in the feeder F4. The positions of the two storages in the feeder F1 and the two in the feeder F5 are more or less the same of the deterministic case (F1 possible locations are the busses 10 or 12 for one lateral and the busses 27, 32, or 34 for the other lateral, and two positions among the bus 83, 84 or 85 for the feeder F5). In the feeder F4, the added storage system has to be installed around the node 77.

The load shedding, in this case, is more reduced and for the critical TD1 is equal to 15.89 MWh/day (about 25% less than the deterministic case), as shown in Figure 26. In the case of autumn working day (TD10), the load shedding amount accounts for 4.24 MWh/day (approximately 65% less than the deterministic case).

Furthermore, it can be observed in Figure 30 that the ESS located around the bus 10 in the feeder F1 has a similar trend of the same ESS in the deterministic case: it charges and discharges mostly in the same hours for solving local contingencies. In particular, it charges when the load demand is low (at the first hours of the day), and finally, at the end of the day for recovering their initial SoC; on the contrary, it discharges in correspondence of the peaks of demand (7:00-21:00).

The same curves shown in Figure 30 for the winter working day are reported in Figure 31 for the autumn working day, with the difference in the location of the storage. In the case of Autumn working day among two storages, one located in the bus 12 and the other one in the bus 27, have the similar trend: they charge and discharge mostly in the same hours for solving local contingencies. In particular, they charge when the load demand is low (at the first hours of the day), and finally, at the end of the day for recovering their initial SoC; on the contrary, they discharge in correspondence of the peaks of demand (7:00-10:00, 12:00-21:00).

#### 6.3.2.3 Robust Case

The third case can be considered as the worst-case analysis. In this case, the budget of uncertainty for uncertain parameters is equal to 1 ($\Gamma = 1$). This budget of uncertainty allows the algorithm to consider the extreme points of the uncertainty set. Compared to the previous cases, the robust case provides six storage systems to be installed in the network. The locations of storage for feeder F1, F4 and F5 are similar to the deterministic and intermediate cases. However, for winter working day, the robust case suggests one more ESS in the feeder F2 (bus 48). On the other hand, for the autumn working day, the additional storage needs to be installed in the feeder F4 (bus 69). In Figure 30, the operation profile of the ESS located around the bus 10, resulting from the optimization for the feeder F1 is shown with the demand and production daily curves. The behavior of the ESS is similar to the one that they have in the other cases: the contribution to reducing the peaks at the cost of a slight increase of demand when they charge. This increase does not alter the network operation and does not produce any technical constraint violation, but it allows a further reduction of load shedding (Figure 26). In particular, for feeder 1 in the critical TD1 the demand is curtailed of 11.10 MWh/day (-30 % than the intermediate case). For TD10, feeder F1 experienced an amount of 3.90 MWh/day as load curtailment (around -8% than the intermediate case).

### 6.3.3 Economic Analysis

In order to analyze the economic feasibility of the investments in storage systems, the comparison between all the cases mentioned above, included the *no storage* one, has been considered. Table 6-2 summarizes the yearly operational costs (operational expenditures – OPEX) for the four considered cases, the amount of load shedding and generation curtailment used for solving the contingencies, the CAPEX for the ESS installation referred to one year only (among the ten years of the ESS life duration), and, in the last column the total yearly cost: CAPEX plus the OPEX. In the *no storage* case, the yearly operational cost, of about 1480 k€, consists of penalty cost for load shedding that accounts for 762.90 k€/year, and penalty cost of CHP curtailment worth 717.46 k€/year. The peak shaving drastically decreases by using the ESS in the deterministic case (the quantity is about halved), and then it is significantly further reduced in the uncertain scenarios. The same behavior can be observed for the generation curtailment of CHP. In the uncertain cases, compared with the base case without storages, the resort to load shedding is much reduced (-44.8% in the deterministic case becomes -60.5% in the intermediate case and -73.9% in the robust one) as well as the generation curtailment (-22.8%, -43.9% and -66.3% in the deterministic, intermediate and robust case respectively). The quantities related to the generation curtailment in Table 6-2 for these four cases are referred only to the curtailment of CHPs.

Consequently, a substantial reduction of the annual operational costs can be observed with the ESS inclusion in the deterministic case and much more in the uncertain cases (-34.2%, -52.4%, and -70.4%, in the deterministic, intermediate and robust case respectively). It is worth noticing that, in the deterministic and uncertain cases, apart from the operational costs, an additional cost factor has to be considered: the CAPEX for the ESS installation, split in ten years (the CAPEX of one 1.0 MW/2 h ESS is assumed equal). This, as expected, negatively impacts on the final cost, much strongly with the increment of budget or uncertainty, due to the growth of the investment costs for the increasing number of storages. However, the reduction of OPEX not only covers such increase, but, the final costs of all the cases that use the storage systems for relieving the contingencies are smaller than the case without them (no storage case). In particular, the percentage of total cost reduction is smaller than the one calculated by considering the OPEX only (i.e., -7.2%, -18.6% and -29.9% for deterministic, intermediate and robust cases, respectively), but the results prove the effectiveness of the optimization. In fact, these results demonstrate that not only the ESS helps to reduce the operational cost, for relieving even the worst-case and reducing even more the resort to load shedding and to the generation curtailment, but also that, with the assumed hypotheses, the ESS CAPEX can be amortized in the ten years of their life duration.

**Table 6-2** *The daily operational cost of the test network and ESS CAPEX*

| Cases | OPEX [k€/year] | Load shedding [MWh/year] | Generation Curtailment [MWh/year] | CAPEX [k€/year] | Total cost CAPEX+OPEX [k€/year] |
|---|---|---|---|---|---|
| No storage | 1480.36 | 6602.12 | 7502.38 | 0 | 1480.36 |
| Deterministic ($\Gamma = 0$) | 974.47 | 3644.95 | 5791.67 | 400 | 1374.47 |
| Intermediate ($\Gamma = 0.5$) | 704.64 | 2605.34 | 4208.2 | 500 | 1204.64 |
| Robust ($\Gamma = 1$) | 437.80 | 1721.07 | 2525.22 | 600 | 1037.80 |

## 6.4 Case Study (Transmission network)

In order to understand the versatility of the proposed approach, it has been applied to a transmission network. The standard IEEE 14 bus system has been considered as a test transmission network. The objective function of storage planning consists of the daily cost of operating conventional generations ($PC_n^g$), the storage investment cost ($SC_n$) per interest period and penalty terms of wind curtailment ($P_n^{wc}$). Therefore, the aim is to reduce the conventional generation cost, storage investment, and wind curtailment. $C_n^g$ and $C_{wc}$ are the specific costs of conventional generator production and the wind curtailment penalty, respectively. The storage investment cost ($SC_n$) is proportional to the number of storage installed ($\Gamma_{n,ESS}$) at each node $n$ and their size in terms of rated power and rated energy. The total storage investment cost appears in the objective function multiplied by a factor $K_s$ that defines the capital recovery factor of storage investment as

$$\min C_{tot} = min\left\{\sum_{n=1}^{N}\sum_{t=1}^{24} C_n^g * PC_n^g(t)\right. \tag{6.18}$$

$$\left. + \sum_{n=1}^{N}\sum_{t=1}^{24} C_{wc} * P_n^{wc}(t) + \sum_{n=1}^{N}\sum_{t=1}^{24} VOLL \cdot L_n^{sh}(t) + \frac{K_s}{365}\sum_{n=1}^{N} SC_n\right\}$$

explained in chapter 5.

Furthermore, in this study, the operational cost of batteries has been disregarded, as well as the impact of the charging/discharging cycles on the battery's life. Actually, a term that takes into account the depreciation of the storages due to their use could be included, but in this study, this cost is assumed negligible.

Apart from the network, generation, and storage constraints explained in chapter 5, the ramping capability of each conventional generator has been considered as in equation 6.19.

$$-RR_n \leq PC_n^g(t) - PC_n^g(t-1) \leq RR_n \tag{6.19}$$

The IEEE 14-bus network has five wind farms connected at nodes 1, 2, 3, 6 and 8, with each having an installed capacity of 30MW. The wind generation profiles were simulated by assuming that the wind speed is Weibull distributed with a scale factor of 11.01 m/s and a shape factor of 2 m/s. The load profile, expressed as a percentage of the annual peak load in the original data set, was computed using specific multiplying coefficients for the week of the year, for the day of the week, and the hour of the day.

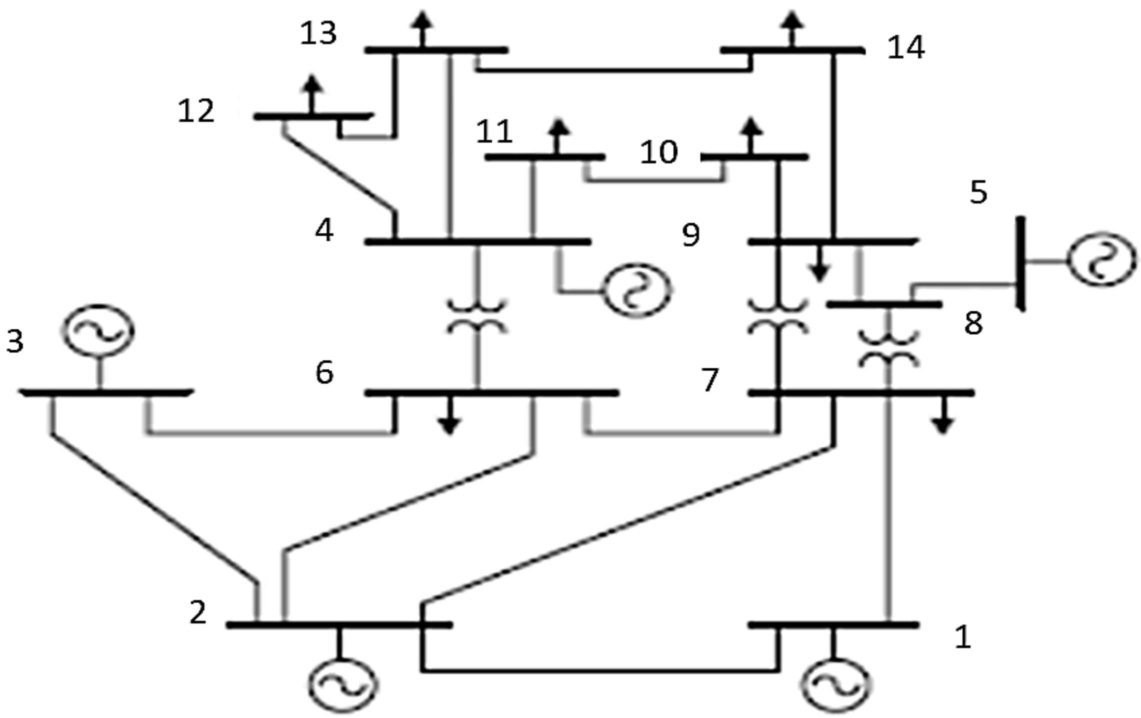


**Figure 32** *IEEE 14 bus test network*

### 6.4.1 Daily Operational Cost

Table 6-3 summarizes the daily operational cost of the dispatch from conventional generators for three different scenarios. A significant reduction of daily operational cost has been observed with the inclusion of storage. The storage devices in this system help to avoid wind curtailment and reduce conventional energy usage. As described in the next section, Storage requirements for a robust problem would always be higher than a deterministic case. Hence, the operational cost would always be higher. In the deterministic model, consideration of uncertainty is avoided by assuming perfect information for all parameters. However, even considering the robust scenario that includes the worst case, the operational cost is much lower compared to the no storage case.

**Table 6-3** *The daily operational cost of 14-bus network*

| Cases | Daily Operational Cost (€) |
|---|---|
| No storage | 120104.39 |
| With Storage (Deterministic) | 16153.74 |
| With Storage (Robust) | 26741.42 |

### 6.4.2 Storage Allocation

All the buses of this 14-bus network were assumed candidates for storage placement. The available storage devices were considered of 20MW/20MWh storage capacity. The efficiencies for charging and discharging were considered 90% each, which gives an overall roundtrip efficiency of 81%. The cost Lithium-ion technology in this study has been considered as €200 for each kW of rated power, €400 for each kWh of rated energy and capital recovery factor, $K_s = 0.01$ assuming a planning horizon of 10 years.

**Table 6-4** *The daily operational cost and energy storage allocation (with varying robustness)*

| Budget of Uncertainty | Number of Storage | Location | Average Daily Dispatch cost(€) |
|---|---|---|---|
| $\Gamma = 0$ | 4 | 3,4,10,14 | 16153 |
| $\Gamma = 0.25$ | 5 | 3,4,9,10,14 | 18428 |
| $\Gamma = 0.50$ | 7 | 3,4,6,7,9,10,14 | 21057 |
| $\Gamma = 0.75$ | 8 | 3,4,6,7,9,10,13,14 | 23959 |
| $\Gamma = 1$ | 10 | 3,4,6,7,9,10,12,13,14 | 26741 |

In Table 6-4, it shows how the investment of storage and daily operational cost change with changing the robustness. The deterministic case ($\Gamma = 0$) suggests 4 storage devices be installed in the network. As the budget of uncertainty increases, the number of storages increase and more charging/discharging cycles that leads to increased energy losses, therefore the daily operational cost also increases.

Since different scenarios can be generated with a different budget of uncertainty, and the algorithm provides the storage and operational cost information, it would be useful for the decision-maker to take a compromised decision. The most robust case ($\Gamma = 1$) may be avoided since it considers the worst case, and it may be very unlikely to happen.

### 6.4.3 Contribution of Storage during the peak load

In order to comprehensively understand the contribution of storage in the power flow, node 4 of Figure 32 has been selected since it is the most representative node in terms of line loading during the peak period. As it has shown in Figure 33, the apparent power flows reach their maximum capacity during the peak period. The storage helps to reduce the peak line flows. Besides, it helps to distribute the power flow in such a way that no branch reaches its maximum capability. Though the deterministic case mostly flattens the load curve, the robust case is more fluctuating to maintain the power flow in the limit.

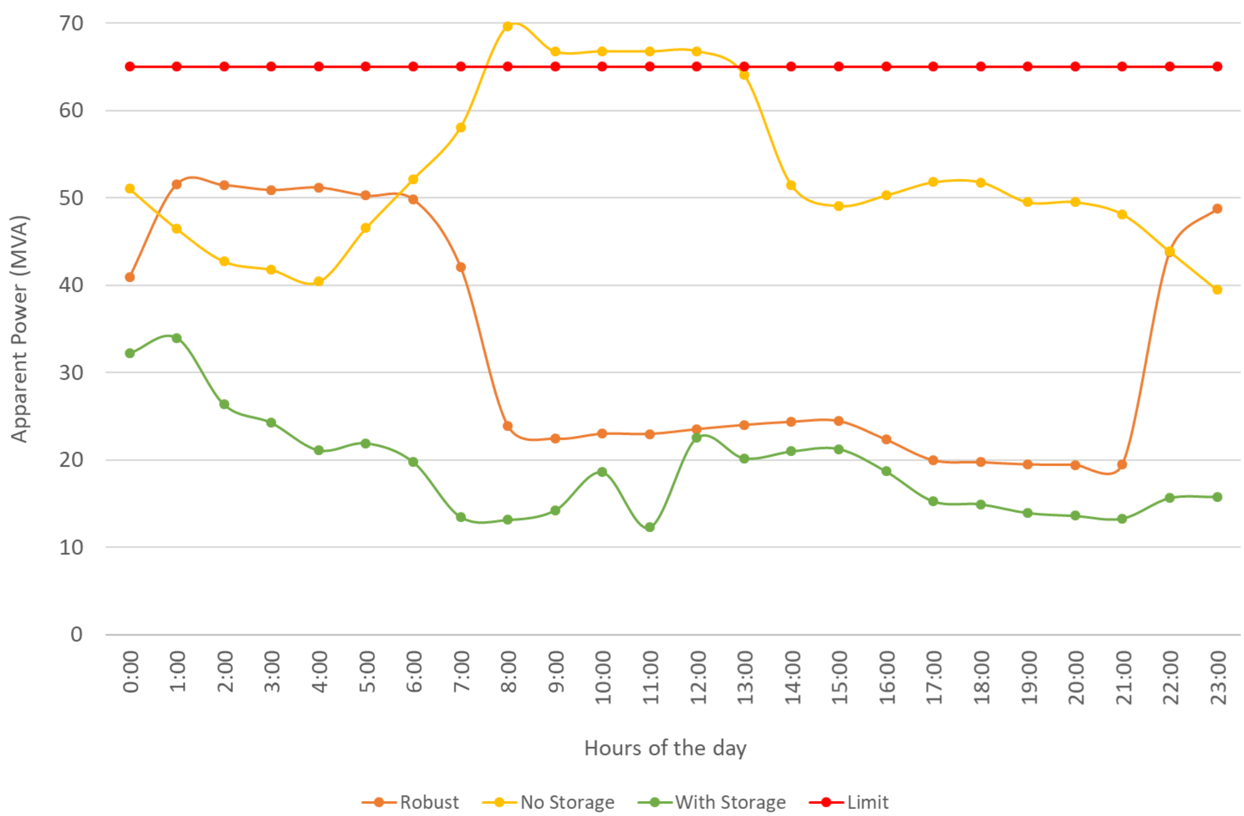


**Figure 33** *Power flow at branch 4-2(with capacity 65MVA)*

### 6.4.4 Storage Activity

In both deterministic and robust cases, the storage at bus 9 behaves similarly except during the peak period, where storage activity changes abruptly for the robust case. It is worthwhile to mention that in the case of planning, the robust solution is quite different from the deterministic one, as depicted in Figure 34. Since, the number of storage system increases in the robust scenario, the operation of individual storage in the network remain analogous for both robust and deterministic cases. Therefore, the pattern of charging and discharging is quite similar. Although the real change of operation due to the robust approach can be understood from the daily operational cost that changes with robustness.

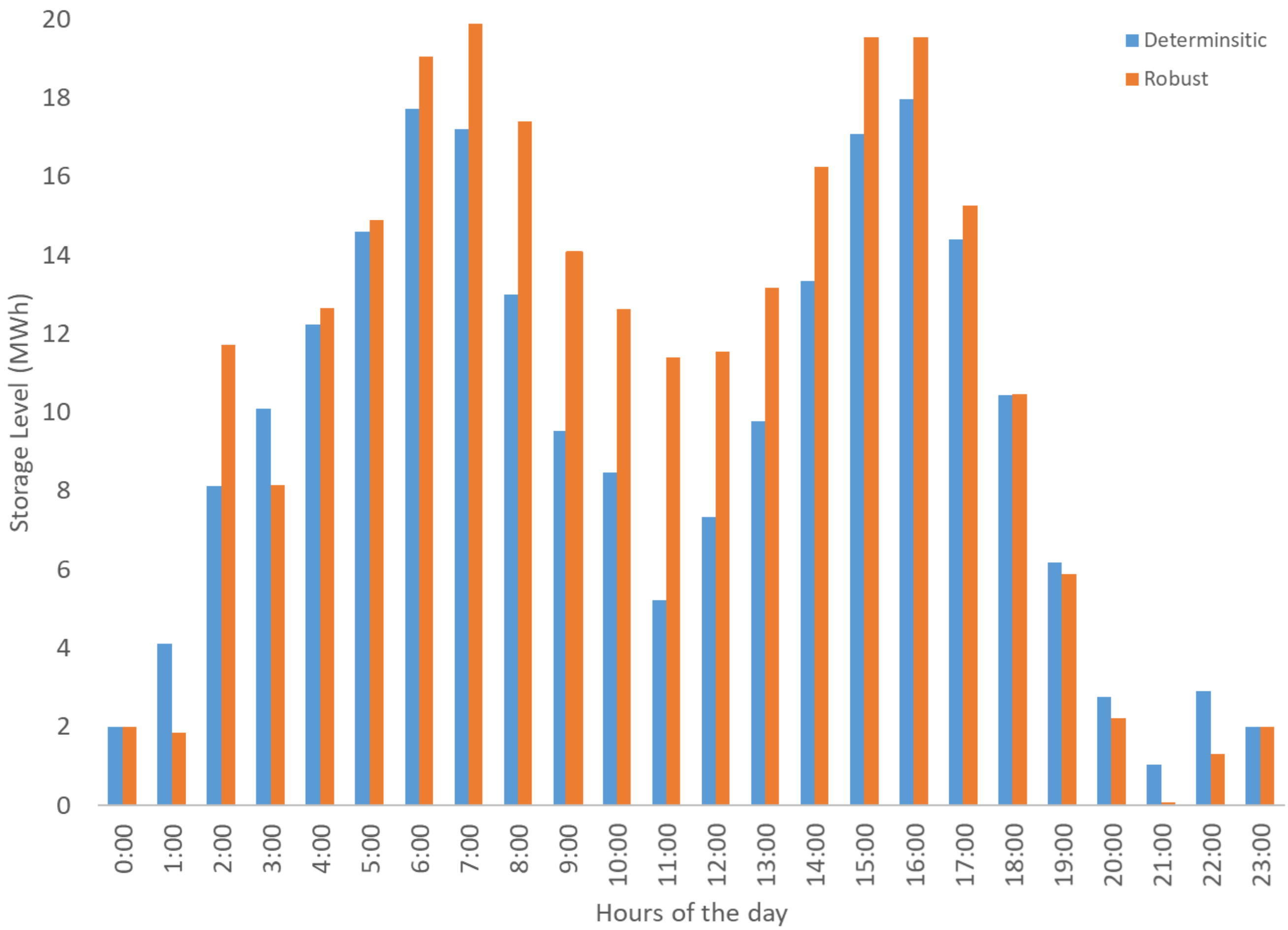


**Figure 34** *Storage operations at bus 9*

## 6.5 Summary

This chapter discusses the methodology for robust optimization application in the energy storage planning problem. Two case studies have been performed to validate the method and justify the scalability and versatility of the proposed approach. The impact of the budget of uncertainty has been demonstrated. It has been observed that with the level of risk the results substantially change. Apart from finding the optimal location of storage, the proposed algorithm also optimized the operation of storage to support the network. The economic analysis indicated that installing storage could reduce significantly network operation costs.

# Conclusion

## 7.1 Conclusion

The transition from conventional fossil fuel to sustainable energy sources as the primary source of energy generation requires a more innovative power system planning approach. The development indicates to have more integration of renewable energy generations. However, this integration brings new challenges that are economically expensive and jeopardize system reliability. Since most of the renewable generators are connected to the distribution network, it is imperative to include more innovative solutions such as storage and optimize the system to avoid expensive network reinforcement. Being said that, this thesis encounters the planning problems of the energy storage system in the network, considering uncertainties.

A detailed literature review has been performed that explains the innovative solution for smart grid planning. The literature review also explored the existing planning methodologies and also the new approaches that improve the current methods. Apart from this, the survey includes different energy storage systems and their possible applications. The need to have an accurate planning tool has well-justified. It argues that DC OPF could provide an inaccurate planning decision whereas the convex relaxation of an AC OPF is able to find the global optima maintaining the computational efficiency.

The necessity to consider the uncertainty in the planning decision has been stressed. An innovative approach, robust optimization, has been described. However, the challenge to include robust optimization in the AC OPF model addressed. To solve that, a robust reformulation approach has been suggested, that keeps the original model intact and solve efficiently.

A multi-period AC OPF model is formulated for the planning of energy storage systems considering wind, solar, and CHP generators. The planning of ESSs in the distribution network considers evaluating the contribution of energy storage to the management of the network. The analysis found the integration of energy storage profitable since it was able to reduce the operating costs significantly. The application of robust optimization allows observing different cases for planning decisions. Four different cases: no storage, deterministic, intermediate, and robust, provided a comprehensive view of the whole planning solution. It was found that with the increment of uncertainty, the number of storage increases. However, this also helps to reduce the load and generation curtailments that incur additional expense to the network operators.

The daily operation of energy storage systems has been optimized. The charging and discharging operations are analogous to network issues. For instance, the storage needs to provide energy in the case of under-voltage incidents to keep the network stable.

A systematic approach of applying robust optimization on an AC OPF based siting of energy storage devices in the electric network has been demonstrated. Since DC OPF neglects the transmission losses and may lead to an infeasible planning solution, the use of AC OPF in this study aimed at increasing accuracy in the planning.

Since the polyhedral uncertainty set has been exploited to represent the uncertainty sets, it allows having the flexibility to do a trade-off between economic efficiency and conservatism. The use of this kind of flexibility also assisted in considering additional scenarios other than the worst-case scenarios that most robust optimization problems account for.

The robust optimization approach aims at efficiently incorporating the uncertainty in the model. By considering the worst-case scenario only, such problems do not provide an optimal solution. Rather, they offer only conservative solutions that could be impractical However, the analytical reformulation technique helped to find the robust counterpart of the original problem that was solved with less computational burden using commercial solvers such as CPLEX.

As planning includes a limited financial budget and resources, this study affords a comprehensive approach, which is a consideration of different situations (budget of uncertainty).

Two case studies have been performed to validate the proposed energy storage planning tool. A real distribution network and an IEEE 14 bus transmission network have been considered as test networks. It was observed that the computational time increase significantly with the size of the network. The results prove that the inclusion of load and wind uncertainties in the problem significantly increases the operational and future planning costs of the system, which indicates the need to include uncertainties in planning.

It should be mentioned that this proposed methodology can be used with different energy storage technologies by considering related costs and performance parameters such as charging/discharging efficiencies.

## 7.2 Future Work

This thesis work brings interesting research paths for future investigation:

- **Considering SDP relaxation**

  In this thesis, the SOCP relaxation technique adopted to formulate convex AC OPF. At this point, the efficient solver for semidefinite programming (SDP) relaxation is scarce. However, it would be interesting to use SDP relaxation for the same planning problem with the help of linearization techniques to solve it efficiently.

- **Integrating different energy storage portfolio**

  There are different energy storage technologies that are mature and becoming economically viable. It is always essential to select the appropriate ESS technology and then the candidate bus. Future research could add a selection of energy storage systems in the planning problem.

- **Implementing the aging of storage devices**

  A term that takes into account the depreciation of the storages due to their use could be included in the objective function.

- **Applying dynamic uncertainty sets**

  To deal with the dynamic relationship between uncertainties across decision stages, a dynamic approach could be interesting to consider. This kind of uncertainty set would be able to find the spatial and temporal correlations in uncertain sources.

- **Adopting the adversarial approach**

  This thesis examines the robust reformulation approach to solve the robust optimization problem. The adversarial approach to solving the same planning problem could help to have an extensive comparison between the two solution methodologies in terms of computational time and accuracy of the solution.

## Reference

1. Change, IPCC Climate. "Mitigation of climate change." Contribution of Working Group III to the Fifth Assessment Report of the Intergovernmental Panel on Climate Change 1454 (2014).
2. Energy, REthinking. "Accelerating the global energy transformation." International Renewable Energy Agency (IRENA). Abu Dhabi (2017).
3. Etta Grover Silva. Optimization of the planning and operations of electric distribution grids in the context of high renewable energy penetration. Electric power. PSL Research University, 2017. English
4. World Energy Council, 2016a. The World Energy Trilemma Index – 2016 - Benchmarking the sustainability of national energy systems. World Energy Council: London, UK. Available at: https://www.worldenergy.org/publications/2016/2016-energy-trilemma-indexbenchmarking-the-sustainability-of-national-energy-systems/ (last accessed 06 September 2019).
5. Context and key issues "Electricity generation is at the core of efforts to reduce carbon dioxide (CO2) emissions" p.21. ©OECD/IEA 2016 Re-powering Markets, IEA Publishing
6. IEA (International Energy Agency) (2017a), "Energy Access Outlook 2017: From Poverty to Prosperity," 2017.
7. Hérault, MC Alvarez. Architecture of the distribution networks of the future in the presence of decentralized production . Diss. PhD thesis, INP Grenoble, 2009.
8. Vinkovic, Anton, Marko Suhadolc, and Rafael Mihalic. "Current-based models of FACTS devices for three-phase load-flow calculations using the Newton–Raphson method." International Journal of Electrical Power & Energy Systems 45.1 (2013): 117-128.
9. Penido, Débora Rosana Ribeiro, et al. "A new tool for multiphase electrical systems analysis based on current injection method." International Journal of Electrical Power & Energy Systems 44.1 (2013): 410-420.
10. Abdel-Akher, Mamdouh, Khalid Mohamed Nor, and AH Abdul Rashid. "Improved three-phase power-flow methods using sequence components." IEEE Transactions on power systems 20.3 (2005): 1389-1397.

11. Farag, Hany E., et al. "A generalized power flow analysis for distribution systems with high penetration of distributed generation." Electric Power Systems Research 81.7 (2011): 1499-1506.
12. Wu, W. C., and B. M. Zhang. "A three-phase power flow algorithm for distribution system power flow based on loop-analysis method." International Journal of Electrical Power & Energy Systems 30.1 (2008): 8-15.
13. Molzahn, Daniel K., et al. "A survey of distributed optimization and control algorithms for electric power systems." IEEE Transactions on Smart Grid 8.6 (2017): 2941-2962.
14. Watson, Jeremy Donald, Neville R. Watson, and Ioannis Lestas. "Optimized dispatch of energy storage systems in unbalanced distribution networks." IEEE Transactions on Sustainable Energy 9.2 (2017): 639-650.
15. Castillo, Anya, and Dennice F. Gayme. "Evaluating the Effects of Real Power Losses in Optimal Power Flow-Based Storage Integration." IEEE Transactions on Control of Network Systems 5.3 (2017): 1132-1145.
16. Maulik, Avirup, and Debapriya Das. "Optimal operation of microgrid using four different optimization techniques." Sustainable Energy Technologies and Assessments 21 (2017): 100-120.
17. Nick, Mostafa, Rachid Cherkaoui, and Mario Paolone. "Optimal planning of distributed energy storage systems in active distribution networks embedding grid reconfiguration." IEEE Transactions on Power Systems 33.2 (2017): 1577-1590.
18. Zidar, Matija, et al. "Review of energy storage allocation in power distribution networks: applications, methods and future research." IET Generation, Transmission & Distribution 10.3 (2016): 645-652.
19. Driesen, Johan, and Ronnie Belmans. "Distributed generation: challenges and possible solutions." 2006 IEEE power engineering society general meeting. IEEE, 2006.
20. Karoui, Karim, Horia Crisciu, and Ludovic Platbrood. "An optimum power flow tool for optimising the expansion plan of reactive power compensation." 2011 IEEE GCC Conference and Exhibition (GCC). IEEE, 2011.

21. Gyuk, Imre P., and S. Eckroad. "Energy storage for grid connected wind generation applications." US Department of Energy, Washington DC, EPRI-DOE Handbook Supplement 1008703 (2004).
22. International Electrotechnical Commission (IEC), Electrical energy storage, 2011
23. Denholm, Paul, et al. Role of energy storage with renewable electricity generation. No. NREL/TP-6A2-47187. National Renewable Energy Lab.(NREL), Golden, CO (United States), 2010.
24. Eyer, Jim, and Garth Corey. "Energy storage for the electricity grid: Benefits and market potential assessment guide." Sandia National Laboratories 20.10 (2010): 5.
25. Telaretti, Enrico, and Luigi Dusonchet. "Battery storage systems for peak load shaving applications: Part 2: Economic feasibility and sensitivity analysis." 2016 IEEE 16th International Conference on Environment and Electrical Engineering (EEEIC). IEEE, 2016.
26. Liao, Qiangqiang, et al. "A techno-economic analysis on NaS battery energy storage system supporting peak shaving." International Journal of Energy Research 40.2 (2016): 241-247.
27. Energinet, D. K. Ancillary services to be delivered in Denmark Tender conditions. Technical report, Energinet, Fredericia, 2012.
28. Rebours, Yann G., et al. "A survey of frequency and voltage control ancillary services—Part I: Technical features." IEEE Transactions on power systems 22.1 (2007): 350-357.
29. Wen, Guanghui, et al. "Frequency regulation of source-grid-load systems: A compound control strategy." IEEE transactions on industrial informatics 12.1 (2015): 69-78.
30. Bragard, Michael, et al. "The balance of renewable sources and user demands in grids: Power electronics for modular battery energy storage systems." IEEE Transactions on Power Electronics 25.12 (2010): 3049-3056.
31. Moreira, Roberto, Rodrigo Moreno, and Goran Strbac. "Synergies and conflicts among energy storage services." 2016 IEEE International Energy Conference (ENERGYCON). IEEE, 2016.
32. Zafirakis, Dimitrios, et al. "The value of arbitrage for energy storage: Evidence from European electricity markets." Applied energy 184 (2016): 971-986.

33. Wang, Yu, et al. "Coordinated control of distributed energy-storage systems for voltage regulation in distribution networks." IEEE transactions on power delivery 31.3 (2015): 1132-1141.
34. Giannitrapani, Antonio, et al. "Optimal allocation of energy storage systems for voltage control in LV distribution networks." IEEE Transactions on Smart Grid 8.6 (2016): 2859-2870.
35. Sharma, Gaurav, and Shelly Vadhera. "Voltage control of the grid connected wind plant using energy storage and FACTS devices." 2015 International Conference on Energy, Power and Environment: Towards Sustainable Growth (ICEPE). IEEE, 2015.
36. Brown, Paul D., JA Peças Lopes, and Manuel A. Matos. "Optimization of pumped storage capacity in an isolated power system with large renewable penetration." IEEE Transactions on Power grid-connected 23.2 (2008): 523-531.
37. Cheng, Meng, Saif Sabah Sami, and Jianzhong Wu. "Virtual energy storage system for smart grids." Energy Procedia 88 (2016): 436-442.
38. Ritchie, A. G. "Recent developments and future prospects for lithium rechargeable batteries." Journal of power Sources 96.1 (2001): 1-4.
39. Zaghib, Karim, et al. "Safe and fast-charging Li-ion battery with long shelf life for power applications." Journal of Power Sources 196.8 (2011): 3949-3954.
40. Hadjipaschalis, Ioannis, Andreas Poullikkas, and Venizelos Efthimiou. "Overview of current and future energy storage technologies for electric power applications." Renewable and sustainable energy reviews 13.6-7 (2009): 1513-1522.
41. Tan, Xingguo, Qingmin Li, and Hui Wang. "Advances and trends of energy storage technology in microgrid." International Journal of Electrical Power & Energy Systems 44.1 (2013): 179-191.
42. Chen, Haisheng, et al. "Progress in electrical energy storage system: A critical review." Progress in natural science 19.3 (2009): 291-312.
43. Baker, John. "New technology and possible advances in energy storage." Energy Policy 36.12 (2008): 4368-4373.
44. Wen, Zhaoyin, et al. "Research on sodium sulfur battery for energy storage." Solid State Ionics 179.27-32 (2008): 1697-1701.

45. Broussely, Michel, and Gianfranco Pistoia, eds. Industrial applications of batteries: from cars to aerospace and energy storage. Elsevier, 2007.
46. Evans, Annette, Vladimir Strezov, and Tim J. Evans. "Assessment of utility energy storage options for increased renewable energy penetration." Renewable and Sustainable Energy Reviews 16.6 (2012): 4141-4147.
47. Divya, K. C., and Jacob Østergaard. "Battery energy storage technology for power systems—An overview." Electric power systems research 79.4 (2009): 511-520.
48. Scamman, Daniel P., Gavin W. Reade, and Edward PL Roberts. "Numerical modelling of a bromide–polysulphide redox flow battery: Part 1: Modelling approach and validation for a pilot-scale system." Journal of Power Sources 189.2 (2009): 1220-1230.
49. Rabiee, Abdorreza, Hossein Khorramdel, and Jamshid Aghaei. "RETRACTED: A review of energy storage systems in microgrids with wind turbines." (2013): 316-326.
50. Ribeiro, Paulo F., et al. "Energy storage systems for advanced power applications." Proceedings of the IEEE 89.12 (2001): 1744-1756.
51. Sharma, Atul, et al. "Review on thermal energy storage with phase change materials and applications." Renewable and Sustainable energy reviews 13.2 (2009): 318-345.
52. Carnegie, Rachel, et al. "Utility Scale Energy Storage Systems, Benefits, Application, and Technologies, by State Utility Forecasting Group, June 2013." Posted at http://www. purdue. edu/discoverypark/energy/assets/pdfs/SUFG/publications/SUFG% 20Ener gy% 20Storage% 20Report. pdf (2013).
53. Chen, Haisheng, et al. "Progress in electrical energy storage system: A critical review." Progress in natural science 19.3 (2009): 291-312.
54. Wen, D. S., et al. "Liquid nitrogen injection into water: Pressure build-up and heat transfer." Cryogenics 46.10 (2006): 740-748.
55. B. Zalba, J.M. Marin, L.F. Cabeza and H. Mehling, “Review on thermal energy storage with phase change: materials, heat transfer analysis and applications”, vol. 23(3), p. 251-283, 2003.
56. Martin, Benoît. Autonomous microgrids for rural electrification: joint investment planning of power generation and distribution through convex optimization. Diss. UCL-Université Catholique de Louvain, 2018.

57. Nemirovski, Arkadi. "Lectures on robust convex optimization." Lecture notes. Georgia Institute of Technology (2012).
58. Birge, John R., and François Louveaux. "The value of information and the stochastic solution." Introduction to Stochastic Programming. Springer, New York, NY, 2011. 163-177.
59. PETRELLI, MARINA. "Robust optimization for the unit commitment of isolated RES-based microgrids in developing countries." (2018).
60. Massachusetts Institute of Technology (MIT) Lecture material, “Duality in Linear Programming.”
61. Bachem, Achim, and Walter Kern. "Linear programming duality." Linear Programming Duality. Springer, Berlin, Heidelberg, 1992. 89-111.
62. Murillo-Sánchez, Carlos E., et al. "Secure planning and operations of systems with stochastic sources, energy storage, and active demand." IEEE Transactions on Smart Grid 4.4 (2013): 2220-2229.
63. Milligan, Michael, Pearl Donohoo, and Mark O'Malley. Stochastic methods for planning and operating power systems with large amounts of wind and solar power. No. NREL/CP-5500-56208. National Renewable Energy Lab.(NREL), Golden, CO (United States), 2012.
64. C. Skar, G. Doorman, and A. Tomasgard, “Large-scale power system planning using enhanced Benders decomposition,” in Power Systems Computation Conference (PSCC),2014, pp. 1–7. DOI: 10.1109/PSCC.2014.7038297
65. L. Roald, M. Vrakopoulou, F. Oldewurtel, and G. Andersson, “Risk-constrained optimal power flow with probabilistic guarantees,” in Power Systems Computation Conference (PSCC), 2014, pp. 1–7. DOI: 10.1109/PSCC.2014.7038342
66. I. A. Sajjad, G. Chicco, and R. Napoli, “A probabilistic approach to study the load variations in aggregated residential load patterns,” in Power Systems Computation Conference (PSCC), 2014, pp. 1–7. DOI: 10.1109/PSCC.2014.7038105
67. R. Wiget, M. Vrakopoulou, and G. Andersson, “Probabilistic security-constrained optimal power flow for a mixed HVAC and HVDC grid with stochastic infeed,” in Power

Systems Computation Conference (PSCC), 2014, pp. 1–7. DOI: 10.1109/PSCC. 2014.7038408

68. T. Summers, J. Warrington, M. Morari, and J. Lygeros, “Stochastic optimal power flow based on convex approximations of chance constraints,” in Power Systems Computation Conference (PSCC), 2014, pp. 1–7. DOI: 10.1109/PSCC.2014.7038376
69. M. Negnevitsky, N. Tomin, D. Panasetsky, N. Voropai, V. Kurbatsky, U. Hager, and C. Rehtanz, “Preventing large-scale blackouts in power systems under uncertainty,” in Power Systems Computation Conference (PSCC), 2014, pp. 1–7. DOI: 10. 1109 /PSCC.2014.7038340.
70. A. Moreira, A. Street, and J. M. Arroyo, “Energy and reserve scheduling under correlated nodal demand uncertainty: An adjustable robust optimization approach,” in Power Systems Computation Conference (PSCC), 2014, pp. 1–8. DOI: 10.1109/PSCC. 2014.7038415.
71. P. Panciatici, M. C. Campi, S. Garatti, S. H. Low, D. K. Molzahn, A. X. Sun, and L. Wehenkel, “Advanced optimization methods for power systems,” in Power Systems Computation Conference (PSCC), 2014, pp. 1–18. DOI: 10.1109/PSCC.2014.7038504.
72. W. Zhang, Y. Xu, Z. Y. Dong, Y.Wang, and R. Zhang, “An efficient approach for robust SCOPF considering load and renewable power uncertainties,” in Power Systems Computation Conference (PSCC), 2016, pp. 1–7. DOI: 10.1109/PSCC.2016.7540823(cit. on p. 37).
73. M. Sun, I. Konstantelos, S. Tindemans, and G. Strbac, “Evaluating composite approaches to modelling high-dimensional stochastic variables in power systems,” in Power Systems Computation Conference (PSCC), 2016, pp. 1–8. DOI: 10.1109/PSCC.2016.7540837.
74. Holttinen, Hannele, et al. "Wind and load variability in the Nordic countries." (2013).
75. Alberta Electric System Operator (AESO), 10 Min Historical Data for TotalWind Power and Alberta Internal Load, http://www.aeso.ca/gridoperations/20544.html
76. Ustun, Taha Selim, and Yuki Aoto. "Analysis of Smart Inverter’s Impact on the Distribution Network Operation." IEEE Access 7 (2019): 9790-9804.

77. Nguyen, Nhi Thi Ai. "Optimal planning of energy storage systems considering uncertainty." (2016).
78. Le, Dinh Duong, et al. "Advanced probabilistic power flow methodology for power systems with renewable resources." Turkish Journal of Electrical Engineering & Computer Sciences 25.2 (2017): 1154-1162.
79. Hussain, Akhtar, Van-Hai Bui, and Hak-Man Kim. "Robust optimization-based scheduling of multi-microgrids considering uncertainties." Energies 9.4 (2016): 278.
80. Kristoffersen, Trine Krogh. "Stochastic programming with applications to power systems." Working Papers, Department of Mathematical Sciences, University of Aarhus 2007.1 (2007).
81. Li, G., and X. P. Zhang. "Stochastic optimal power flow approach considering correlated probabilistic load and wind farm generation." (2011): 31-31.
82. Dantzig, George B. "Linear programming under uncertainty." Stochastic programming. Springer, New York, NY, 2010. 1-11.
83. Shapiro, Alexander, Darinka Dentcheva, and Andrzej Ruszczyński. Lectures on stochastic programming: modeling and theory. Society for Industrial and Applied Mathematics, 2009.
84. Zhu, Jizhong. Optimization of power system operation. Vol. 47. John Wiley & Sons, 2015.
85. Soyster, Allen L. "Convex programming with set-inclusive constraints and applications to inexact linear programming." Operations research 21.5 (1973): 1154-1157.
86. Kouvelis, Panos, and Gang Yu. Robust discrete optimization and its applications. Vol. 14. Springer Science & Business Media, 2013.
87. Ben-Tal, Aharon, and Arkadi Nemirovski. "Robust convex optimization." Mathematics of operations research 23.4 (1998): 769-805.
88. El Ghaoui, Laurent, and Hervé Lebret. "Robust solutions to least-squares problems with uncertain data." SIAM Journal on matrix analysis and applications 18.4 (1997): 1035-1064.
89. El Ghaoui, Laurent, Francois Oustry, and Hervé Lebret. "Robust solutions to uncertain semidefinite programs." SIAM Journal on Optimization 9.1 (1998): 33-52.

90. Bertsimas, Dimitris, and Melvyn Sim. "The price of robustness." Operations research 52.1 (2004): 35-53.
91. Aissi, Hassene, Cristina Bazgan, and Daniel Vanderpooten. "Min–max and min–max regret versions of combinatorial optimization problems: A survey." European journal of operational research 197.2 (2009): 427-438.
92. Li, Zukui, Ran Ding, and Christodoulos A. Floudas. "A comparative theoretical and computational study on robust counterpart optimization: I. Robust linear optimization and robust mixed integer linear optimization." Industrial & engineering chemistry research 50.18 (2011): 10567-10603.
93. Gorissen, Bram L., İhsan Yanıkoğlu, and Dick den Hertog. "A practical guide to robust optimization." Omega 53 (2015): 124-137.
94. Takriti, Samer, John R. Birge, and Erik Long. "A stochastic model for the unit commitment problem." IEEE Transactions on Power Systems 11.3 (1996): 1497-1508.
95. Carpentier, Pierre, et al. "Stochastic optimization of unit commitment: a new decomposition framework." IEEE Transactions on Power Systems 11.2 (1996): 1067-1073.
96. Dentcheva, Darinka, and Werner Römisch. "Optimal power generation under uncertainty via stochastic programming." Stochastic programming methods and technical applications. Springer, Berlin, Heidelberg, 1998. 22-56.
97. Wallace, Stein W., and Stein-Erik Fleten. "Stochastic programming models in energy." Handbooks in operations research and management science 10 (2003): 637-677.
98. Bertsimas, Dimitris, et al. "Adaptive robust optimization for the security constrained unit commitment problem." IEEE transactions on power systems 28.1 (2012): 52-63.
99. Ben-Tal, Aharon, and Arkadi Nemirovski. "Robust solutions of linear programming problems contaminated with uncertain data." Mathematical programming 88.3 (2000): 411-424.
100. Zugno, Marco, et al. "Modeling demand response in electricity retail markets as a stackelberg game." 12th IAEE European Energy Conference: Energy challenge and environmental sustainability. 2012.

101. Zugno, Marco, and Antonio J. Conejo. "A robust optimization approach to energy and reserve dispatch in electricity markets." European Journal of Operational Research 247.2 (2015): 659-671.

102. Jabr, Rabih A. "Adjustable robust OPF with renewable energy sources." IEEE Transactions on Power Systems 28.4 (2013): 4742-4751.

103. Jabr, Rabih A., Izudin Džafić, and Bikash C. Pal. "Robust optimization of storage investment on transmission networks." IEEE Transactions on Power Systems 30.1 (2014): 531-539.

104. Street, Alexandre, Fabrício Oliveira, and José M. Arroyo. "Contingency-constrained unit commitment with $ n-k $ security criterion: A robust optimization approach." IEEE Transactions on Power Systems 26.3 (2010): 1581-1590.

105. Jiang, Ruiwei, Jianhui Wang, and Yongpei Guan. "Robust unit commitment with wind power and pumped storage hydro." IEEE Transactions on Power Systems 27.2 (2011): 800-810.

106. Zhao, Long, and Bo Zeng. "Robust unit commitment problem with demand response and wind energy." 2012 IEEE power and energy society general meeting. IEEE, 2012.

107. Jiang, Ruiwei, et al. "Two-stage minimax regret robust unit commitment." IEEE Transactions on Power Systems 28.3 (2013): 2271-2282.

108. Zhang, Yu, and Georgios B. Giannakis. "Robust optimal power flow with wind integration using conditional value-at-risk." 2013 IEEE International Conference on Smart Grid Communications (SmartGridComm). IEEE, 2013.

109. Bai, Xiaoqing, Liyan Qu, and Wei Qiao. "Robust AC optimal power flow for power networks with wind power generation." IEEE Transactions on Power Systems 31.5 (2015): 4163-4164.

110. Soares, Tiago, et al. "Active distribution grid management based on robust AC optimal power flow." IEEE Transactions on Smart Grid 9.6 (2017): 6229-6241.

111. Martin, Benoît, Emmanuel De Jaeger, and François Glineur. "A robust convex optimization framework for autonomous network planning under load uncertainty." 2017 IEEE Manchester PowerTech. IEEE, 2017.

112. Liu, Ping. Stochastic and robust optimal operation of energy-efficient building with combined heat and power systems. Mississippi State University, 2014.

113. Kouvelis, Panos, and Gang Yu. Robust discrete optimization and its applications. Vol. 14. Springer Science & Business Media, 2013.

114. Volko, Claus-Dieter. "Robust Discrete Optimization." (2012).

115. Ben-Tal, Aharon, Laurent El Ghaoui, and Arkadi Nemirovski. Robust optimization. Vol. 28. Princeton University Press, 2009.

116. Bienstock, Daniel, and Nuri ÖZbay. "Computing robust basestock levels." Discrete Optimization 5.2 (2008): 389-414.

117. Nick, Mostafa, et al. "Optimal location and sizing of distributed storage systems in active distribution networks." 2013 IEEE Grenoble Conference. IEEE, 2013.

118. Qing, Zhong, et al. "Optimal siting & sizing of battery energy storage system in active distribution network." IEEE PES ISGT Europe 2013. IEEE, 2013.

119. El-Zonkoly, Amany. "Optimal placement and schedule of multiple grid-connected hybrid energy systems." International Journal of Electrical Power & Energy Systems 61 (2014): 239-247.

120. Motalleb, Mahdi, Ehsan Reihani, and Reza Ghorbani. "Optimal placement and sizing of the storage supporting transmission and distribution networks." Renewable Energy 94 (2016): 651-659.

121. Paudyal, Sumit, Claudio A. Canizares, and Kankar Bhattacharya. "Three-phase distribution OPF in smart grids: Optimality versus computational burden." 2011 2nd IEEE PES International Conference and Exhibition on Innovative Smart Grid Technologies. IEEE, 2011.

122. Mashayekh, Salman, et al. "A mixed integer linear programming approach for optimal DER portfolio, sizing, and placement in multi-energy microgrids." Applied Energy 187 (2017): 154-168.

123. Gan, Lingwen, and Steven H. Low. "Convex relaxations and linear approximation for optimal power flow in multiphase radial networks." 2014 Power Systems Computation Conference. IEEE, 2014.

124. Nazaripouya, Hamidreza, et al. "Optimal sizing and placement of battery energy storage in distribution system based on solar size for voltage regulation." 2015 IEEE Power & Energy Society General Meeting. IEEE, 2015.

125. Thrampoulidis, Christos, Subhonmesh Bose, and Babak Hassibi. "Optimal placement of distributed energy storage in power networks." IEEE Transactions on Automatic Control 61.2 (2015): 416-429.

126. Ghofrani, Mahmoud, et al. "A framework for optimal placement of energy storage units within a power system with high wind penetration." IEEE Transactions on Sustainable Energy 4.2 (2013): 434-442.

127. Sharma, Isha, and Kankar Bhattacharya. "Optimal sizing of battery energy storage systems in unbalanced distribution feeders." IECON 2013-39th Annual Conference of the IEEE Industrial Electronics Society. IEEE, 2013.

128. Li, Qifeng, Raja Ayyanar, and Vijay Vittal. "Convex optimization for DES planning and operation in radial distribution systems with high penetration of photovoltaic resources." IEEE Transactions on Sustainable Energy 7.3 (2016): 985-995.

129. Subhonmesh, Bose, Steven H. Low, and K. Mani Chandy. "Equivalence of branch flow and bus injection models." 2012 50th Annual Allerton Conference on Communication, Control, and Computing (Allerton). IEEE, 2012.

130. Bose, Subhonmesh, et al. "Equivalent relaxations of optimal power flow." IEEE Transactions on Automatic Control 60.3 (2014): 729-742.

131. Coffrin, Carleton, Hassan L. Hijazi, and Pascal Van Hentenryck. "DistFlow extensions for AC transmission systems." arXiv preprint arXiv:1506.04773 (2015).

132. Farivar, Masoud, et al. "Optimal inverter VAR control in distribution systems with high PV penetration." 2012 IEEE Power and Energy Society general meeting. IEEE, 2012.

133. Bracale, A., Caldon, R., Celli, et Al., 2012, “Analysis of the Italian distribution system evolution through reference networks”, Proc. IEEE PES ISGT Europe, 2012.

## List of Publications

- Nayeem Chowdhury, Fabrizio Pilo, Giuditta Pisano, and Matteo Troncia. "Optimal location of energy storage systems with robust optimization." CIRED 2019.
- Nayeem Chowdhury, Giuditta Pisano, and Fabrizio Pilo. "Energy Storage Placement in the Transmission Network: A Robust Optimization Approach." In *2019 AEIT International Annual Conference (AEIT)*, pp. 1-6. IEEE, 2019.
- Pisano, G.; Chowdhury, N.; Coppo, M.; Natale, N.; Petretto, G.; Soma, G.G.; Turri, R.; Pilo, F. Synthetic Models of Distribution Networks Based on Open Data and Georeferenced Information. Energies 2019, 12, 4500.
- Nayeem Chowdhury, Fabrizio Pilo, and Giuditta Pisano. "Robust Optimization for Managing Uncertainties in Energy Storage System Positioning" Energies 2019. (Under Review)